Supplement of Atmos. Chem. Phys., 25, 15969–15990, 2025
https://doi.org/10.5194/acp-25-15969-2025-supplement

Supplement of

Intercomparison of global ground-level ozone datasets for health-relevant metrics

Hantao Wang et al.

Correspondence to: J. Jason West (jasonwest@unc.edu)

SUPPLEMENTARY INFORMATION

Section S1. Grouping method used in pairwise spatial similarity comparison

The Grouping method is based on the pairwise correlation between each dataset. Initially, all datasets are re-gridded to a resolution of 0.1° by 0.1°. Subsequently, the pairwise correlation coefficient (R) is computed for each pair of datasets spanning the period from 2006 to 2016. The mean pairwise correlation for each grouping over the same timeframe is then calculated to construct Figure 5(a). Then, we generate a random groups table. For this comparison, involving 6 datasets, there are 203 possible combinations for grouping. For each grouping combination, 4 variables are computed: the sum of pairwise correlations within groups (C_i), the sum of pairwise correlations outside the groups (C_o), the number of dataset pairs within groups (N_i), and the number of dataset pairs outside the groups (N_o). The objective is to ascertain the grouping combination that maximizes the difference between $\frac{Ci}{Ni}$ and $\frac{Co}{No}$.

For example, consider a grouping scenario where:
Group A: BME, NJML, UKML
Group B: CAMS, GEOS, TCR-2.

“pwcorr” denotes the operation to compute the pairwise correlation between two datasets. The calculations proceed as follows:

Equation S1. Correlation inside the groups
C_i = pwcorr(BME, NJML)+ pwcorr(BME, UKML)+ pwcorr(NJML, UKML)+ pwcorr(CAMS, GEOS)+ pwcorr(CAMS, TCR-2)+ pwcorr(TCR-2, GEOS)
Equation S2. Correlation outside the groups
C_o = pwcorr(BME, GEOS)+ pwcorr(BME, TCR-2)+ pwcorr(BME, CAMS)+ pwcorr(NJML, GEOS)+ pwcorr(NJML, TCR-2)+ pwcorr(NJML, CAMS)+ pwcorr(UKML, GEOS)+ pwcorr(UKML, TCR-2)+ pwcorr(UKML, CAMS)

In this case, $N_i = 6$, $N_o = 9$, Thus

Equation S3. Difference between mean correlation inside the groups and mean correlation outside the groups
Difference = $\frac{Ci}{Ni} - \frac{Co}{No}$

This analysis is conducted for all 203 combinations, identifying the optimal grouping that maximizes the difference.
Group A: BME, UKML, CAMS, GEOS, TCR-2
Group B: NJML

We also use the hierarchical clustering method to group 6 datasets based on pairwise correlation (R) and get the same result. The hierarchical clustering is typically used with a dissimilarity (distance) matrix, where the elements represent the distances or dissimilarities between data (Bishop, 2006).

Section S2. Calculation method used for area weighted mean and population weighted mean

The weighted means of each dataset in this study were calculated using regridded data at 0.1° × 0.1° spatial resolution, excluding ocean areas.

The area-weighted mean represents the average ozone concentration calculated by weighting each grid cell equally based on its geographic area. This metric provides a spatially representative estimate of ozone levels across a given region or the globe.

Equation S4. Area-weighted mean
Area-weighted mean = ∑(OSDAM8 × area) / ∑(area)

The population-weighted mean accounts for the number of people residing in each grid cell, giving greater weight to densely populated areas. This approach better reflects average human exposure to ground-level ozone across a region or globally.

Equation S5. Population-weighted mean
Population-weighted mean = ∑ (OSDAM8 × POP) / ∑ (POP)

Here, *OSDAM8* refers to the yearly ground-level ozone concentration in each grid cell, *area* is the area of the grid cell calculated with latitude-based correction, and *POP* represents the population in each grid cell, based on the GBD2019.

Table S1. Inputs to the BME dataset include nine chemistry models and observations from TOAR-I and CNEMC. Table based on DeLang et al. (2021)

Model/Observation	Years	Resolution	Experiment	Reference
TOAR-I	1990-2017	7269 monitoring stations	Tropospheric Ozone Assessment Report	(Schultz et al., 2017)
CNEMC	2014-2017	1565 monitoring stations	the Chinese National Environmental Monitoring Center Network	(Lu et al., 2018)
CESM1 CAM4-CHEM	1990-2010	1.9° × 2.5°	CCMI REF-C1SD	(Tilmes et al., 2015)
CESMI WACCM	1990-2010	1.9° × 2.5°	CCMI REF-C1SD	(Marsh et al., 2013; Garcia et al., 2017)
CHASER	1990-2010	2.8° × 2.8°	CCMI REF-C1SD	(Sudo et al., 2002; Watanabe et al., 2011)
GFDL AM3	1990-2014	2° × 2.5°	CCMI REF-C1SD	(Lin et al., 2017)
GFDL AM4	2010-2016	1° × 1.25°	CMIP6 nudged to NCEP wind	(Zhang et al., 2020; Horowitz et al., 2020)
MERRA2-GMI	1990-2017	0.5° × 0.625°	MACCity and GFED-4s emissions	(Ziemke et al., 2019; Strode et al., 2019)
MOCAGE	1990-2016	2° × 2°	CCMI REF-C1SD	(Josse et al., 2004; Teyssèdre et al., 2007)
MRI-ESM1r1	1990-2010	2.8° × 2.8°	CCMI REF-C1SD	(Adachi et al., 2013)
MRI-ESM2.0	2011-2017	2.8° × 2.8°	CMIP6 historical and ssp370	(Yukimoto et al., 2019c)

Table S2. Inputs to the UKML dataset include multiple CMIP6 Chemistry−Climate Models. In situ observations from TOAR-I (1990−2014) and CNEMC (2015−2019) are used as labels for supervised learning. Table based on Sun et al. (2022)

Model[a]	Grids[b]	Hist[c]	Ssp245[d]	Reference
BCC-ESM1	128×64	3		(Wu et al., 2020; Zhang et al., 2018)
MPI-ESM1.2-HAM	192×96	3		(Neubauer et al., 2019)
MPI-ESM1.2-HR	384×192	19	3	(Von Storch et al., 2017; Gutjahr et al., 2019; Schupfner et al., 2019)
UKESM1-0-LL	192×144	3		(Tang et al., 2019; Good et al., 2019; Yool et al., 2020; Sellar et al., 2020; Sellar et al., 2019; Mulcahy et al., 2018; Archibald et al., 2020)
MRI-ESM2.0	128×64	5	5	(Yukimoto et al., 2019a; Yukimoto et al., 2012; Yukimoto et al., 2019b)
NASA-GISS-E2.1-G	144×90	19	20	(Studies, 2018b, a, 2020; Shindell et al., 2013)
NASA-GISS-E2.1-H	144×90	10		
NCAR-CESM2-WACCM	288×192	3		(Danabasoglu, 2019; Gettelman et al., 2019)
NCC-NorESM-MM	288×192	3	2	(Seland et al., 2019; Bentsen et al., 2019)
NOAA-GFDL-ESM4	288×180	1	1	(John et al., 2018; Horowitz et al., 2018; Krasting et al., 2018)
EC-Earth3	120×90	2		(Consortium, 2020)
BCC-CSM2	320×160	1		(Hegglin et al., 2016; Wu et al., 2021)

[a]The names of coupled earth system models are abbreviated.

[b]The planar dimensional spatial resolutions are presented in longitudinal latitudinal grids.

[c]Numbers of simulation ensembles for historical period (1990−2014, using historical experiments)

[d]Numbers of simulation ensembles for recent years (2015−2019, using ssp245 experiments)

Table S3. Inputs to the NJML dataset include meteorology terms, chemical models, landcover and satellite observations. Ground observation from TOAR-I (2003–2019) are used as labels for training. Table based on Liu et al. (2022)

Variable	Years	Resolution	Source	Reference
10m wind speed	2003-2019	30 km/0.25 °	ERA5	(Hersbach et al., 2020)
2m temperature	2003-2019	30 km/0.25 °	ERA5	
Boundary layer height	2003-2019	30 km/0.25 °	ERA5	
Forecast surface roughness	2003-2019	30 km/0.25 °	ERA5	
Mean sea level pressure	2003-2019	30 km/0.25 °	ERA5	
Mean surface downward short-wave radiation flux	2003-2019	30 km/0.25 °	ERA5	
Mean surface downward UV radiation flux	2003-2019	30 km/0.25 °	ERA5	
Total precipitation	2003-2019	30 km/0.25 °	ERA5	
Soil temperature level 1	2003-2019	30 km/0.25 °	ERA5	
Surface latent heat flux	2003-2019	30 km/0.25 °	ERA5	
Surface sensible heat flux	2003-2019	30 km/0.25 °	ERA5	
Total cloud cover	2003-2019	30 km/0.25 °	ERA5	
Total column ozone	2003-2019	30 km/0.25 °	ERA5	
Forecast albedo	2003-2019	30 km/0.25 °	ERA5	
Evaporation	2003-2019	30 km/0.25 °	ERA5	
2m dewpoint temperature	2003-2019	30 km/0.25 °	ERA5	
Volumetric soil water layer 1	2003-2019	30 km/0.25 °	ERA5	
2m temperature one month lag	2003-2019	30 km/0.25 °	ERA5	
2m dewpoint temperature one month lag	2003-2019	30 km/0.25 °	ERA5	

Total precipitation one month lag	2003-2019	30 km/0.25 °	ERA5	
Mean sea level pressure one month lag	2003-2019	30 km/0.25 °	ERA5	
Total aerosol optical depth at 550 nm	2003-2019	80 km/0.75 °	CAMS	(Inness et al., 2019)
Total column hydroxyl radical	2003-2019	80 km/0.75 °	CAMS	
Total column methane	2003-2019	80 km/0.75 °	CAMS	
Total column nitrogen dioxide	2003-2019	80 km/0.75 °	CAMS	
Total column ozone/GEMS Total column ozone	2003-2019	80 km/0.75 °	CAMS	
Particulate matter d < 2.5 µm (PM2.5)	2003-2019	80 km/0.75 °	CAMS	
Total column carbon monoxide	2003-2019	80 km/0.75 °	CAMS	
Total column formaldehyde	2003-2019	80 km/0.75 °	CAMS	
Total column nitrogen monoxide	2003-2019	80 km/0.75 °	CAMS	
Carbon monoxide	2003-2019	80 km/0.75 °	CAMS	
Dust aerosol (0.55 - 0.9 µm) mixing ratio	2003-2019	80 km/0.75 °	CAMS	
Dust aerosol (0.03 - 0.55 µm) mixing ratio	2003-2019	80 km/0.75 °	CAMS	
Dust aerosol (0.9 - 20 µm) mixing ratio	2003-2019	80 km/0.75 °	CAMS	
Hydrophilic organic matter aerosol mixing ratio	2003-2019	80 km/0.75 °	CAMS	
Hydrophobic organic matter aerosol mixing ratio	2003-2019	80 km/0.75 °	CAMS	
Nitrogen monoxide	2003-2019	80 km/0.75 °	CAMS	
SO2 precursor mixing ratio	2003-2019	80 km/0.75 °	CAMS	
Sea salt aerosol (0.5 - 5 µm) mixing ratio	2003-2019	80 km/0.75 °	CAMS	
Sulphur dioxide	2003-2019	80 km/0.75 °	CAMS	
Formaldehyde	2003-2019	80 km/0.75 °	CAMS	
Hydrophilic black carbon aerosol mixing ratio	2003-2019	80 km/0.75 °	CAMS	
Hydrophobic black carbon aerosol mixing ratio	2003-2019	80 km/0.75 °	CAMS	
Hydroxyl radical	2003-2019	80 km/0.75 °	CAMS	
Methane (chemistry)	2003-2019	80 km/0.75 °	CAMS	
Nitrogen dioxide	2003-2019	80 km/0.75 °	CAMS	
Ozone/GEMS Ozone	2003-2019	80 km/0.75 °	CAMS	
Sea salt aerosol (0.03 - 0.5 µm) mixing ratio	2003-2019	80 km/0.75 °	CAMS	
Sea salt aerosol (5 - 20 µm) mixing ratio	2003-2019	80 km/0.75 °	CAMS	
Sulphate aerosol mixing ratio	2003-2019	80 km/0.75 °	CAMS	
Black Carbon Surface Mass Concentration	2003-2019	0.5 °×0.625 °	MERRA2	Global Modeling and Assimilation Office (GMAO) (2015)
Dust Surface Mass Concentration	2003-2019	0.5 °×0.625 °	MERRA2	
Organic Carbon Surface Mass Concentration	2003-2019	0.5 °×0.625 °	MERRA2	

Sea Salt Surface Mass Concentration	2003-2019	0.5 °×0.625 °	MERRA2	
SO4 Surface Mass Concentration	2003-2019	0.5 °×0.625 °	MERRA2	
SO2 Surface Mass Concentration	2003-2019	0.5 °×0.625 °	MERRA2	
Total Aerosol Extinction AOT [550 nm]	2003-2019	0.5 °×0.625 °	MERRA2	
CO Column Burden	2003-2019	0.5 °×0.625 °	MERRA2	
CO Surface Concentration in ppbv	2003-2019	0.5 °×0.625 °	MERRA2	
total_column_ozone	2003-2019	0.5 °×0.625 °	MERRA2	
Nitrogen dioxide	2003-2019	0.9 °×1.25 °	CAM_CHEM	Atmospheric Chemistry Observations & Modeling, National Center for Atmospheric Research, University Corporation for Atmospheric Research (2020)
Ozone	2003-2019	0.9 °×1.25 °	CAM_CHEM	
Nitrogen monoxide	2003-2019	0.9 °×1.25 °	CAM_CHEM	
Population	2003-2019	1 km	Worldpop	(Lloyd et al., 2019)
Elevation mean	2003-2019	1 arc-minute	NOAA/NGDC/ETOPO1	(Amante and Eakins, 2009)
Elevation sd	2003-2019	1 arc-minute	NOAA/NGDC/ETOPO1	
Water percentage	2003-2019	0.05 °	MODIS	(Friedl, 2015)
Shrublands percentage	2003-2019	0.05 °	MODIS	
Savannas percentage	2003-2019	0.05 °	MODIS	
Non Vegetated percentage	2003-2019	0.05 °	MODIS	
Grasslands percentage	2003-2019	0.05 °	MODIS	
Croplands percentage	2003-2019	0.05 °	MODIS	
Forests percentage	2003-2019	0.05 °	MODIS	
Urban percentage	2003-2019	0.05 °	MODIS	
Dark Target and Deep Blue AOD @ 0.55 micron	2003-2019	1 °	CERES	(Doelling et al., 2016)
Tropospheric vertical column densities (VCDs) of NO2	2004-2019	0.25 °	OMI/Aura	(Krotkov et al., 2017)
tropospheric ozone	2004-2019	1 °	OMI/Aura	
Total ozone column	2003-2019	1.25 °×1 °	TCO	(Greg E. Bodeker, 2022)
Total ozone column uncertainty	2003-2019	1.25 °×1 °	TCO	
Leaf area index	2003-2019	0.5 °	MODIS	(Lin et al., 2023)
bc emission	2003-2019	0.5 °	CEDS	DOI: 10.5281/zenodo.3592072
nox emission	2003-2019	0.5 °	CEDS	
co emission	2003-2019	0.5 °	CEDS	
nmvoc emission	2003-2019	0.5 °	CEDS	
ch4 emission	2003-2019	0.5 °	CEDS	
so2 emission	2003-2019	0.5 °	CEDS	
oc emission	2003-2019	0.5 °	CEDS	

Table S4. Satellite observations used for ozone assimilation in TCR-2. Table based on Miyazaki et al. (2020)

Species	Instrument	Period	Data typea	Reference
NO_2 , SO_2	OMI (Aura)	2005-2020	TrC for NO2, PBL for SO2	(Boersma et al., 2011; Boersma et al., 2017; Krotkov et al., 2016; Li et al., 2013)
NO_2	SCIAMACHY (Envisat)	2005-2012	TrC	(Boersma et al., 2004)
NO_2	GOME-2 (Metop-A)	2007-2020	TrC	
Ozone	TES (Aura)	2005-2011	PROF	(Bowman et al., 2006; Herman and Kulawik, 2013)
Ozone, HNO_3	MLS (Aura)	2005-2020	PROF	(Livesey et al., 2017)
CO	MOPITT (Terra)	2005-2020	PROF	(Deeter et al., 2017; Deeter et al., 2013)

[a]Satellite retrievals of atmospheric composition that were assimilated in the chemistry reanalysis. TC is total column, TRC is tropospheric column, PROF is profiles, PC is partial columns. PBL is planetary boundary layer.

Table S5. Satellite observations used for ozone assimilation in CAMS (CAMS global ECMWF Atmospheric Composition Reanalysis 4). Table based on Inness et al. (2019)

Species	Instrument	Period	Data typea	Reference
Ozone, NO2	SCIAMACHY (Envisat)	2003-2012	TC for Ozone, TRC for NO2	(Lerot et al., 2009)
Ozone	MIPAS (Envisat)	2003-2012	PROF	(Von Clarmann et al., 2009)
Ozone	MLS (Aura)	2004-2016	PROF	(Schwartz, 2015)
Ozone, NO2	OMI (Aura)	2004-2020	TC for Ozone, TRC for NO2	(Liu et al., 2010)
Ozone, NO2	GOME-2 (Metop-A)	2007-2020	TC for Ozone, TRC for NO2	(Hao et al., 2014)
Ozone, NO2	GOME-2 (Metop-B)	2013-2020	TC for Ozone, TRC for NO2	
Ozone	SBUV/2 (NOAA-14–NOAA-19)	2003-2020	PC	(Bhartia et al., 1996; Mcpeters et al., 2013)
CO	MOPITT (Terra)	2002-2020	TC	(Deeter et al., 2014)

[a]Satellite retrievals of atmospheric composition that were assimilated in the chemistry reanalysis. TC is total column, TRC is tropospheric column, PROF is profiles, PC is partial columns.

Table S6. Inputs used for ozone assimilation in GEOS. Table based on Qu et al. (2020)

Variable	Years	Source	Reference
NO_2 tropospheric column	2005-2016	OMNO2	(Qu et al., 2020b)
NO_2 tropospheric column	2005-2016	DOMINO	(Qu et al., 2020a)
Meteorological fields	2005-2016	MERRA-2	Global Modeling and Assimilation Office (GMAO) (2015)
Anthropogenic emissionsa	2005-2016	HTAP 2010 inventory version 2	(Janssens-Maenhout et al., 2015)
Anthropogenic emissions	2005-2016	CEDS	(Hoesly et al., 2018)
Nonanthropogenic emissionsb	2005-2016	Follows Qu et al. 2017	(Qu et al., 2017)

[a]Anthropogenic emissions include NO_x, SO_2, NH_3, CO, $NMVOC_S$ (non-methane volatile organic compounds), and primary aerosols.
[b]Nonanthropogenic emissions include biomass burning emissions, NO_x emissions from lightning, and soil NO_x emissions.

Table S7. The regions defined by Hemispheric Transport Air Pollution(HTAP)2 (Koffi et al., 2016)

	Tier 1		Tier 2
01	**GLO***	World	
02	OCN	Non-arctic/Antarctic Ocean	020 Baltic Sea 021 North Atlantic 022 South Atlantic 023 North Pacific 024 South Pacific 025 Indian Ocean 026 Hudson Bay 027 Mediterranean Sea 028 Black and Caspian Sea
03	**NAM***	US+Canada (upto 66 N; polar circle)	031 NE US (all divided on state or provincial lines) 032 SE US 033 NW US 034 SW US 035 E. Canada 036 W. Canada + Alaska up to 66 N.
04	**EUR***	Western + Eastern EU+Turkey (upto 66 N polar circle)	041 NW Europe 042 SW Europe (France follows provinces level at ca. 46 N). 043 Eastern Europe 044 Greece+Turkey+Cyprus
05	**SAS***	South Asia: India, Pakistan, Nepal, Bangadesh, Sri Lanka	051 North India+Pakistan+Nepal+Bangladesh 052 South India+Sri Lanka 053 Indian Himalaya (above an elevation of 1500 m)

06	**EAS***	E Asia: China, Korea, Japan	061 North East China 062 South East China 063 West China +Mongolia (excl. Himalaya) 064 North/South Korea 065 Japan 066 China/Tibet Himalaya (above an elevation of 1500 m)
07	**SEA***	South East Asia	071 Indonesia+Malaysia+Singapore 072 Thailand+Myanmar+Vietnam
08	PAN	Pacific, Australia+ New Zealand	081 Pacific 082 Australia 083 New Zealand
09	NAF	Northern Africa	091 Egypt 092 Rest of Northern Africa
10	**SAF***	Sub Saharan Africa	101 West and Central Africa: Côte d'Ivoire, Angola, Benin, Burkina Faso, Cameroon, Cape Verde, Chad, Congo Brazzaville, Democratic Republic of Congo, Equatorial Guinea, Gambia, Ghana, Guinea, Guinea Bissau, Liberia, Mali, Niger, Nigeria, Senegal, Sierra Leone and Togo 102 East Africa: Burundi, Djibouti, Eritrea, Ethiopia, Kenya, Sudan, Rwanda, Uganda, Somalia and Tanzania. 103 Southern Africa: Angola, Botswana, Lesotho, Madagascar, Malawi, Mauritius, Mozambique, Namibia, South Africa, Swaziland, Tanzania, Zambia, and Zimbabwe
11	**MDE***	Middle East; S. Arabia etc, Iran, Iraq	111 Middle East 112 S.Arabia; Yemen; Oman; etc 113 Iran, Iraq
12	MCA	Mexico, Central America, Caribbean, Guyanas, Venezuela, Columbia	121 Mexico 122 Central America 123 Caribbean 124 Guyanas, Columbia, Venezuela
13	SAM	S. America	131 South Brazil 132 Rest of Brazil 133 Uruguay, Paraguay, Argentina, Chile 134 Peru, Ecuador
14	RBU	Russia, Belarussia, Ukraine, Central Asia	141 Russia West 142 Russia East 143 Belarussia+Ukraine
15	CAS	Central Asia	144 Uzbekistan, Kazakhstan, Kyrgyzstan, Tajikistan, Turkmenistan
16	NPO	Arctic Circle (North of 66 N)+Greenland	150 Arctic (includes ocean and all of Greenland)
17	SPO	Antarctic	160 Antarctic 161 Southern Ocean, south of 60S

*Regions in bold characters defined as priority regions in this paper.

Table S8. Performance evaluation of six datasets for countries (unions) with the most monitors from 2006 to 2015 against TOAR-II observations of OSDMA8. Number is the number of the TOAR-II monitor stations in each country. Density (per km2) is the density of the TOAR-II monitors in each country based on land area. Estimate is the average of the grid estimates for each dataset at the TOAR-II monitor locations in each country. Linear regression R2 and root mean squared error (RMSE) against TOAR-II observations in each country are presented. Country names are in ISO 3166-1 alpha-3, United States of America (USA), Japan (JPN), China (CHN), South Korea (KOR), Canada (CAN), United Kingdom of Great Britain and Northern Ireland (GBR). EU-27 includes Austria, Belgium, Bulgaria, Croatia, Cyprus, Czech Republic, Denmark, Estonia, Finland, France, Germany, Greece, Hungary, Ireland, Italy, Latvia, Lithuania, Luxembourg, Malta, Netherlands, Poland, Portugal, Romania, Slovakia, Slovenia, Spain, Sweden. "Others" is all other countries apart from those listed. The order of countries or regions is determined based on the number of ground monitoring stations.

2006	Country	EU-27	USA	JPN	KOR	CAN	GBR	Others
	Number	1755	717	643	226	198	82	94
	Density	4.39E-04	7.84E-05	1.76E-03	2.32E-03	2.25E-05	3.39E-04	4.53E-06
	TOAR	46.66	51.15	49.33	41.21	39.16	39.38	44.56
BME	R^2	0.55	0.84	0.44	0.04	0.71	0.46	0.73
	RMSE	3.91	2.42	2.73	4.30	2.31	2.66	4.98
	Estimate	46.19	51.24	48.75	43.19	40.35	39.03	42.36
	Lower	40.20	45.26	42.76	37.20	34.37	33.04	36.38
	Upper	52.18	57.23	54.73	49.18	46.34	45.01	48.35
NJML	R^2	0.48	0.59	0.16	0.40	0.50	0.38	0.67
	RMSE	11.58	11.55	4.78	6.23	10.87	10.17	10.01
	Estimate	57.66	62.34	50.19	48.82	50.08	49.15	51.26
	Lower	49.64	54.32	42.17	40.80	42.06	41.13	43.24
	Upper	65.68	70.36	58.21	56.84	58.10	57.17	59.28
UKML	R^2	0.10	0.31	0.36	0.02	0.15	0.06	0.60
	RMSE	11.22	8.47	13.70	22.66	10.22	11.05	8.71
	Estimate	56.13	58.18	61.88	65.27	49.02	49.69	49.19
	Lower	46.56	48.60	52.30	55.69	39.44	40.11	39.61
	Upper	65.71	67.76	71.46	74.85	58.60	59.27	58.77
CAMS	R^2	0.18	0.38	0.00	0.13	0.11	0.05	0.52
	RMSE	7.09	5.93	6.54	7.48	4.65	8.53	7.31
	Estimate	44.00	51.95	45.96	50.88	40.08	32.58	40.57
	Lower	31.51	39.46	33.48	38.39	27.59	20.08	28.08
	Upper	56.49	64.44	58.45	63.37	52.57	45.09	53.06
GEOS	R^2	0.41	0.57	0.43	0.45	0.23	0.07	0.84
	RMSE	6.39	5.02	8.61	17.70	7.94	5.89	4.30
	Estimate	49.83	51.71	55.31	62.40	45.33	44.79	40.42
	Lower	40.81	42.69	46.28	53.32	36.30	35.76	31.36
	Upper	58.85	60.73	64.35	71.49	54.36	53.82	49.47
TCR-2	R^2	0.29	0.36	0.27	0.09	0.26	0.22	0.59
	RMSE	8.99	9.20	9.71	15.95	8.08	5.86	7.07
	Estimate	52.52	57.45	54.84	59.90	46.38	44.39	42.27
	Lower	40.84	45.76	43.16	48.21	34.69	32.70	30.57
	Upper	64.21	69.13	66.52	71.59	58.07	56.09	53.97
2007	Country	EU-27	USA	JPN	KOR	CAN	GBR	Others
	Number	1840	745	751	237	197	50	95
	Density	4.67E-04	8.14E-05	2.06E-03	2.43E-03	2.24E-05	2.07E-04	4.18E-06
	TOAR	44.01	50.23	51.22	42.83	38.13	35.36	42.73
BME	R^2	0.63	0.90	0.55	0.17	0.80	0.11	0.73
	RMSE	3.54	2.16	3.22	4.71	2.15	3.22	6.29
	Estimate	43.40	50.29	49.69	43.19	39.26	34.83	40.85
	Lower	37.69	44.59	43.98	37.48	33.55	29.12	35.14

	Upper	49.11	56.00	55.40	48.90	44.96	40.54	46.56
NJML	R^2	0.57	0.67	0.20	0.29	0.67	0.19	0.71
	RMSE	11.72	11.96	5.30	5.24	11.80	8.87	10.77
	Estimate	55.15	61.80	51.75	49.19	49.83	44.02	51.16
	Lower	46.90	53.55	43.50	40.94	41.58	35.76	42.91
	Upper	63.40	70.05	60.00	57.44	58.08	52.27	59.41
UKML	R^2	0.24	0.47	0.31	0.07	0.36	0.00	0.68
	RMSE	12.83	9.37	11.32	21.06	11.17	14.31	8.45
	Estimate	55.66	58.49	60.79	65.23	49.32	48.98	48.19
	Lower	46.86	49.69	51.99	56.43	40.52	40.18	39.39
	Upper	64.46	67.29	69.59	74.03	58.12	57.78	56.99
CAMS	R^2	0.37	0.65	0.08	0.00	0.38	0.00	0.67
	RMSE	5.90	4.47	6.15	6.27	3.72	5.63	6.62
	Estimate	42.25	50.01	47.13	50.45	39.52	32.37	39.39
	Lower	32.03	39.80	36.92	40.24	29.31	22.15	29.18
	Upper	52.46	60.23	57.34	60.66	49.73	42.59	49.60
GEOS	R^2	0.59	0.56	0.69	0.42	0.57	0.01	0.75
	RMSE	6.39	5.37	8.01	16.86	7.57	6.55	5.63
	Estimate	47.95	50.12	55.29	62.87	44.22	42.14	39.83
	Lower	39.18	41.35	46.50	54.04	35.44	33.35	31.04
	Upper	56.73	58.90	64.08	71.71	53.00	50.93	48.63
TCR-2	R^2	0.52	0.62	0.32	0.10	0.57	0.00	0.62
	RMSE	9.17	8.72	9.15	13.48	8.13	7.47	7.12
	Estimate	50.92	56.57	54.80	58.87	45.77	42.79	42.54
	Lower	40.99	46.64	44.87	48.93	35.84	32.85	32.61
	Upper	60.85	66.50	64.73	68.80	55.71	52.73	52.48
2008	Country	EU-27	USA	JPN	KOR	CAN	GBR	Others
	Number	1962	746	808	255	197	87	113
	Density	4.91E-04	8.16E-05	2.22E-03	2.61E-03	2.24E-05	3.60E-04	4.74E-06
	TOAR	44.20	49.18	51.58	45.17	39.11	37.61	41.39
BME	R^2	0.60	0.89	0.63	0.02	0.75	0.26	0.85
	RMSE	3.23	1.99	2.58	5.12	2.13	3.10	4.93
	Estimate	44.02	48.90	50.64	45.70	40.08	37.65	39.52
	Lower	38.77	43.65	45.40	40.45	34.84	32.41	34.27
	Upper	49.26	54.14	55.89	50.94	45.33	42.90	44.76
NJML	R^2	0.52	0.71	0.30	0.39	0.57	0.30	0.73
	RMSE	9.87	11.00	4.15	4.76	9.52	7.68	9.89
	Estimate	53.82	59.61	51.80	51.32	48.92	45.72	48.20
	Lower	46.51	52.30	44.49	44.00	41.60	38.41	40.88
	Upper	61.13	66.92	59.11	58.63	56.23	53.04	55.51
UKML	R^2	0.24	0.49	0.45	0.08	0.17	0.01	0.74
	RMSE	11.72	10.02	12.87	22.33	10.19	10.99	7.86
	Estimate	55.27	58.04	62.99	68.54	49.25	48.49	46.04
	Lower	46.32	49.09	54.04	59.59	40.30	39.54	37.09
	Upper	64.22	66.99	71.94	77.49	58.20	57.44	54.99
CAMS	R^2	0.20	0.54	0.00	0.02	0.05	0.01	0.62
	RMSE	7.13	4.76	6.75	4.99	4.35	6.31	8.42
	Estimate	38.98	45.73	47.04	50.83	38.51	34.02	35.82
	Lower	30.07	36.82	38.13	41.91	29.60	25.10	26.90
	Upper	47.89	54.65	55.95	59.74	47.42	42.93	44.73
GEOS	R^2	0.65	0.61	0.67	0.12	0.27	0.03	0.79
	RMSE	5.92	4.77	7.75	15.11	6.54	5.81	5.01
	Estimate	47.83	49.35	55.60	63.38	44.10	44.35	38.48

	Lower	39.74	41.26	47.50	55.23	36.01	36.26	30.37
	Upper	55.92	57.43	63.71	71.53	52.19	52.45	46.59
TCR-2	R^2	0.47	0.41	0.26	0.26	0.39	0.01	0.58
	RMSE	8.45	9.06	7.49	10.58	5.72	5.57	7.25
	Estimate	49.84	55.19	51.42	57.82	43.86	42.59	39.13
	Lower	38.15	43.49	39.73	46.13	32.17	30.89	27.42
	Upper	61.53	66.88	63.11	69.52	55.55	54.29	50.83
2009	Country	EU-27	USA	JPN	KOR	CAN	GBR	Others
	Number	2056	767	1115	262	195	87	128
	Density	5.14E-04	8.38E-05	3.06E-03	2.68E-03	2.22E-05	3.60E-04	5.15E-06
	TOAR	44.34	46.77	51.37	48.14	38.08	35.65	40.39
BME	R^2	0.67	0.87	0.41	0.09	0.67	0.39	0.72
	RMSE	3.30	1.93	3.69	4.17	1.81	2.88	5.04
	Estimate	43.98	46.61	50.01	48.23	39.22	35.45	38.15
	Lower	38.61	41.24	44.64	42.87	33.85	30.08	32.78
	Upper	49.35	51.98	55.37	53.60	44.59	40.82	43.51
NJML	R^2	0.59	0.70	0.08	0.35	0.53	0.48	0.69
	RMSE	10.16	10.48	4.55	3.85	9.40	7.63	9.89
	Estimate	53.81	56.59	50.13	53.16	48.22	43.49	47.05
	Lower	46.53	49.31	42.85	45.87	40.94	36.21	39.77
	Upper	61.09	63.87	57.41	60.44	55.50	50.78	54.34
UKML	R^2	0.32	0.47	0.24	0.00	0.06	0.06	0.68
	RMSE	11.45	11.20	9.51	15.81	9.56	12.93	8.29
	Estimate	54.87	56.94	60.31	65.04	47.63	48.59	45.01
	Lower	46.26	48.33	51.70	56.42	39.02	39.98	36.40
	Upper	63.48	65.55	68.92	73.65	56.24	57.20	53.63
CAMS	R^2	0.40	0.54	0.17	0.04	0.04	0.00	0.58
	RMSE	5.60	4.14	7.36	6.42	4.05	6.66	6.43
	Estimate	42.52	46.67	45.84	54.25	38.26	32.05	37.11
	Lower	32.58	36.72	35.90	44.31	28.32	22.11	27.17
	Upper	52.46	56.61	55.78	64.20	48.20	42.00	47.05
GEOS	R^2	0.73	0.51	0.69	0.02	0.44	0.09	0.75
	RMSE	6.50	5.34	5.96	14.42	7.31	6.57	5.96
	Estimate	48.91	48.59	56.11	65.55	44.59	43.35	38.85
	Lower	41.24	40.92	48.43	57.81	36.91	35.68	31.16
	Upper	56.58	56.26	63.80	73.29	52.26	51.03	46.54
TCR-2	R^2	0.57	0.31	0.28	0.10	0.25	0.01	0.57
	RMSE	9.30	10.52	6.73	10.68	8.04	7.05	7.95
	Estimate	51.39	54.80	54.62	60.39	46.07	43.11	42.35
	Lower	41.01	44.42	44.24	50.00	35.68	32.72	31.96
	Upper	61.76	65.18	65.00	70.78	56.45	53.49	52.74
2010	Country	EU-27	USA	JPN	KOR	CAN	GBR	Others
	Number	2119	799	1057	265	200	87	121
	Density	5.30E-04	8.73E-05	2.90E-03	2.72E-03	2.28E-05	3.60E-04	5.07E-06
	TOAR	44.06	48.31	43.52	43.13	38.60	34.09	40.30
BME	R^2	0.72	0.85	0.34	0.12	0.71	0.31	0.60
	RMSE	2.93	2.14	5.47	3.61	2.29	2.41	4.91
	Estimate	43.56	47.98	48.35	45.02	38.97	34.23	38.26
	Lower	38.06	42.49	42.85	39.52	33.48	28.74	32.77
	Upper	49.05	53.48	53.84	50.51	44.47	39.73	43.76
NJML	R^2	0.62	0.65	0.14	0.35	0.63	0.30	0.67
	RMSE	10.72	9.87	6.33	4.56	9.28	8.42	11.02
	Estimate	53.43	57.77	48.06	48.87	48.00	42.60	47.46

	Lower	46.65	50.99	41.28	42.09	41.22	35.82	40.67
	Upper	60.21	64.56	54.84	55.65	54.78	49.39	54.24
UKML	R^2	0.29	0.52	0.08	0.11	0.25	0.17	0.38
	RMSE	12.18	8.96	15.64	19.96	9.36	14.55	10.72
	Estimate	54.64	56.50	58.78	64.14	47.61	48.82	45.75
	Lower	46.02	47.87	50.16	55.52	38.99	40.20	37.13
	Upper	63.26	65.12	67.40	72.76	56.23	57.44	54.38
CAMS	R^2	0.28	0.53	0.10	0.13	0.09	0.08	0.40
	RMSE	7.06	4.38	4.02	4.18	3.80	5.22	7.27
	Estimate	38.32	45.39	45.54	48.51	39.10	30.84	35.08
	Lower	29.18	36.25	36.39	39.37	29.95	21.69	25.94
	Upper	47.47	54.53	54.68	57.66	48.24	39.99	44.23
GEOS	R^2	0.67	0.47	0.27	0.41	0.31	0.42	0.67
	RMSE	7.00	5.14	10.99	14.67	8.29	7.40	6.36
	Estimate	48.31	49.42	54.58	60.98	45.80	42.61	39.32
	Lower	39.72	40.83	45.97	52.33	37.21	34.00	30.70
	Upper	56.90	58.02	63.18	69.62	54.40	51.21	47.93
TCR-2	R^2	0.45	0.43	0.10	0.02	0.39	0.04	0.46
	RMSE	9.06	10.04	10.74	11.91	6.88	6.05	8.29
	Estimate	49.88	55.85	52.47	57.28	44.69	40.07	40.75
	Lower	38.71	44.68	41.30	46.10	33.52	28.89	29.57
	Upper	61.05	67.03	63.64	68.45	55.87	51.25	51.93
2011	Country	EU-27	USA	JPN	KOR	CAN	GBR	Others
	Number	2142	741	822	277	205	93	127
	Density	5.36E-04	8.10E-05	2.26E-03	2.84E-03	2.33E-05	3.84E-04	3.16E-06
	TOAR	44.57	49.27	41.89	43.93	38.31	34.76	39.92
BME	R^2	0.65	0.89	0.29	0.10	0.79	0.31	0.82
	RMSE	3.46	2.09	5.53	3.79	1.67	2.21	3.64
	Estimate	43.94	48.74	46.81	45.64	39.56	35.14	39.34
	Lower	38.53	43.34	41.41	40.24	34.15	29.74	33.93
	Upper	49.34	54.15	52.22	51.05	44.96	40.55	44.74
NJML	R^2	0.57	0.65	0.05	0.29	0.56	0.14	0.76
	RMSE	10.86	9.89	6.53	3.73	8.53	8.81	10.86
	Estimate	54.04	58.90	46.68	48.93	47.57	43.55	47.91
	Lower	46.77	51.62	39.41	41.66	40.30	36.28	40.64
	Upper	61.32	66.17	53.96	56.21	54.85	50.83	55.19
UKML	R^2	0.27	0.46	0.02	0.00	0.04	0.01	0.71
	RMSE	11.50	7.97	20.39	20.30	9.00	14.92	7.94
	Estimate	54.28	56.16	61.95	65.67	46.96	49.67	45.06
	Lower	44.66	46.54	52.32	56.04	37.33	40.04	35.43
	Upper	63.91	65.79	71.58	75.29	56.59	59.30	54.69
CAMS	R^2	0.33	0.42	0.04	0.07	0.10	0.11	0.59
	RMSE	5.96	5.19	5.67	3.93	3.97	5.05	5.71
	Estimate	41.90	49.15	45.80	48.66	38.32	31.49	37.32
	Lower	31.59	38.84	35.49	38.35	28.01	21.17	27.00
	Upper	52.21	59.47	56.11	58.97	48.63	41.81	47.63
GEOS	R^2	0.60	0.54	0.34	0.35	0.30	0.47	0.66
	RMSE	6.30	5.41	11.43	13.32	6.88	6.93	7.14
	Estimate	48.47	50.30	53.52	59.82	45.01	42.60	38.23
	Lower	40.14	41.97	45.19	51.45	36.68	34.26	29.87
	Upper	56.80	58.63	61.86	68.19	53.34	50.94	46.59
TCR-2	R^2	0.46	0.40	0.03	0.20	0.24	0.07	0.62
	RMSE	9.15	9.17	12.54	11.56	7.21	7.59	7.42

	Estimate	50.85	55.73	53.03	57.47	45.58	42.66	40.45
	Lower	40.26	45.14	42.44	46.87	34.98	32.07	29.84
	Upper	61.44	66.32	63.62	68.06	56.17	53.26	51.05
2012	Country	EU-27	USA	JPN	KOR	CAN	GBR	Others
	Number	2527	262	1094	286	207	91	129
	Density	6.32E-04	2.86E-05	3.00E-03	2.93E-03	2.36E-05	3.76E-04	3.14E-06
	TOAR	44.30	53.11	43.63	47.65	39.05	33.77	39.36
BME	R^2	0.73	0.87	0.44	0.11	0.86	0.43	0.78
	RMSE	2.99	3.13	4.96	3.47	1.81	1.84	3.84
	Estimate	44.26	52.15	46.60	48.49	40.60	34.86	39.89
	Lower	38.89	46.79	41.23	43.12	35.23	29.49	34.53
	Upper	49.62	57.51	51.96	53.85	45.96	40.22	45.26
NJML	R^2	0.57	0.61	0.15	0.12	0.72	0.27	0.71
	RMSE	9.88	7.67	6.67	3.18	9.77	8.18	10.20
	Estimate	53.40	60.75	47.31	51.57	49.06	42.36	47.34
	Lower	46.08	53.42	39.99	44.25	41.74	35.03	40.01
	Upper	60.73	68.08	54.64	58.90	56.39	49.69	54.67
UKML	R^2	0.28	0.59	0.34	0.00	0.27	0.01	0.63
	RMSE	11.18	7.01	18.39	17.66	8.71	13.98	8.05
	Estimate	54.30	58.85	60.57	66.08	47.50	47.96	44.51
	Lower	44.55	49.10	50.81	56.33	37.75	38.20	34.75
	Upper	64.06	68.61	70.33	75.84	57.26	57.72	54.27
CAMS	R^2	0.35	0.66	0.03	0.04	0.55	0.10	0.49
	RMSE	7.19	6.75	5.21	3.50	3.31	4.20	7.24
	Estimate	38.65	47.77	45.11	47.98	39.16	32.22	34.57
	Lower	29.67	38.79	36.12	38.99	30.18	23.24	25.59
	Upper	47.63	56.76	54.09	56.97	48.14	41.21	43.55
GEOS	R^2	0.75	0.69	0.34	0.16	0.53	0.28	0.80
	RMSE	6.55	4.88	12.77	14.58	8.55	8.30	5.90
	Estimate	49.04	51.58	55.13	62.74	46.77	43.44	39.48
	Lower	40.17	42.72	46.25	53.82	37.90	34.57	30.59
	Upper	57.90	60.45	64.00	71.66	55.63	52.31	48.36
TCR-2	R^2	0.56	0.64	0.15	0.02	0.55	0.00	0.71
	RMSE	8.49	6.18	10.88	11.44	7.51	7.90	6.58
	Estimate	50.52	54.53	51.88	58.99	46.21	42.14	40.36
	Lower	40.32	44.33	41.69	48.78	36.02	31.94	30.16
	Upper	60.71	64.72	62.08	69.19	56.41	52.34	50.56
2013	Country	EU-27	USA	JPN	KOR	CAN	GBR	Others
	Number	2120	866	1046	291	197	94	172
	Density	5.30E-04	9.47E-04	2.87E-03	2.98E-03	2.24E-05	3.89E-04	4.19E-06
	TOAR	44.07	47.09	44.37	49.23	38.14	36.01	39.78
BME	R^2	0.54	0.86	0.60	0.16	0.71	0.36	0.54
	RMSE	4.18	2.27	4.65	3.41	2.14	1.93	6.19
	Estimate	45.04	46.04	46.58	50.03	39.02	36.59	40.93
	Lower	38.67	39.67	40.21	43.66	32.65	30.22	34.56
	Upper	51.41	52.42	52.95	56.40	45.40	42.97	47.31
NJML	R^2	0.51	0.68	0.25	0.01	0.59	0.02	0.65
	RMSE	9.85	8.60	6.44	3.26	8.52	8.75	10.60
	Estimate	52.39	55.39	47.37	52.86	47.00	44.95	47.03
	Lower	45.71	48.71	40.70	46.19	40.33	38.27	40.36
	Upper	59.06	62.06	54.05	59.54	53.68	51.62	53.71
UKML	R^2	0.23	0.42	0.32	0.00	0.19	0.01	0.66
	RMSE	10.97	10.08	16.90	15.20	9.86	11.51	8.84

	Estimate	53.14	56.21	59.72	65.33	47.81	47.58	45.36
	Lower	44.30	47.37	50.88	56.49	38.96	38.74	36.52
	Upper	61.99	65.06	68.57	74.18	56.65	56.43	54.21
CAMS	R^2	0.35	0.36	0.32	0.00	0.05	0.00	0.51
	RMSE	4.99	5.05	6.85	5.12	4.94	3.73	6.63
	Estimate	42.96	48.15	49.29	54.45	41.94	35.22	38.51
	Lower	33.61	38.80	39.94	45.10	32.59	25.87	29.16
	Upper	52.30	57.50	58.64	63.81	51.29	44.57	47.86
GEOS	R^2	0.52	0.56	0.53	0.41	0.29	0.18	0.76
	RMSE	6.62	5.61	12.77	13.87	8.68	7.43	7.04
	Estimate	49.17	49.82	55.68	63.65	45.98	44.49	40.10
	Lower	40.60	41.24	47.09	55.01	37.40	35.91	31.50
	Upper	57.75	58.39	64.27	72.29	54.56	53.07	48.69
TCR-2	R^2	0.31	0.30	0.24	0.02	0.37	0.13	0.64
	RMSE	8.79	9.60	13.38	11.54	8.15	7.90	7.50
	Estimate	50.13	54.13	54.83	61.52	45.83	44.23	40.91
	Lower	38.92	42.92	43.62	50.29	34.62	33.02	29.68
	Upper	61.34	65.34	66.04	72.74	57.04	55.45	52.13
2014	Country	EU-27	USA	JPN	KOR	CAN	GBR	Others
	Number	1787	856	1127	224	204	94	114
	Density	4.47E-04	9.36E-05	3.09E-03	2.30E-03	2.32E-05	3.89E-04	2.76E-06
	TOAR	43.00	46.44	45.16	51.09	37.37	35.51	36.99
BME	R^2	0.52	0.83	0.22	0.11	0.43	0.42	0.73
	RMSE	5.54	2.42	5.25	5.08	3.19	2.32	5.09
	Estimate	45.04	46.71	46.51	53.82	39.64	36.11	39.87
	Lower	38.49	40.16	39.96	47.27	33.09	29.56	33.32
	Upper	51.59	53.26	53.06	60.37	46.19	42.66	46.42
NJML	R^2	0.56	0.73	0.14	0.01	0.36	0.24	0.62
	RMSE	10.91	8.45	6.44	4.35	8.86	8.04	11.19
	Estimate	51.33	54.26	48.43	55.18	46.11	43.16	46.21
	Lower	44.78	47.71	41.88	48.63	39.56	36.60	39.66
	Upper	57.88	60.81	54.98	61.73	52.66	49.71	52.76
UKML	R^2	0.11	0.55	0.23	0.19	0.08	0.05	0.40
	RMSE	13.56	10.34	16.71	14.55	10.81	12.65	10.86
	Estimate	53.40	55.77	60.25	66.63	47.97	47.82	44.87
	Lower	44.21	46.58	51.06	57.44	38.78	38.63	35.68
	Upper	62.60	64.96	69.45	75.82	57.16	57.01	54.06
CAMS	R^2	0.22	0.32	0.18	0.15	0.03	0.05	0.41
	RMSE	5.87	5.28	4.82	4.39	4.86	5.36	7.28
	Estimate	42.40	47.12	47.39	55.75	40.77	33.84	38.41
	Lower	33.05	37.77	38.04	46.39	31.42	24.48	29.06
	Upper	51.75	56.47	56.74	65.11	50.12	43.20	47.76
GEOS	R^2	0.34	0.51	0.29	0.07	0.37	0.02	0.62
	RMSE	8.59	5.70	12.07	13.30	7.86	10.33	6.73
	Estimate	48.89	48.86	55.48	66.06	44.12	44.28	37.29
	Lower	39.54	39.51	46.11	56.60	34.77	34.93	27.90
	Upper	58.24	58.21	64.85	75.52	53.48	53.64	46.68
TCR-2	R^2	0.19	0.34	0.07	0.10	0.32	0.04	0.52
	RMSE	10.70	9.87	12.73	9.12	7.64	9.08	8.38
	Estimate	50.12	53.53	54.56	61.03	44.17	43.10	40.36
	Lower	38.50	41.91	42.94	49.39	32.55	31.47	28.72
	Upper	61.74	65.15	66.19	72.67	55.80	54.73	52.00
2015	Country	EU-27	CHN	JPN	USA	KOR	CAN	Others

	Number	1849	1427	1123	875	312	204	267
	Density	4.63E-04	1.52E-04	3.08E-03	9.57E-05	3.20E-03	2.32E-05	6.10E-06
	TOAR	45.64	50.39	44.03	46.41	50.40	38.58	38.24
BME	R^2	0.81	0.65	0.04	0.86	0.11	0.54	0.57
	RMSE	2.84	5.01	4.93	2.47	4.37	2.55	4.83
	Estimate	44.03	48.01	44.20	44.51	51.84	38.56	39.13
	Lower	37.66	41.65	37.84	38.15	45.47	32.19	32.77
	Upper	50.39	54.38	50.57	50.88	58.21	44.93	45.50
NJML	R^2	0.74	0.61	0.02	0.68	0.07	0.35	0.53
	RMSE	9.51	5.56	6.09	8.30	3.49	7.68	9.86
	Estimate	53.12	51.53	47.57	53.79	55.34	46.59	46.02
	Lower	44.61	43.02	39.06	45.28	46.83	38.08	37.51
	Upper	61.63	60.04	56.08	62.30	63.85	55.10	54.53
UKML	R^2	0.29	0.31	0.07	0.54	0.00	0.18	0.44
	RMSE	10.99	17.77	15.87	8.44	13.25	10.39	12.20
	Estimate	54.02	65.56	59.26	53.46	65.11	49.38	48.69
	Lower	41.36	52.90	46.61	40.80	52.46	36.72	36.04
	Upper	66.67	78.21	71.92	66.12	77.77	62.04	61.35
CAMS	R^2	0.43	0.21	0.24	0.25	0.01	0.10	0.42
	RMSE	4.97	8.96	4.42	5.78	5.56	3.84	6.51
	Estimate	43.73	54.46	46.70	47.42	57.20	40.90	38.10
	Lower	32.37	43.10	35.34	36.06	45.84	29.54	26.74
	Upper	55.09	65.82	58.06	58.78	68.56	52.26	49.46
GEOS	R^2	0.59	0.41	0.28	0.58	0.42	0.30	0.60
	RMSE	6.71	11.67	12.30	6.04	13.46	7.09	7.93
	Estimate	48.80	59.22	55.52	48.98	65.45	44.92	41.49
	Lower	38.37	48.78	45.09	38.55	54.99	34.49	31.05
	Upper	59.23	69.66	65.95	59.41	75.92	55.36	51.93
TCR-2	R^2	0.52	0.25	0.04	0.27	0.36	0.39	0.61
	RMSE	8.37	15.18	13.67	9.64	11.39	7.01	9.00
	Estimate	50.46	62.05	55.31	53.05	63.13	45.23	43.66
	Lower	37.28	48.87	42.13	39.87	49.95	32.05	30.47
	Upper	63.64	75.23	68.49	66.22	76.32	58.42	56.84

Table S9. Population weighted trend of six datasets over priority regions (NAM, EUR, SAS, EAS, SEA, SAF, MDE) from 2006 to 2016 with 95% confidence intervals and p-values.

Dataset	Region	Slope(ppb/year)	LowerCI(ppb/year)	UpperCI(ppb/year)	pValue
BME	NAM	-0.47	-0.70	-0.23	0.00
	EUR	-0.08	-0.26	0.10	0.34
	SAS	0.52	0.06	0.97	0.03
	EAS	-0.87	-1.39	-0.35	0.00
	SEA	0.31	-0.18	0.79	0.19
	SAF	0.23	-0.47	0.93	0.47
	MDE	0.00	-0.47	0.47	0.99
NJML	NAM	-1.14	-1.64	-0.64	0.00
	EUR	-0.41	-0.63	-0.19	0.00

	SAS	-0.34	-0.53	-0.15	0.00
	EAS	-0.20	-0.37	-0.03	0.03
	SEA	0.00	-0.24	0.24	0.99
	SAF	0.03	-0.05	0.11	0.43
	MDE	-0.30	-0.40	-0.20	0.00
UKML	NAM	-0.50	-0.63	-0.37	0.00
	EUR	-0.20	-0.27	-0.13	0.00
	SAS	0.78	0.67	0.90	0.00
	EAS	0.30	0.05	0.55	0.02
	SEA	0.34	0.19	0.49	0.00
	SAF	0.20	0.08	0.31	0.00
	MDE	0.02	-0.03	0.07	0.38
CAMS	NAM	-0.15	-0.77	0.47	0.61
	EUR	0.02	-0.47	0.51	0.92
	SAS	0.19	-0.04	0.42	0.09
	EAS	0.11	-0.41	0.63	0.64
	SEA	-0.05	-0.44	0.34	0.78
	SAF	-0.05	-0.35	0.25	0.72
	MDE	0.09	-0.42	0.59	0.71
GEOS	NAM	-0.10	-0.34	0.14	0.36
	EUR	0.07	-0.06	0.19	0.26
	SAS	0.15	-0.07	0.37	0.16
	EAS	0.07	-0.14	0.28	0.45
	SEA	-0.02	-0.27	0.24	0.89
	SAF	0.00	-0.11	0.12	0.99
	MDE	0.16	-0.01	0.32	0.06
TCR-2	NAM	-0.36	-0.52	-0.20	0.00
	EUR	-0.15	-0.26	-0.03	0.02
	SAS	0.48	0.31	0.66	0.00
	EAS	0.27	0.06	0.48	0.02
	SEA	0.37	0.03	0.72	0.04
	SAF	0.12	0.02	0.23	0.03
	MDE	0.16	0.02	0.30	0.03

Table S10. The share of population exposed to ozone above particular thresholds in each world region for each year (from 2006 to 2016). The unit of thresholds is ppb and unit of share is percentage (%).

2006		EAS	EUR	MDE	NAM	SAF	SAS	SEA	GLO
BME	>30	100[99,100]	100[96,100]	100[100,100]	100[97,100]	93[76,100]	100[99,100]	77[51,89]	95[86,99]
	>50	58[36,90]	19[3,60]	74[39,88]	47[13,74]	10[3,32]	80[57,94]	0[0,8]	42[25,64]
	>70	0[0,3]	0[0,1]	0[0,0]	1[0,1]	0[0,0]	0[0,8]	0[0,0]	0[0,3]
NJML	>30	100[100,100]	100[100,100]	100[100,100]	100[100,100]	100[94,100]	100[100,100]	93[78,100]	99[95,100]
	>50	79[48,99]	92[53,100]	100[85,100]	91[81,100]	35[6,73]	98[83,100]	32[9,61]	74[49,89]
	>70	3[0,13]	2[1,8]	17[2,62]	9[2,54]	0[0,0]	14[0,53]	0[0,0]	6[0,25]
UKML	>30	100[100,100]	100[100,100]	100[98,100]	100[100,100]	96[54,100]	100[100,100]	98[77,100]	97[86,100]
	>50	100[71,100]	88[26,100]	91[76,98]	89[32,99]	11[1,48]	96[60,100]	30[2,75]	69[39,84]
	>70	20[9,64]	0[0,18]	0[0,64]	0[0,25]	0[0,1]	7[0,55]	0[0,1]	6[2,35]
CAMS	>30	100[96,100]	98[64,100]	100[99,100]	100[88,100]	86[33,100]	100[99,100]	91[59,98]	94[72,100]
	>50	71[8,99]	21[0,80]	91[40,100]	62[17,97]	7[1,51]	95[49,100]	29[9,76]	52[17,81]
	>70	3[0,23]	0[0,3]	9[5,68]	4[0,29]	0[0,1]	13[0,70]	7[6,12]	5[1,28]
GEOS	>30	100[100,100]	100[100,100]	100[100,100]	100[100,100]	99[80,100]	100[100,100]	94[79,98]	98[90,100]
	>50	95[67,100]	55[3,99]	100[76,100]	71[8,100]	13[3,65]	92[57,99]	5[0,45]	61[33,83]
	>70	5[0,51]	0[0,0]	4[0,42]	0[0,0]	0[0,1]	0[0,24]	0[0,0]	1[0,18]
TCR-2	>30	100[100,100]	100[99,100]	100[100,100]	100[99,100]	97[72,100]	100[99,100]	86[45,99]	97[85,100]
	>50	94[66,100]	79[14,100]	93[80,100]	89[47,100]	18[4,82]	87[60,99]	20[1,57]	65[37,88]
	>70	37[1,76]	0[0,21]	33[0,85]	3[0,56]	1[0,6]	3[0,72]	0[0,1]	11[0,44]
2007		EAS	EUR	MDE	NAM	SAF	SAS	SEA	GLO
BME	>30	100[100,100]	97[88,99]	100[100,100]	99[94,100]	97[84,100]	100[99,100]	86[66,95]	96[88,99]
	>50	77[52,94]	20[3,48]	80[61,91]	42[16,73]	13[2,39]	86[68,94]	1[0,9]	48[32,65]
	>70	17[6,30]	0[0,0]	0[0,8]	1[0,1]	0[0,0]	0[0,15]	0[0,0]	4[1,10]
NJML	>30	100[100,100]	100[100,100]	100[100,100]	100[100,100]	100[95,100]	100[100,100]	85[72,100]	99[96,100]
	>50	79[38,99]	80[38,97]	99[83,100]	91[78,99]	39[3,79]	98[78,100]	31[2,60]	73[44,91]
	>70	4[2,15]	0[0,10]	18[2,61]	12[1,59]	0[0,0]	10[0,49]	0[0,0]	5[1,25]
UKML	>30	100[100,100]	100[100,100]	100[100,100]	100[100,100]	98[62,100]	100[100,100]	96[75,100]	98[88,100]
	>50	100[84,100]	81[35,99]	92[78,98]	90[46,99]	11[1,45]	97[73,100]	36[1,62]	69[47,82]
	>70	24[13,57]	0[0,10]	0[0,53]	0[0,17]	0[0,0]	15[0,57]	0[0,0]	9[3,32]
CAMS	>30	100[100,100]	92[56,100]	100[100,100]	100[88,100]	91[43,100]	100[100,100]	87[68,96]	95[76,99]
	>50	77[19,100]	20[1,56]	88[43,100]	52[17,87]	13[0,42]	95[56,100]	28[8,67]	53[21,76]
	>70	0[0,18]	0[0,1]	8[4,41]	4[0,16]	0[0,0]	8[0,55]	7[6,8]	3[1,21]
GEOS	>30	100[100,100]	100[100,100]	100[100,100]	100[100,100]	98[82,100]	100[100,100]	84[62,97]	97[89,100]
	>50	97[66,100]	40[2,87]	99[76,100]	58[5,99]	11[2,66]	94[59,99]	3[0,35]	60[33,82]
	>70	3[0,51]	0[0,0]	4[0,47]	0[0,0]	0[0,0]	0[0,23]	0[0,0]	1[0,18]
TCR-2	>30	100[100,100]	100[99,100]	100[100,100]	100[99,100]	99[82,100]	100[99,100]	79[39,97]	97[87,100]
	>50	93[71,100]	71[19,99]	93[82,100]	87[52,99]	20[6,77]	85[67,98]	7[1,34]	63[41,85]
	>70	37[2,66]	0[0,14]	34[1,80]	2[0,46]	0[0,4]	3[0,59]	0[0,0]	11[0,36]
2008		EAS	EUR	MDE	NAM	SAF	SAS	SEA	GLO
BME	>30	100[100,100]	99[95,100]	100[100,100]	100[97,100]	89[69,98]	100[99,100]	76[39,87]	94[84,98]
	>50	77[50,93]	15[3,40]	84[74,91]	30[10,60]	4[1,16]	87[78,93]	0[0,7]	45[30,57]
	>70	1[0,13]	0[0,0]	4[0,19]	1[1,2]	0[0,0]	1[0,26]	0[0,0]	1[0,6]
NJML	>30	100[100,100]	100[100,100]	100[100,100]	100[100,100]	100[96,100]	100[100,100]	90[77,100]	99[96,100]
	>50	77[41,98]	78[26,99]	100[87,100]	89[72,100]	39[7,73]	98[78,100]	25[0,54]	71[44,89]
	>70	3[2,8]	0[0,4]	9[2,58]	4[2,27]	0[0,1]	8[0,31]	0[0,0]	4[1,16]
UKML	>30	100[100,100]	100[100,100]	100[100,100]	100[100,100]	98[61,100]	100[100,100]	98[80,100]	97[87,100]
	>50	100[77,100]	76[31,100]	89[77,99]	87[35,99]	10[1,45]	98[73,100]	30[5,68]	68[45,83]
	>70	33[21,63]	0[0,11]	0[0,59]	0[0,21]	0[0,1]	28[0,62]	0[0,0]	14[5,34]
CAMS	>30	100[100,100]	97[55,100]	100[100,100]	100[89,100]	91[45,99]	100[100,100]	88[73,97]	94[76,99]
	>50	66[10,97]	2[0,23]	80[27,98]	14[0,62]	9[0,26]	94[61,99]	21[7,55]	45[18,65]
	>70	0[0,4]	0[0,0]	5[3,9]	0[0,0]	0[0,0]	4[0,36]	6[5,7]	2[1,10]
GEOS	>30	100[100,100]	100[100,100]	100[100,100]	100[100,100]	99[90,100]	100[100,100]	92[73,98]	97[90,100]
	>50	94[71,99]	36[1,92]	99[78,100]	46[5,99]	16[3,62]	93[57,99]	0[0,24]	58[34,79]
	>70	2[0,51]	0[0,0]	0[0,33]	0[0,0]	0[0,1]	0[0,13]	0[0,0]	0[0,15]
TCR-2	>30	100[98,100]	100[98,100]	100[100,100]	100[99,100]	96[68,100]	100[98,100]	83[45,98]	96[82,100]
	>50	89[58,99]	70[12,99]	93[80,100]	82[40,99]	20[4,74]	87[62,99]	4[1,36]	61[35,84]
	>70	32[7,65]	0[0,18]	33[0,83]	1[0,47]	0[0,5]	6[0,70]	0[0,1]	10[1,40]
2009		EAS	EUR	MDE	NAM	SAF	SAS	SEA	GLO
BME	>30	100[100,100]	98[90,100]	100[99,100]	100[95,100]	70[45,88]	99[99,100]	80[44,94]	90[80,97]
	>50	77[50,94]	18[3,43]	79[64,88]	13[5,46]	1[0,9]	85[64,91]	0[0,7]	45[30,57]
	>70	6[0,20]	0[0,0]	0[0,15]	0[0,1]	0[0,0]	0[0,5]	0[0,0]	1[0,6]
NJML	>30	100[100,100]	100[100,100]	100[100,100]	100[100,100]	100[95,100]	100[100,100]	90[77,100]	99[96,100]
	>50	79[42,98]	77[29,91]	99[85,100]	88[46,99]	36[6,69]	99[88,100]	33[7,57]	72[46,87]
	>70	4[2,11]	0[0,5]	5[2,55]	3[1,9]	0[0,0]	19[1,46]	0[0,0]	7[1,20]
UKML	>30	100[100,100]	100[100,100]	100[100,100]	100[100,100]	98[61,100]	100[100,100]	98[80,100]	97[87,100]
	>50	100[82,100]	79[25,99]	92[75,99]	85[25,97]	10[1,44]	98[77,100]	34[0,73]	68[45,82]
	>70	20[12,60]	0[0,8]	0[0,47]	0[0,14]	0[0,0]	30[2,62]	0[0,0]	11[3,33]
CAMS	>30	100[97,100]	92[62,100]	100[100,100]	100[82,100]	91[46,99]	100[100,100]	88[73,97]	94[76,99]
	>50	73[22,97]	15[0,56]	88[42,99]	29[6,76]	7[1,39]	95[63,100]	31[9,65]	50[23,73]

	>70	0[0,17]	0[0,0]	7[3,34]	4[0,6]	0[0,1]	10[1,56]	7[6,8]	3[1,20]
GEOS	>30	100[100,100]	100[100,100]	100[100,100]	100[100,100]	99[90,100]	100[100,100]	92[73,98]	97[90,100]
	>50	96[69,100]	44[2,90]	98[78,100]	37[1,99]	11[2,58]	97[72,99]	2[0,33]	59[36,79]
	>70	3[0,50]	0[0,0]	3[0,37]	0[0,0]	0[0,0]	1[0,48]	0[0,0]	1[0,23]
TCR-2	>30	100[100,100]	100[100,100]	100[100,100]	100[100,100]	98[73,100]	100[99,100]	83[45,98]	96[83,100]
	>50	93[70,100]	75[16,99]	93[81,100]	86[37,99]	16[5,71]	89[64,99]	13[1,42]	63[35,85]
	>70	36[3,66]	0[0,14]	34[0,79]	0[0,33]	1[0,5]	10[0,62]	0[0,3]	12[1,37]
2010		EAS	EUR	MDE	NAM	SAF	SAS	SEA	GLO
BME	>30	100[100,100]	97[87,100]	99[97,100]	99[95,100]	81[55,95]	99[95,100]	72[29,92]	92[80,98]
	>50	66[39,91]	11[1,37]	62[30,80]	27[4,61]	1[0,12]	74[50,85]	0[0,3]	39[22,56]
	>70	0[0,6]	0[0,0]	0[0,0]	0[0,1]	0[0,0]	0[0,3]	0[0,0]	0[0,2]
NJML	>30	100[100,100]	100[100,100]	100[100,100]	100[100,100]	100[98,100]	100[100,100]	82[77,97]	99[97,100]
	>50	63[35,92]	73[30,89]	99[87,100]	88[66,98]	34[8,74]	98[82,99]	21[2,50]	68[44,86]
	>70	3[2,5]	0[0,3]	8[2,54]	3[0,15]	0[0,0]	9[0,32]	0[0,0]	4[1,15]
UKML	>30	100[100,100]	100[100,100]	100[100,100]	100[100,100]	97[61,100]	100[100,100]	96[76,100]	98[87,100]
	>50	98[77,100]	80[23,99]	93[78,98]	82[23,98]	8[2,47]	98[79,100]	28[0,67]	67[45,83]
	>70	32[18,58]	0[0,5]	0[0,48]	0[0,4]	0[0,1]	29[5,66]	0[0,0]	14[5,32]
CAMS	>30	100[100,100]	88[41,100]	100[100,100]	100[91,100]	74[38,98]	100[100,100]	84[68,93]	89[74,98]
	>50	32[4,93]	2[0,23]	76[29,98]	15[0,71]	4[0,25]	96[66,100]	23[7,57]	37[18,66]
	>70	0[0,1]	0[0,0]	6[4,18]	0[0,0]	0[0,0]	25[1,51]	5[3,6]	6[1,13]
GEOS	>30	100[100,100]	100[100,100]	100[100,100]	100[100,100]	99[90,100]	100[100,100]	81[58,96]	97[91,100]
	>50	88[62,100]	35[3,89]	100[82,100]	51[0,100]	17[3,69]	95[66,99]	2[0,35]	58[34,83]
	>70	4[0,39]	0[0,0]	4[0,50]	0[0,0]	0[0,0]	0[0,40]	0[0,0]	1[0,20]
TCR-2	>30	100[100,100]	100[93,100]	100[100,100]	100[99,100]	98[71,100]	100[97,100]	76[36,99]	96[83,100]
	>50	93[63,100]	64[10,97]	92[81,100]	85[41,100]	18[4,82]	86[59,99]	14[1,39]	63[35,86]
	>70	38[2,69]	0[0,19]	41[2,84]	0[0,50]	1[0,6]	7[0,68]	0[0,3]	12[1,41]
2011		EAS	EUR	MDE	NAM	SAF	SAS	SEA	GLO
BME	>30	100[99,100]	99[89,100]	99[98,100]	99[95,100]	94[82,100]	100[100,100]	81[60,89]	96[88,99]
	>50	69[38,90]	15[2,40]	73[42,87]	27[8,64]	9[0,32]	90[73,99]	8[0,25]	46[28,64]
	>70	0[0,4]	0[0,0]	0[0,0]	0[0,1]	0[0,0]	2[0,21]	0[0,0]	1[0,6]
NJML	>30	100[100,100]	100[100,100]	100[100,100]	100[100,100]	100[98,100]	100[100,100]	88[77,100]	99[96,100]
	>50	73[42,98]	76[30,93]	99[84,100]	88[68,98]	38[8,77]	99[83,99]	25[0,54]	70[45,89]
	>70	3[2,8]	0[0,5]	5[1,56]	4[0,18]	0[0,1]	9[0,35]	0[0,0]	4[1,17]
UKML	>30	100[100,100]	100[100,100]	100[100,100]	100[99,100]	97[57,100]	100[100,100]	97[78,100]	98[86,100]
	>50	100[79,100]	76[15,100]	94[70,99]	85[19,99]	12[1,53]	99[75,100]	44[15,77]	70[43,85]
	>70	29[18,74]	0[0,11]	0[0,66]	0[0,13]	0[0,1]	35[8,73]	0[0,13]	15[6,40]
CAMS	>30	100[100,100]	92[54,100]	100[100,100]	100[87,100]	92[48,99]	100[100,100]	89[73,97]	94[77,99]
	>50	67[19,100]	14[0,53]	92[48,100]	55[7,87]	12[1,48]	97[62,100]	28[8,73]	51[22,77]
	>70	3[0,18]	0[0,0]	10[4,48]	0[0,7]	0[0,1]	9[0,61]	7[5,8]	4[1,22]
GEOS	>30	100[100,100]	100[100,100]	100[100,100]	100[100,100]	99[86,100]	100[100,100]	90[72,98]	98[91,100]
	>50	97[65,99]	39[1,89]	100[76,100]	55[3,100]	15[4,64]	95[65,99]	0[0,32]	59[34,80]
	>70	2[0,44]	0[0,0]	2[0,40]	0[0,0]	0[0,1]	1[0,34]	0[0,0]	1[0,19]
TCR-2	>30	100[100,100]	100[100,100]	100[100,100]	100[99,100]	98[78,100]	100[99,100]	82[42,98]	97[86,100]
	>50	94[68,100]	69[9,100]	96[81,100]	86[45,99]	20[5,78]	90[74,99]	11[0,42]	64[40,86]
	>70	40[2,69]	0[0,9]	35[1,82]	0[0,45]	0[0,5]	17[0,74]	0[0,0]	14[1,41]
2012		EAS	EUR	MDE	NAM	SAF	SAS	SEA	GLO
BME	>30	100[99,100]	98[86,100]	100[99,100]	99[95,100]	94[82,100]	100[100,100]	81[60,89]	96[88,99]
	>50	61[25,87]	21[3,46]	73[61,92]	35[8,72]	9[0,32]	90[73,99]	8[0,25]	46[28,64]
	>70	0[0,3]	0[0,0]	0[0,3]	0[0,2]	0[0,0]	2[0,21]	0[0,0]	1[0,6]
NJML	>30	100[100,100]	100[100,100]	100[100,100]	100[100,100]	100[98,100]	100[100,100]	88[77,100]	99[96,100]
	>50	69[44,96]	73[26,90]	99[87,100]	91[74,99]	38[8,77]	99[83,100]	25[0,54]	70[45,89]
	>70	3[2,16]	0[0,4]	8[2,59]	3[1,32]	0[0,1]	9[0,35]	0[0,0]	4[1,17]
UKML	>30	100[100,100]	100[100,100]	100[99,100]	100[100,100]	97[54,100]	100[100,100]	97[78,100]	98[86,100]
	>50	100[86,100]	75[11,100]	93[65,99]	85[16,100]	12[1,52]	99[75,100]	43[15,77]	69[43,85]
	>70	33[21,81]	0[0,10]	0[0,55]	0[0,13]	0[0,1]	35[8,73]	0[0,13]	15[6,40]
CAMS	>30	100[100,100]	90[49,100]	100[100,100]	100[91,100]	92[48,99]	100[100,100]	89[73,97]	94[76,99]
	>50	34[6,92]	1[0,25]	83[29,99]	14[0,76]	12[1,48]	96[62,100]	28[8,73]	51[22,77]
	>70	0[0,2]	0[0,0]	5[3,13]	0[0,0]	0[0,1]	9[0,61]	7[5,8]	4[1,15]
GEOS	>30	100[100,100]	100[100,100]	100[100,100]	100[100,100]	99[86,100]	100[100,100]	90[72,98]	98[91,100]
	>50	96[67,100]	47[3,96]	100[86,100]	55[3,100]	15[4,64]	95[65,99]	1[0,32]	59[34,80]
	>70	6[0,58]	0[0,0]	13[0,72]	0[0,0]	0[0,1]	1[0,34]	0[0,0]	1[0,19]
TCR-2	>30	100[100,100]	100[99,100]	100[100,100]	100[99,100]	98[78,100]	100[99,100]	82[42,98]	97[86,100]
	>50	95[74,100]	68[17,99]	96[86,100]	84[45,99]	20[5,78]	90[74,99]	11[0,42]	64[40,86]
	>70	43[9,70]	0[0,13]	45[6,85]	0[0,45]	0[0,5]	17[0,74]	0[0,0]	15[1,41]
2013		EAS	EUR	MDE	NAM	SAF	SAS	SEA	GLO
BME	>30	99[95,100]	100[90,100]	100[99,100]	99[94,100]	93[76,100]	100[99,100]	79[52,91]	96[85,99]
	>50	35[10,74]	22[3,53]	74[44,88]	12[4,54]	1[0,22]	85[59,94]	0[0,14]	36[18,58]
	>70	0[0,1]	0[0,0]	0[0,1]	0[0,1]	0[0,0]	0[0,19]	0[0,0]	0[0,5]
NJML	>30	100[100,100]	100[100,100]	100[100,100]	100[100,100]	100[99,100]	100[100,100]	89[77,100]	99[96,100]
	>50	73[48,96]	73[21,96]	99[86,100]	85[34,97]	30[6,74]	98[70,100]	26[7,60]	69[42,88]
	>70	3[1,13]	0[0,3]	5[1,49]	2[1,7]	0[0,1]	5[0,22]	0[0,0]	2[0,18]
UKML	>30	100[100,100]	100[100,100]	100[100,100]	100[100,100]	96[54,100]	100[100,100]	98[78,100]	98[86,100]
	>50	100[85,100]	69[15,100]	92[77,99]	85[19,99]	10[0,47]	100[84,100]	43[11,78]	69[43,85]
	>70	35[22,74]	0[0,6]	0[0,60]	0[0,10]	0[0,0]	35[8,72]	0[0,10]	15[6,40]
CAMS	>30	100[100,100]	100[73,100]	100[100,100]	100[97,100]	86[45,99]	100[100,100]	89[68,97]	90[76,99]

	>50	74[26,100]	11[0,59]	87[45,99]	45[2,94]	5[0,28]	96[68,100]	19[8,54]	50[25,74]
	>70	1[0,17]	0[0,0]	10[4,37]	0[0,1]	0[0,0]	14[1,57]	5[5,7]	4[1,15]
GEOS	>30	100[100,100]	100[100,100]	100[100,100]	100[100,100]	98[84,100]	100[100,100]	88[67,97]	97[89,100]
	>50	92[63,100]	43[2,96]	100[79,100]	46[1,100]	14[3,61]	95[62,99]	1[0,52]	62[35,84]
	>70	1[0,44]	0[0,0]	7[0,50]	0[0,0]	0[0,1]	0[0,30]	0[0,0]	2[0,28]
TCR-2	>30	100[100,100]	100[99,100]	100[100,100]	100[99,100]	97[71,100]	100[99,100]	87[48,99]	97[85,100]
	>50	95[72,100]	71[5,100]	96[79,100]	83[23,100]	17[4,72]	90[62,99]	16[1,43]	65[44,85]
	>70	40[5,78]	0[0,13]	40[3,86]	0[0,38]	1[1,5]	13[0,74]	0[0,1]	15[2,41]
2014		EAS	EUR	MDE	NAM	SAF	SAS	SEA	GLO
BME	>30	99[95,100]	99[86,100]	100[99,100]	99[93,100]	100[96,100]	100[100,99]	87[67,96]	96[88,99]
	>50	46[15,78]	20[1,57]	80[44,97]	11[3,55]	27[2,70]	96[81,99]	8[0,34]	46[25,69]
	>70	1[0,3]	0[0,0]	0[0,4]	0[0,1]	0[0,0]	8[0,50]	0[0,0]	2[0,13]
NJML	>30	100[100,100]	100[100,100]	100[100,100]	100[100,100]	100[98,100]	100[100,100]	92[81,100]	99[97,100]
	>50	65[39,90]	65[17,88]	99[80,100]	83[33,96]	29[7,68]	99[81,100]	31[7,56]	66[42,84]
	>70	4[2,10]	0[0,0]	4[1,34]	2[0,4]	0[0,0]	9[2,26]	0[0,0]	3[1,11]
UKML	>30	100[100,100]	100[100,100]	100[100,100]	100[100,100]	99[64,100]	100[100,100]	98[81,100]	98[88,100]
	>50	100[86,100]	72[12,99]	94[78,100]	83[12,99]	11[1,51]	100[84,100]	46[4,77]	69[46,85]
	>70	32[19,72]	0[0,4]	0[0,65]	0[0,8]	0[0,0]	41[19,73]	0[0,0]	17[8,38]
CAMS	>30	100[100,100]	99[70,100]	100[100,100]	100[94,100]	83[38,99]	100[100,100]	91[75,97]	93[78,99]
	>50	69[34,99]	9[0,53]	89[37,99]	39[3,88]	7[0,28]	92[58,99]	27[9,68]	48[24,72]
	>70	0[0,22]	0[0,0]	9[4,30]	0[0,0]	0[0,0]	12[0,50]	6[5,8]	4[1,19]
GEOS	>30	100[100,100]	100[100,100]	100[100,100]	100[100,100]	99[82,100]	100[100,100]	90[72,98]	98[90,100]
	>50	94[70,100]	47[1,98]	100[79,100]	44[0,98]	13[3,64]	96[66,99]	2[0,46]	59[35,83]
	>70	23[0,61]	0[0,0]	6[0,51]	0[0,0]	0[0,1]	0[0,44]	0[0,0]	5[0,25]
TCR-2	>30	100[100,100]	100[99,100]	100[100,100]	100[99,100]	97[74,100]	100[99,100]	91[55,99]	98[87,100]
	>50	95[77,100]	70[6,100]	94[83,100]	81[28,99]	16[3,78]	91[72,99]	22[1,58]	64[41,88]
	>70	48[15,82]	0[0,11]	41[2,85]	0[0,36]	1[0,4]	15[0,76]	0[0,1]	16[3,44]
2015		EAS	EUR	MDE	NAM	SAF	SAS	SEA	GLO
BME	>30	99[95,100]	97[83,100]	100[100,100]	99[93,100]	91[73,99]	100[99,100]	85[59,94]	96[84,99]
	>50	47[21,77]	20[3,56]	82[44,96]	14[3,54]	2[0,34]	93[78,98]	7[2,28]	40[25,63]
	>70	0[0,3]	0[0,0]	0[0,6]	0[0,1]	0[0,0]	0[0,40]	1[0,1]	0[0,11]
NJML	>30	100[100,100]	100[99,100]	100[100,100]	100[100,100]	100[95,100]	100[100,100]	95[80,100]	100[96,100]
	>50	65[29,95]	70[31,92]	99[73,100]	81[17,99]	38[5,84]	97[45,100]	30[3,72]	67[28,90]
	>70	3[0,15]	0[0,9]	4[1,56]	2[0,5]	0[0,2]	6[0,29]	0[0,0]	3[0,16]
UKML	>30	100[100,100]	100[100,100]	100[100,100]	100[99,100]	99[48,100]	100[100,100]	98[75,100]	98[84,100]
	>50	100[60,100]	81[0,100]	96[14,100]	63[0,100]	13[3,83]	99[71,100]	46[0,90]	70[31,92]
	>70	34[13,94]	0[0,24]	1[1,86]	0[0,20]	1[0,5]	44[4,95]	0[0,7]	18[4,54]
CAMS	>30	100[99,100]	100[59,100]	100[99,100]	100[87,100]	85[31,100]	100[100,100]	91[67,99]	93[73,100]
	>50	72[25,100]	14[0,74]	91[34,100]	40[0,98]	5[0,49]	95[48,100]	35[10,79]	50[19,81]
	>70	1[0,36]	0[0,1]	12[5,47]	0[0,3]	0[0,1]	12[0,66]	8[5,13]	4[1,27]
GEOS	>30	100[100,100]	100[92,100]	100[100,100]	100[100,100]	99[63,100]	100[99,100]	91[45,99]	98[82,100]
	>50	92[59,100]	50[0,100]	100[54,100]	43[0,100]	16[2,80]	92[38,100]	1[0,72]	58[24,89]
	>70	14[0,69]	0[0,1]	2[0,81]	0[0,1]	0[0,4]	0[0,59]	0[0,0]	3[0,33]
TCR-2	>30	100[99,100]	100[87,100]	100[99,100]	100[98,100]	98[63,100]	100[98,100]	90[45,100]	98[81,100]
	>50	94[63,100]	71[1,100]	93[71,100]	80[1,100]	21[4,91]	91[70,100]	20[1,75]	65[34,93]
	>70	42[0,86]	0[0,29]	37[0,87]	0[0,50]	1[0,9]	30[0,83]	1[0,10]	18[0,51]
2016		EAS	EUR	MDE	NAM	SAF	SAS	SEA	GLO
BME	>30	100 [97, 100]	97 [77, 100]	100 [99, 100]	100 [97, 100]	93 [66, 100]	100 [100,100]	88 [57, 97]	97 [87, 100]
	>50	54 [26, 80]	13 [1, 48]	81 [49, 96]	26 [5, 75]	3 [0, 30]	91 [71, 99]	1 [0, 18]	48 [28, 69]
	>70	1 [0, 8]	0 [0, 0]	1 [0, 7]	0 [0, 2]	0 [0, 0]	5 [0, 31]	0 [0, 0]	1 [0, 8]
NJML	>30	100[100,100]	100 [100,100]	100 [100,100]	100 [99, 100]	99 [95, 100]	100 [100,100]	91 [81, 100]	99 [96, 100]
	>50	66 [34, 92]	64 [7, 91]	98 [73, 100]	16 [4, 91]	40 [5, 82]	97 [54, 99]	19 [0, 63]	63 [29, 88]
	>70	3 [0, 21]	0 [0, 4]	3 [0, 53]	0 [0, 3]	0 [0, 1]	7 [0, 32]	0 [0, 0]	3 [0, 17]
UKML	>30	100[100,100]	100 [100,100]	100 [99, 100]	100 [100,100]	99 [53, 100]	100 [100,100]	98 [77, 100]	98 [85, 100]
	>50	100 [67, 100]	81 [0, 100]	96 [41, 100]	63 [0, 100]	13 [4, 72]	98 [80, 100]	48 [0, 82]	70 [36, 89]
	>70	33 [14, 88]	0 [0, 10]	1 [1, 77]	0 [0, 8]	1 [0, 5]	51 [14, 92]	0 [0, 5]	19 [6, 48]
CAMS	>30	100[100,100]	99 [55, 100]	100 [99, 100]	100 [85, 100]	84 [38, 100]	100 [100,100]	86 [60, 97]	93 [74, 100]
	>50	68 [11, 100]	11 [0, 60]	89 [36, 99]	42 [6, 91]	13 [1, 43]	97 [63, 100]	21 [7, 65]	50 [20, 76]
	>70	1 [0, 14]	0 [0, 0]	15 [10, 41]	0 [0, 7]	0 [0, 1]	26 [0, 69]	6 [3, 7]	7 [1, 23]
GEOS	>30	100[100,100]	100 [100,100]	100 [100,100]	100 [100,100]	99 [74, 100]	100 [100,100]	83 [46, 97]	97 [85, 100]
	>50	86 [58, 100]	50 [0, 100]	100 [66, 100]	46 [0, 100]	14 [1, 77]	97 [54, 100]	0 [0, 48]	58 [28, 86]
	>70	2 [0, 59]	0 [0, 0]	9 [0, 70]	0 [0, 0]	0 [0, 2]	0 [0, 56]	0 [0, 0]	1 [0, 29]
TCR-2	>30	100[100,100]	100 [96, 100]	100 [100,100]	100 [98, 100]	98 [76, 100]	100 [99, 100]	84 [40, 99]	97 [85, 100]
	>50	94 [67, 100]	67 [3, 100]	96 [81, 100]	84 [27, 100]	23 [4, 85]	94 [78, 99]	18 [3, 49]	66 [40, 89]
	>70	40 [1, 75]	0 [0, 17]	41 [2, 86]	0 [0, 42]	1 [0, 6]	33 [0, 84]	0 [0, 5]	15 [0, 46]

Table S11. Different quantiles of TOAR-II observations for 2006 to 2015. The unit of TOAR-II observations is ppb.

Year	2006	2007	2008	2009	2010	2011	2012	2013	2014	2015
0%	12.52	15.74	15.32	13.25	12.28	8.25	12.01	9.07	8.76	12.24
10%	37.73	36.42	37.29	37.16	36.35	36.00	36.01	37.00	36.52	36.85
20%	41.58	39.46	40.32	40.14	39.35	38.83	38.79	39.52	39.25	39.92
30%	43.69	41.75	42.32	42.19	41.16	40.77	40.67	41.42	41.09	42.02
40%	45.56	43.96	44.13	44.06	42.64	42.49	42.29	42.96	42.74	43.89
50%	47.24	46.03	45.93	45.92	43.97	43.92	43.90	44.43	44.20	45.63
60%	48.87	48.08	47.76	48.13	45.28	45.28	45.53	45.71	45.59	47.44
70%	50.63	50.40	49.78	50.10	46.92	46.99	47.58	47.29	47.14	49.60
80%	52.81	52.96	52.18	52.45	49.07	49.61	49.91	49.33	48.87	52.58
90%	55.82	56.31	55.51	55.50	52.57	53.50	53.29	52.60	51.98	57.07
100%	78.83	79.95	79.33	80.38	72.17	82.24	80.63	83.21	75.16	92.03

Figure S1. Blue and red dots are TOAR-II January 2016 to March 2017 monitor stations with valid monthly data for more than 11 months (which used for evaluation), red dots are BME inputs from TOAR-I and CNEMC in 2016, blue dots are new TOAR-II stations compared to TOAR-I in 2016 which used for evaluation in Figure S9

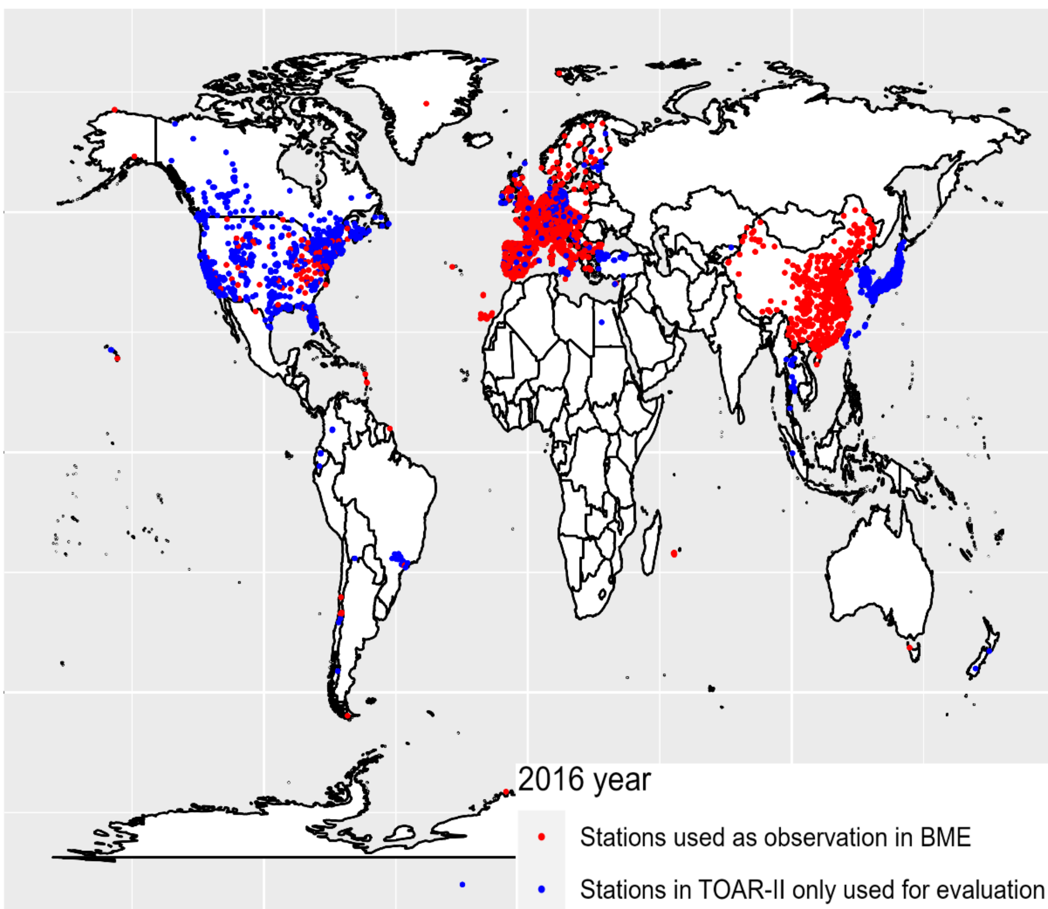

Figure S2. Performance evaluations of six datasets with TOAR-II observations for OSDMA8 for each year from 2006 to 2015. The evaluation using grid-to-grid and includes all monitor stations in the TOAR-II network for each year (2006 to 2015).

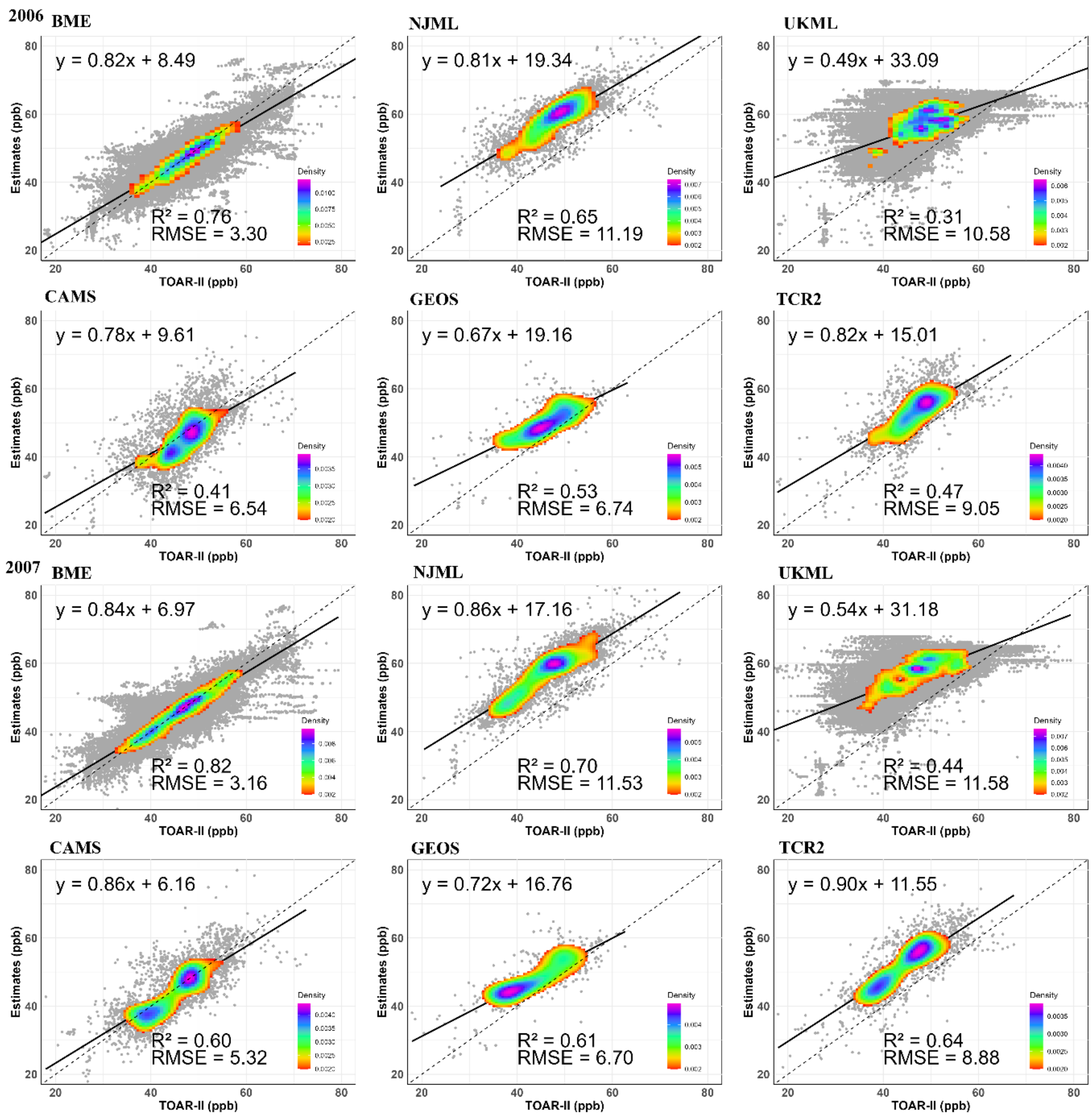

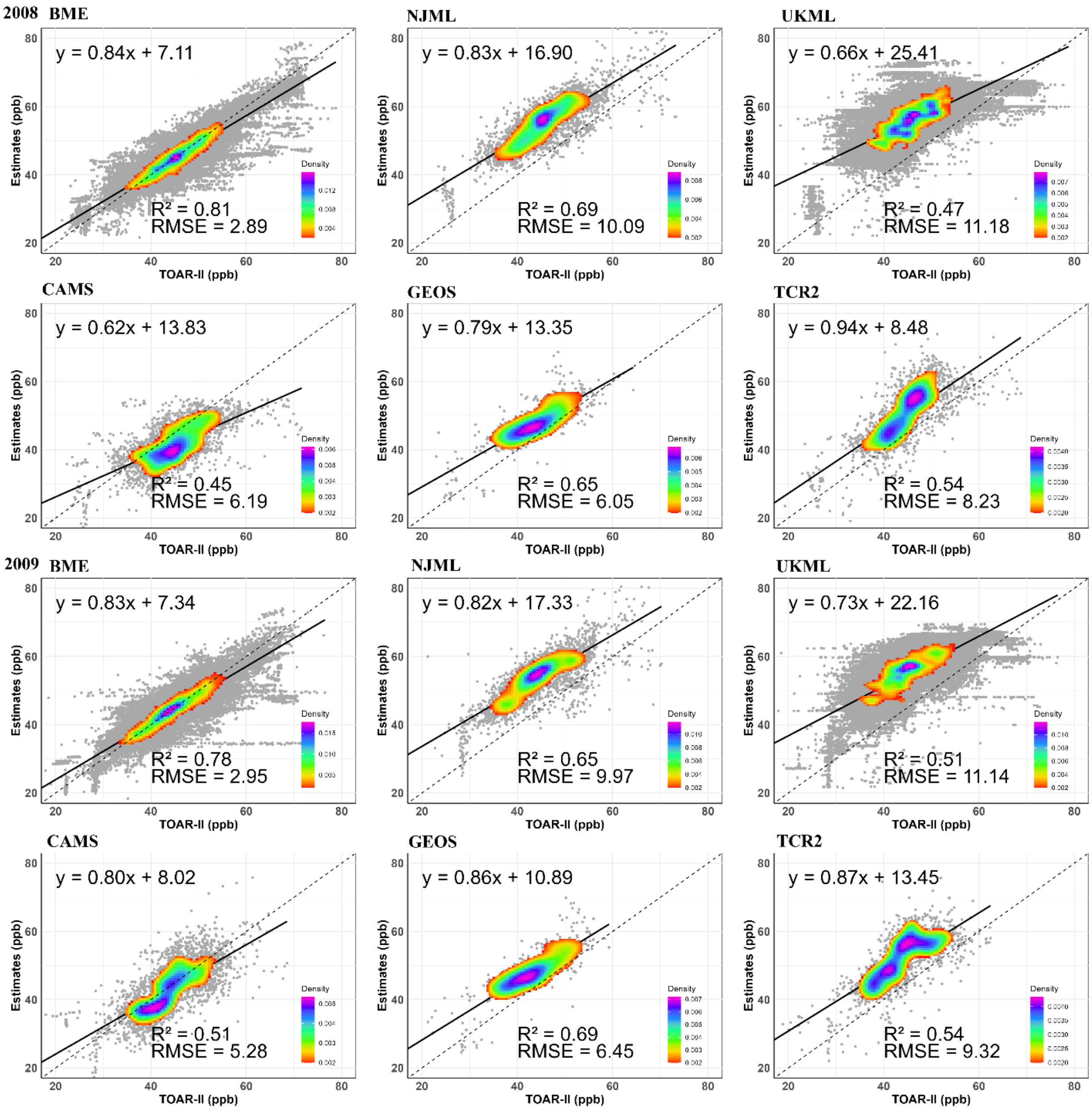
2008 BME
y = 0.84x + 7.11
R² = 0.81
RMSE = 2.89
NJML
y = 0.83x + 16.90
R² = 0.69
RMSE = 10.09
UKML
y = 0.66x + 25.41
R² = 0.47
RMSE = 11.18
CAMS
y = 0.62x + 13.83
R² = 0.45
RMSE = 6.19
GEOS
y = 0.79x + 13.35
R² = 0.65
RMSE = 6.05
TCR2
y = 0.94x + 8.48
R² = 0.54
RMSE = 8.23
2009 BME
y = 0.83x + 7.34
R² = 0.78
RMSE = 2.95
NJML
y = 0.82x + 17.33
R² = 0.65
RMSE = 9.97
UKML
y = 0.73x + 22.16
R² = 0.51
RMSE = 11.14
CAMS
y = 0.80x + 8.02
R² = 0.51
RMSE = 5.28
GEOS
y = 0.86x + 10.89
R² = 0.69
RMSE = 6.45
TCR2
y = 0.87x + 13.45
R² = 0.54
RMSE = 9.32
Estimates (ppb)
TOAR-II (ppb)
Density

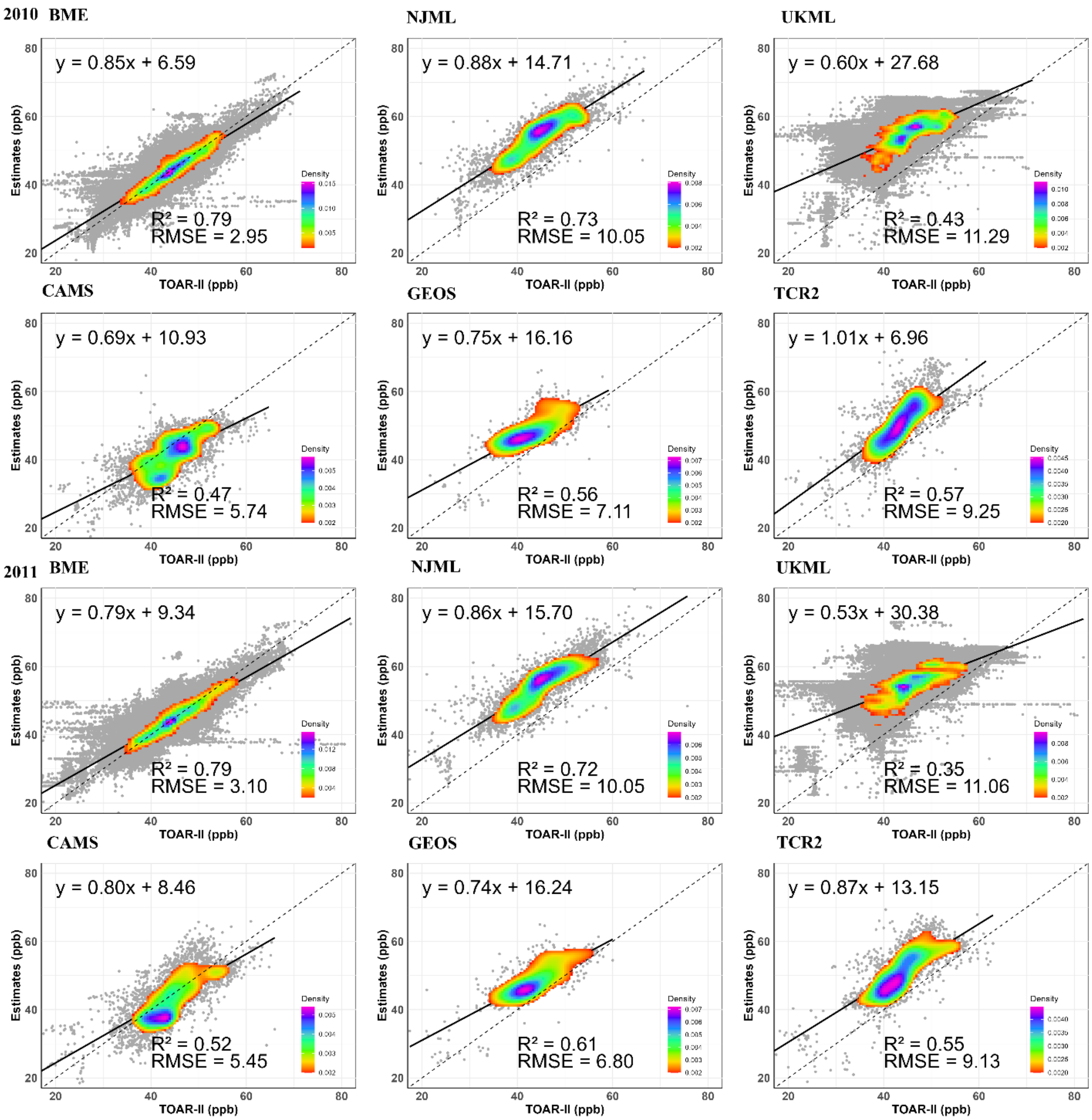

2010 BME
y = 0.85x + 6.59
R² = 0.79
RMSE = 2.95
NJML
y = 0.88x + 14.71
R² = 0.73
RMSE = 10.05
UKML
y = 0.60x + 27.68
R² = 0.43
RMSE = 11.29
CAMS
y = 0.69x + 10.93
R² = 0.47
RMSE = 5.74
GEOS
y = 0.75x + 16.16
R² = 0.56
RMSE = 7.11
TCR2
y = 1.01x + 6.96
R² = 0.57
RMSE = 9.25
2011 BME
y = 0.79x + 9.34
R² = 0.79
RMSE = 3.10
NJML
y = 0.86x + 15.70
R² = 0.72
RMSE = 10.05
UKML
y = 0.53x + 30.38
R² = 0.35
RMSE = 11.06
CAMS
y = 0.80x + 8.46
R² = 0.52
RMSE = 5.45
GEOS
y = 0.74x + 16.24
R² = 0.61
RMSE = 6.80
TCR2
y = 0.87x + 13.15
R² = 0.55
RMSE = 9.13
Estimates (ppb)
TOAR-II (ppb)
Density

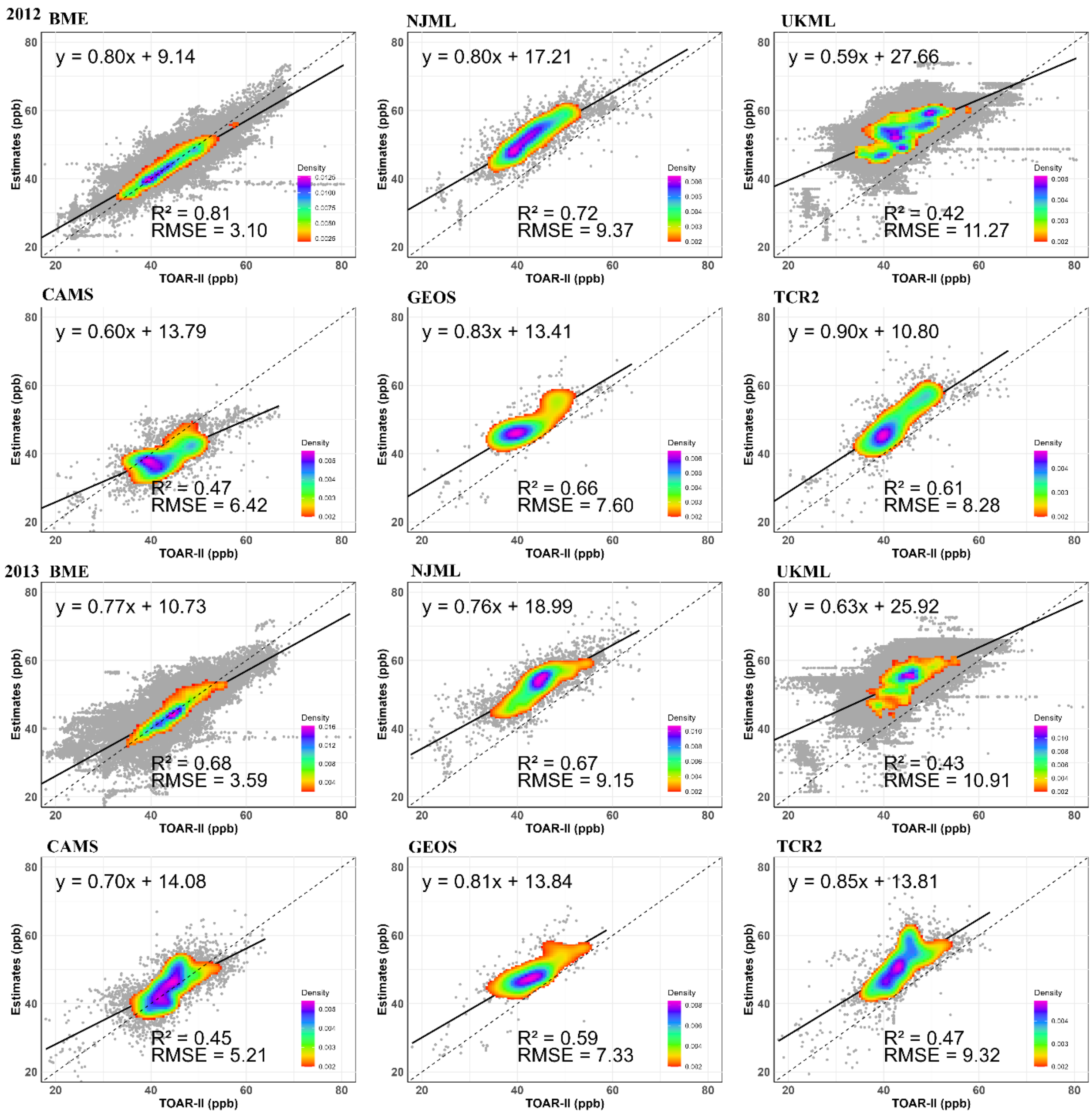
2012
BME
y = 0.80x + 9.14
R² = 0.81
RMSE = 3.10
NJML
y = 0.80x + 17.21
R² = 0.72
RMSE = 9.37
UKML
y = 0.59x + 27.66
R² = 0.42
RMSE = 11.27
CAMS
y = 0.60x + 13.79
R² = 0.47
RMSE = 6.42
GEOS
y = 0.83x + 13.41
R² = 0.66
RMSE = 7.60
TCR2
y = 0.90x + 10.80
R² = 0.61
RMSE = 8.28
2013
BME
y = 0.77x + 10.73
R² = 0.68
RMSE = 3.59
NJML
y = 0.76x + 18.99
R² = 0.67
RMSE = 9.15
UKML
y = 0.63x + 25.92
R² = 0.43
RMSE = 10.91
CAMS
y = 0.70x + 14.08
R² = 0.45
RMSE = 5.21
GEOS
y = 0.81x + 13.84
R² = 0.59
RMSE = 7.33
TCR2
y = 0.85x + 13.81
R² = 0.47
RMSE = 9.32
Estimates (ppb)
TOAR-II (ppb)
Density

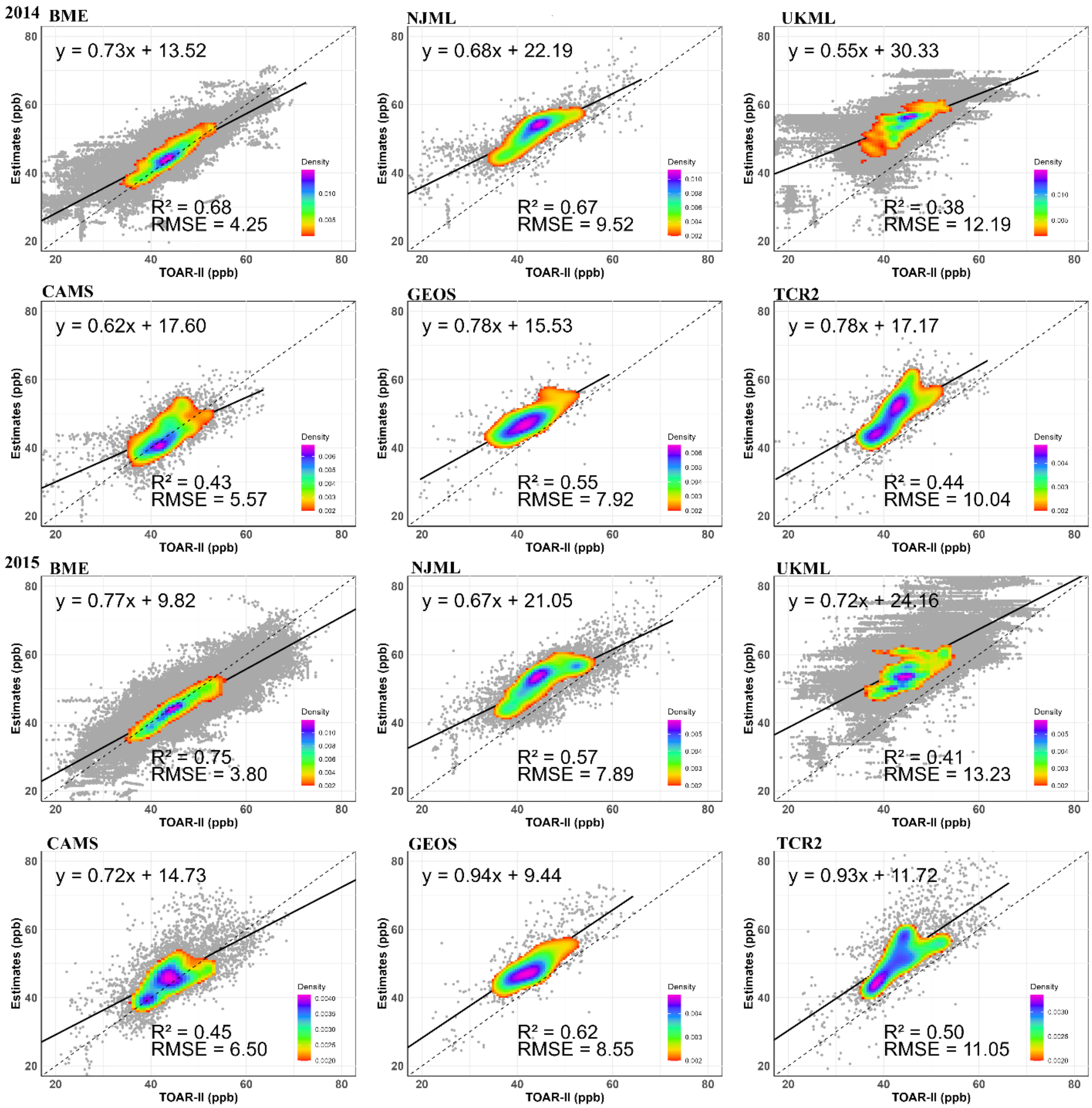
2014
BME
y = 0.73x + 13.52
R² = 0.68
RMSE = 4.25
NJML
y = 0.68x + 22.19
R² = 0.67
RMSE = 9.52
UKML
y = 0.55x + 30.33
R² = 0.38
RMSE = 12.19
CAMS
y = 0.62x + 17.60
R² = 0.43
RMSE = 5.57
GEOS
y = 0.78x + 15.53
R² = 0.55
RMSE = 7.92
TCR2
y = 0.78x + 17.17
R² = 0.44
RMSE = 10.04
2015
BME
y = 0.77x + 9.82
R² = 0.75
RMSE = 3.80
NJML
y = 0.67x + 21.05
R² = 0.57
RMSE = 7.89
UKML
y = 0.72x + 24.16
R² = 0.41
RMSE = 13.23
CAMS
y = 0.72x + 14.73
R² = 0.45
RMSE = 6.50
GEOS
y = 0.94x + 9.44
R² = 0.62
RMSE = 8.55
TCR2
y = 0.93x + 11.72
R² = 0.50
RMSE = 11.05
Estimates (ppb)
TOAR-II (ppb)
Density

Figure S3. Performance evaluations of six datasets with TOAR-II observations for OSDMA8 for each year from 2006 to 2015. The evaluation using grid-to-point and includes all monitor stations in the TOAR-II network for each year (2006 to 2015).

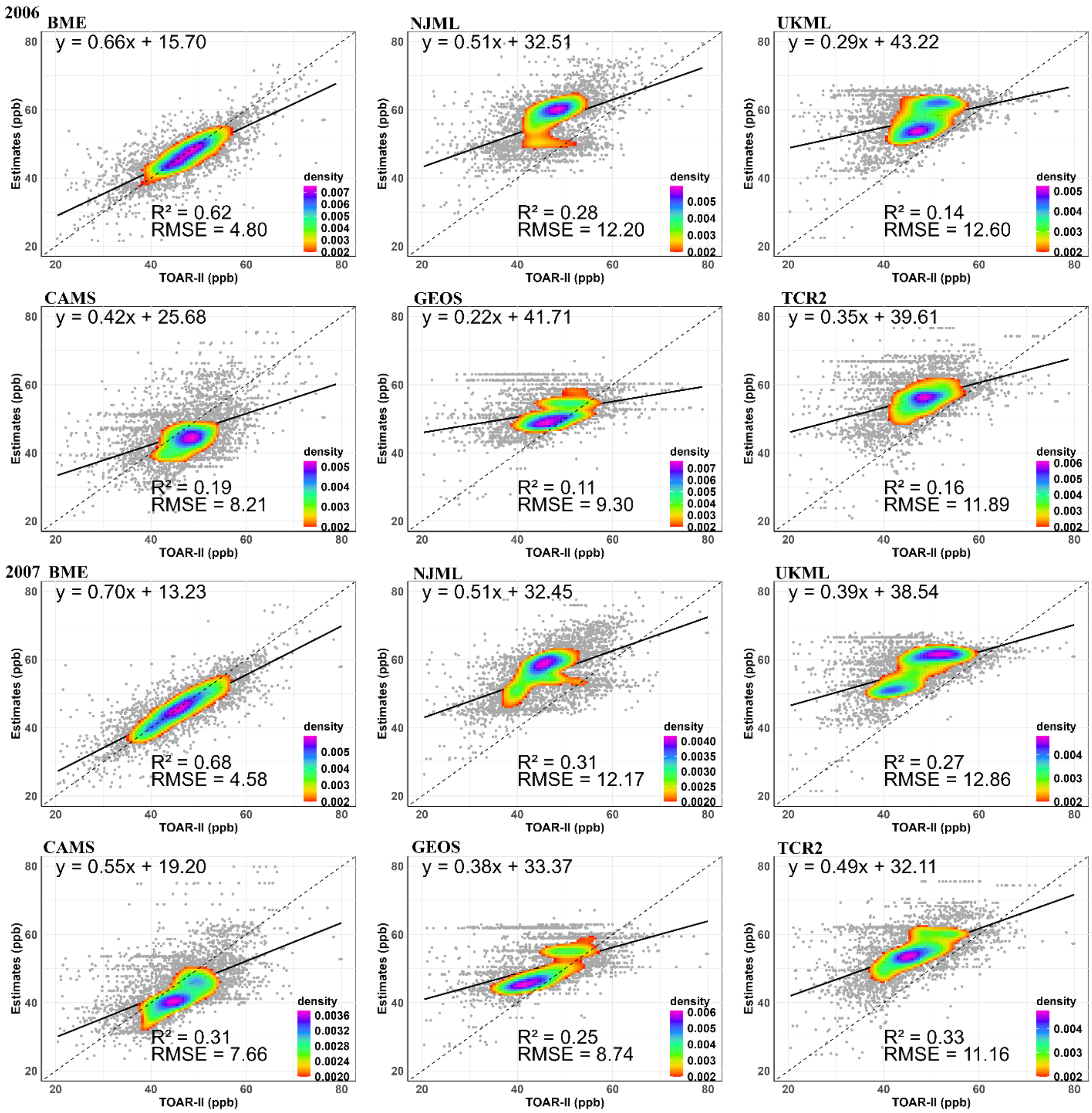

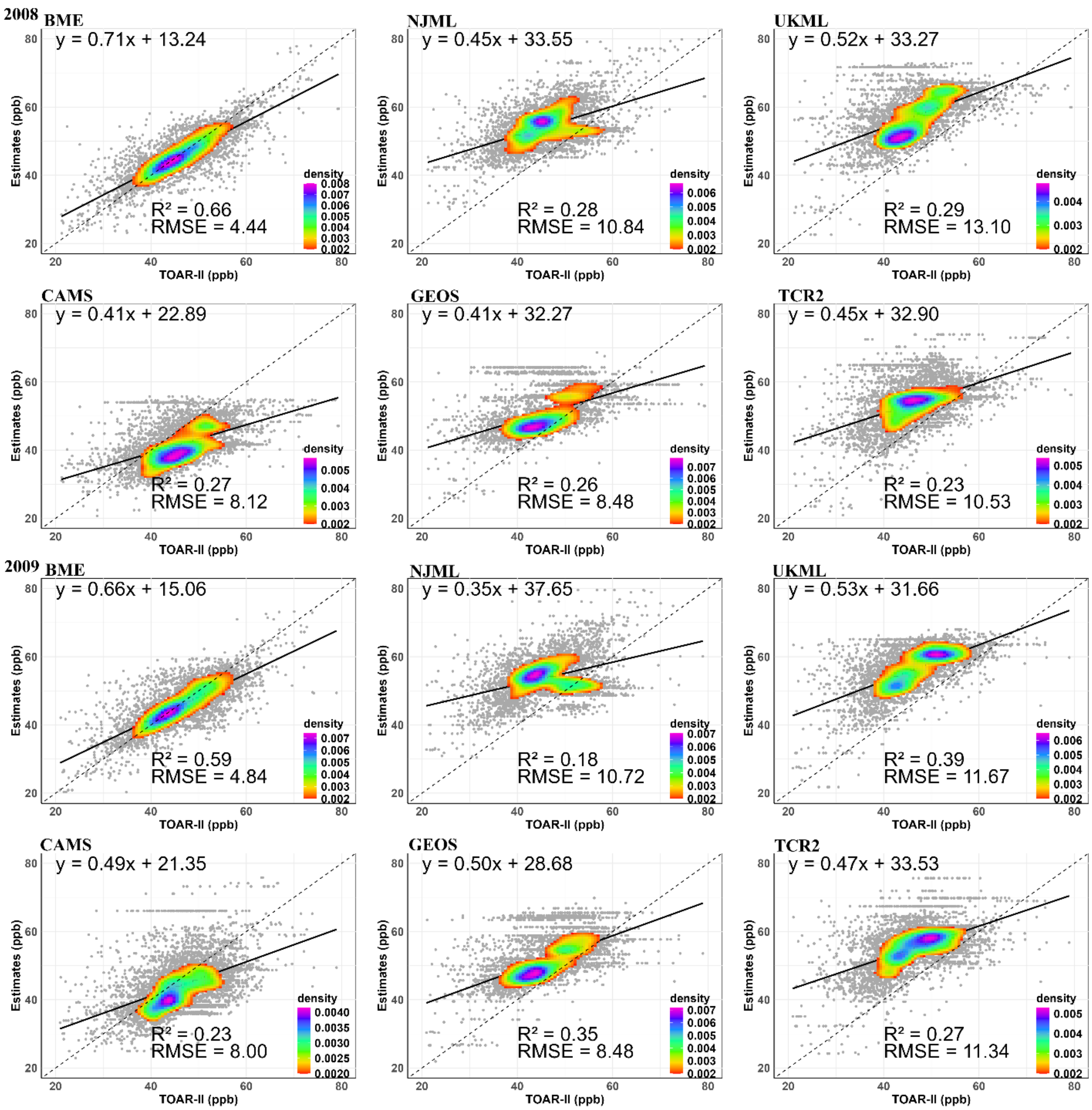
2008 BME
y = 0.71x + 13.24
R² = 0.66
RMSE = 4.44
NJML
y = 0.45x + 33.55
R² = 0.28
RMSE = 10.84
UKML
y = 0.52x + 33.27
R² = 0.29
RMSE = 13.10
CAMS
y = 0.41x + 22.89
R² = 0.27
RMSE = 8.12
GEOS
y = 0.41x + 32.27
R² = 0.26
RMSE = 8.48
TCR2
y = 0.45x + 32.90
R² = 0.23
RMSE = 10.53
2009 BME
y = 0.66x + 15.06
R² = 0.59
RMSE = 4.84
NJML
y = 0.35x + 37.65
R² = 0.18
RMSE = 10.72
UKML
y = 0.53x + 31.66
R² = 0.39
RMSE = 11.67
CAMS
y = 0.49x + 21.35
R² = 0.23
RMSE = 8.00
GEOS
y = 0.50x + 28.68
R² = 0.35
RMSE = 8.48
TCR2
y = 0.47x + 33.53
R² = 0.27
RMSE = 11.34
Estimates (ppb)
TOAR-II (ppb)
density

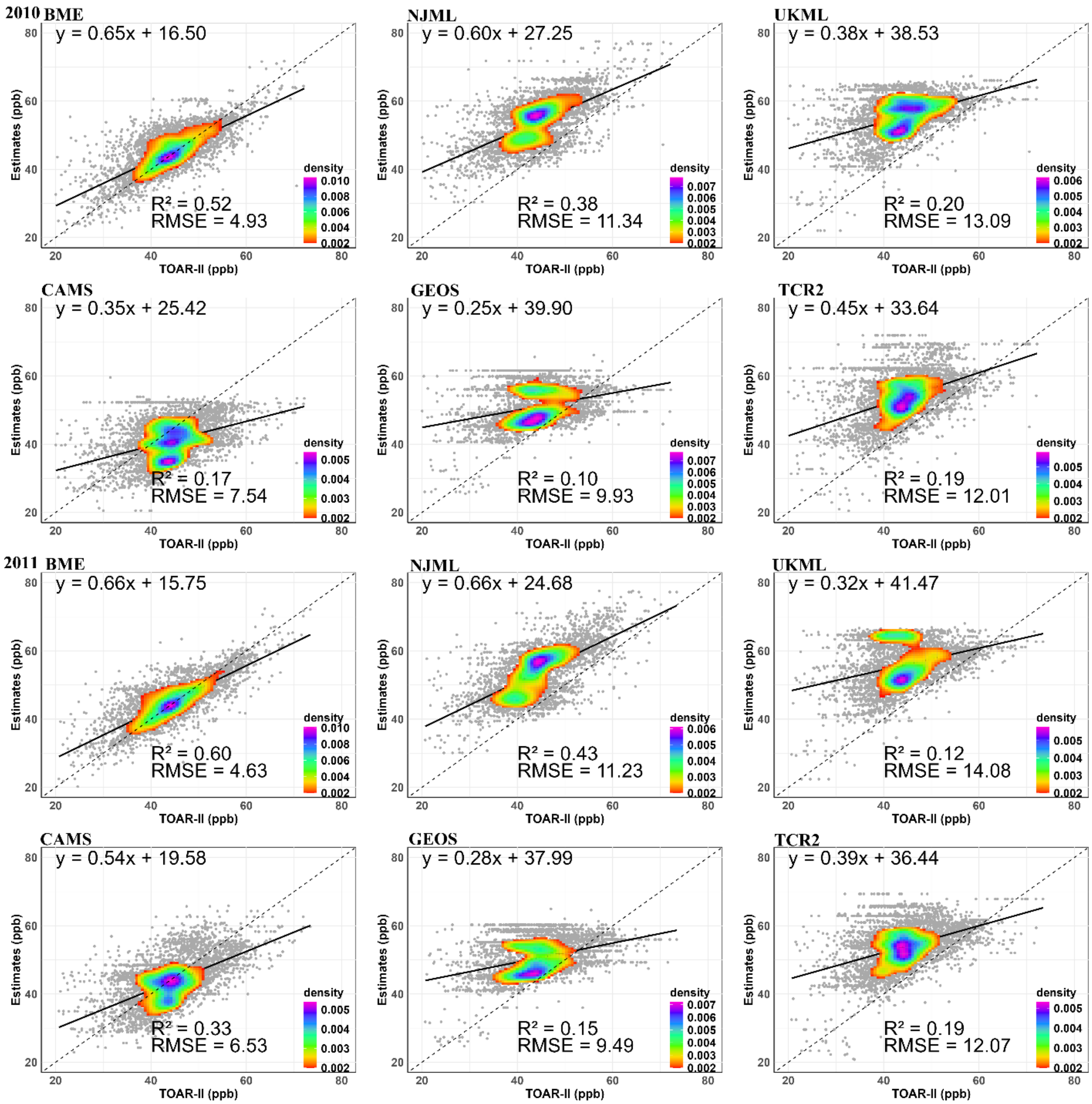
2010 BME
y = 0.65x + 16.50
R² = 0.52
RMSE = 4.93
NJML
y = 0.60x + 27.25
R² = 0.38
RMSE = 11.34
UKML
y = 0.38x + 38.53
R² = 0.20
RMSE = 13.09
CAMS
y = 0.35x + 25.42
R² = 0.17
RMSE = 7.54
GEOS
y = 0.25x + 39.90
R² = 0.10
RMSE = 9.93
TCR2
y = 0.45x + 33.64
R² = 0.19
RMSE = 12.01
2011 BME
y = 0.66x + 15.75
R² = 0.60
RMSE = 4.63
NJML
y = 0.66x + 24.68
R² = 0.43
RMSE = 11.23
UKML
y = 0.32x + 41.47
R² = 0.12
RMSE = 14.08
CAMS
y = 0.54x + 19.58
R² = 0.33
RMSE = 6.53
GEOS
y = 0.28x + 37.99
R² = 0.15
RMSE = 9.49
TCR2
y = 0.39x + 36.44
R² = 0.19
RMSE = 12.07
Estimates (ppb)
TOAR-II (ppb)
density

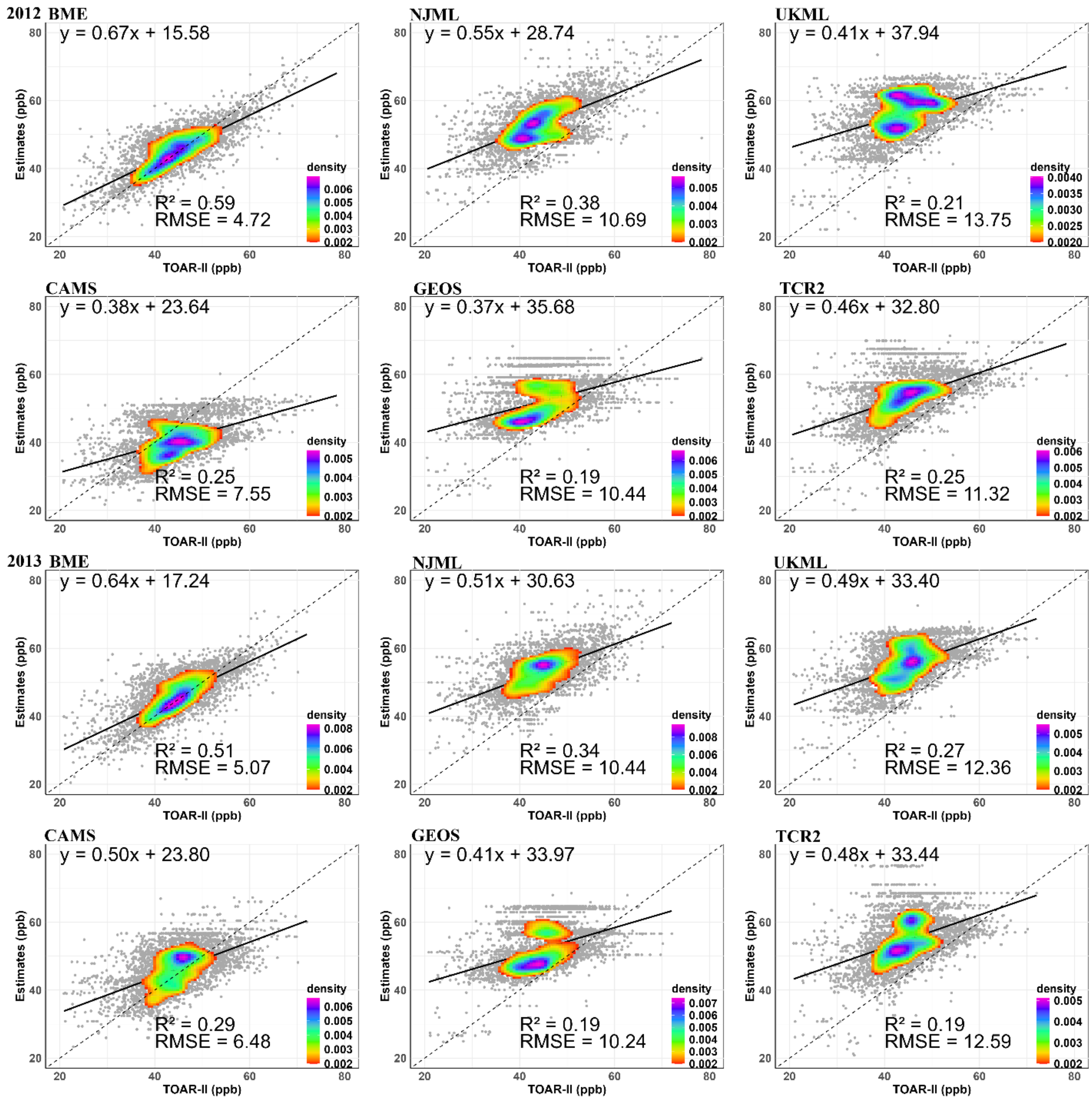
2012 BME
y = 0.67x + 15.58
R² = 0.59
RMSE = 4.72
NJML
y = 0.55x + 28.74
R² = 0.38
RMSE = 10.69
UKML
y = 0.41x + 37.94
R² = 0.21
RMSE = 13.75
CAMS
y = 0.38x + 23.64
R² = 0.25
RMSE = 7.55
GEOS
y = 0.37x + 35.68
R² = 0.19
RMSE = 10.44
TCR2
y = 0.46x + 32.80
R² = 0.25
RMSE = 11.32
2013 BME
y = 0.64x + 17.24
R² = 0.51
RMSE = 5.07
NJML
y = 0.51x + 30.63
R² = 0.34
RMSE = 10.44
UKML
y = 0.49x + 33.40
R² = 0.27
RMSE = 12.36
CAMS
y = 0.50x + 23.80
R² = 0.29
RMSE = 6.48
GEOS
y = 0.41x + 33.97
R² = 0.19
RMSE = 10.24
TCR2
y = 0.48x + 33.44
R² = 0.19
RMSE = 12.59
Estimates (ppb)
TOAR-II (ppb)
density

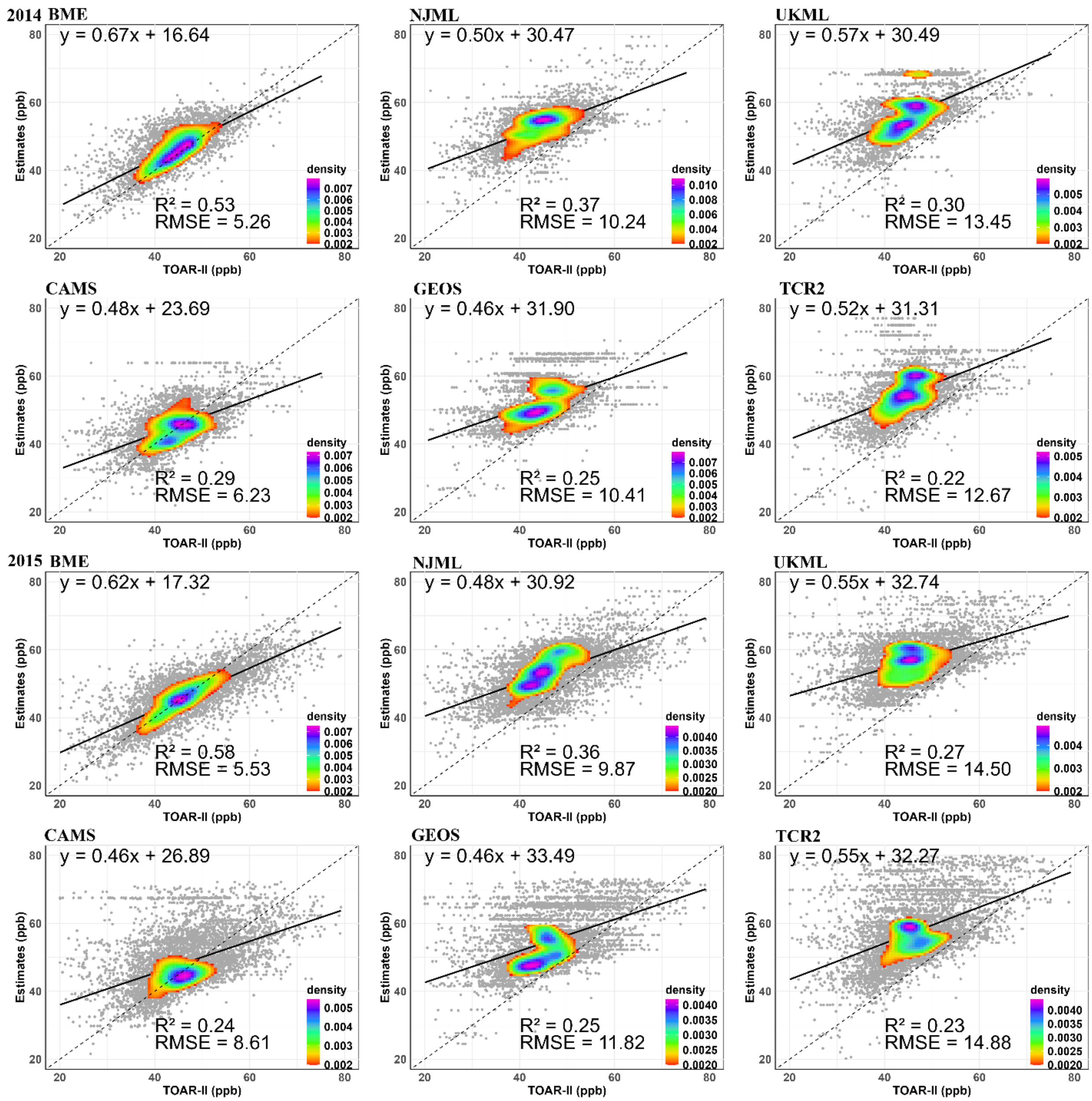
2014 BME
y = 0.67x + 16.64
R² = 0.53
RMSE = 5.26
NJML
y = 0.50x + 30.47
R² = 0.37
RMSE = 10.24
UKML
y = 0.57x + 30.49
R² = 0.30
RMSE = 13.45
CAMS
y = 0.48x + 23.69
R² = 0.29
RMSE = 6.23
GEOS
y = 0.46x + 31.90
R² = 0.25
RMSE = 10.41
TCR2
y = 0.52x + 31.31
R² = 0.22
RMSE = 12.67
2015 BME
y = 0.62x + 17.32
R² = 0.58
RMSE = 5.53
NJML
y = 0.48x + 30.92
R² = 0.36
RMSE = 9.87
UKML
y = 0.55x + 32.74
R² = 0.27
RMSE = 14.50
CAMS
y = 0.46x + 26.89
R² = 0.24
RMSE = 8.61
GEOS
y = 0.46x + 33.49
R² = 0.25
RMSE = 11.82
TCR2
y = 0.55x + 32.27
R² = 0.23
RMSE = 14.88
density
Estimates (ppb)
TOAR-II (ppb)

Figure S4. Performance evaluations of six datasets with TOAR-II observations in 2016 for OSDMA8. The evaluation excludes the monitoring stations used as input in BME data fusion in 2016. Location of monitoring stations used as input in BME data fusion in 2016 can be found in Figure S1. (a) is using grid-to-grid evaluation; (b) is using grid-to-point evaluation.

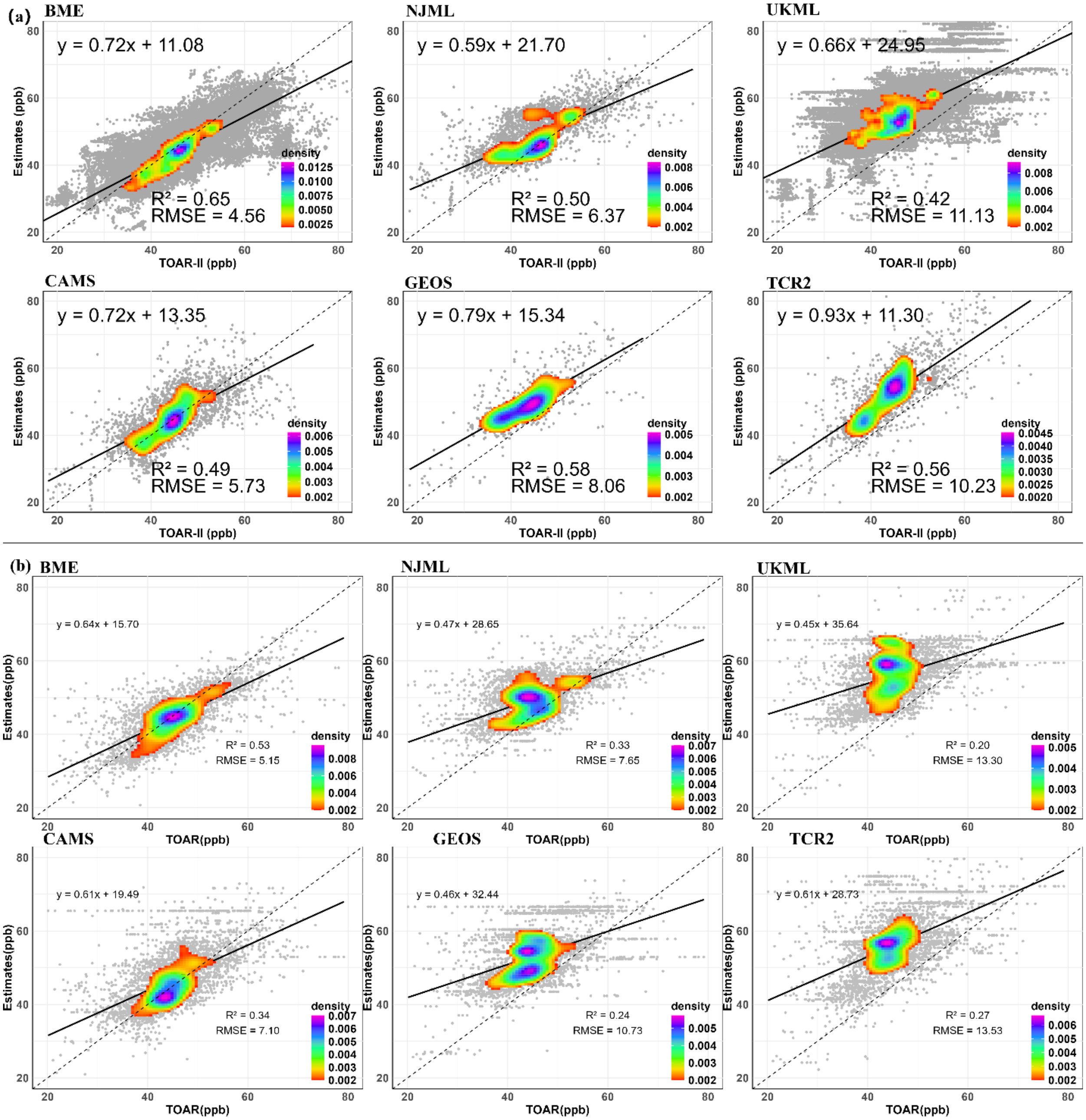

Figure S5. Normalized mean bias of six databases against TOAR-II observations (OSDMA8) at different quantiles for each year from 2006 to 2015. Different quantiles of TOAR-II observations for each year are shown in Table S9.

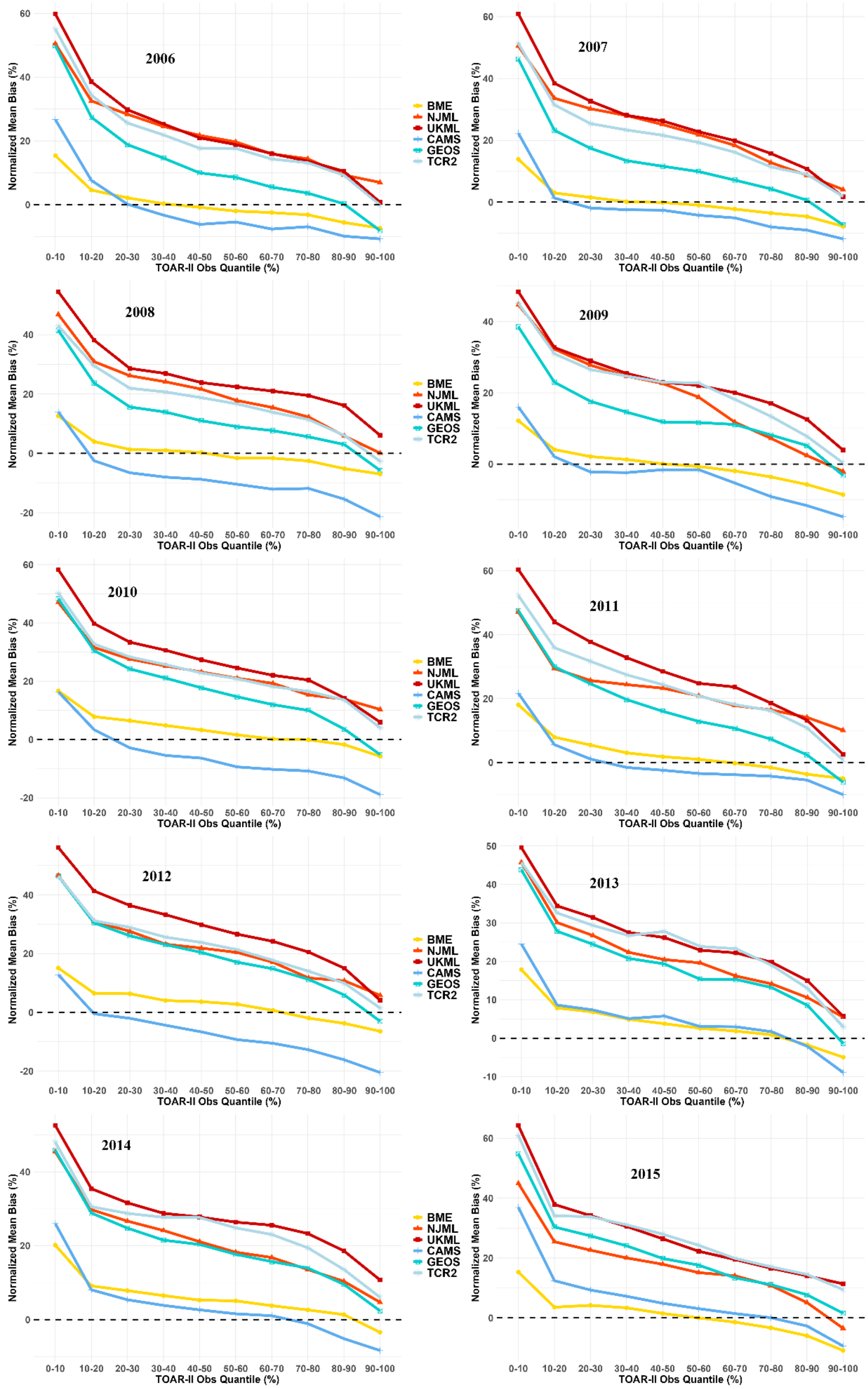

Figure S6: Population-weighted exposure distributions for OSDMA8 from 2006 to 2015 in three regions: East Asia (EAS), Europe (EUR), and North America (NAM) (regions defined in Table S7). Each panel compares the distribution derived from the TOAR-II observations (black line) with estimates from six datasets (colored lines), calculating the population-weighted kernel density estimate, only for grid cells where TOAR-II measurements exist.

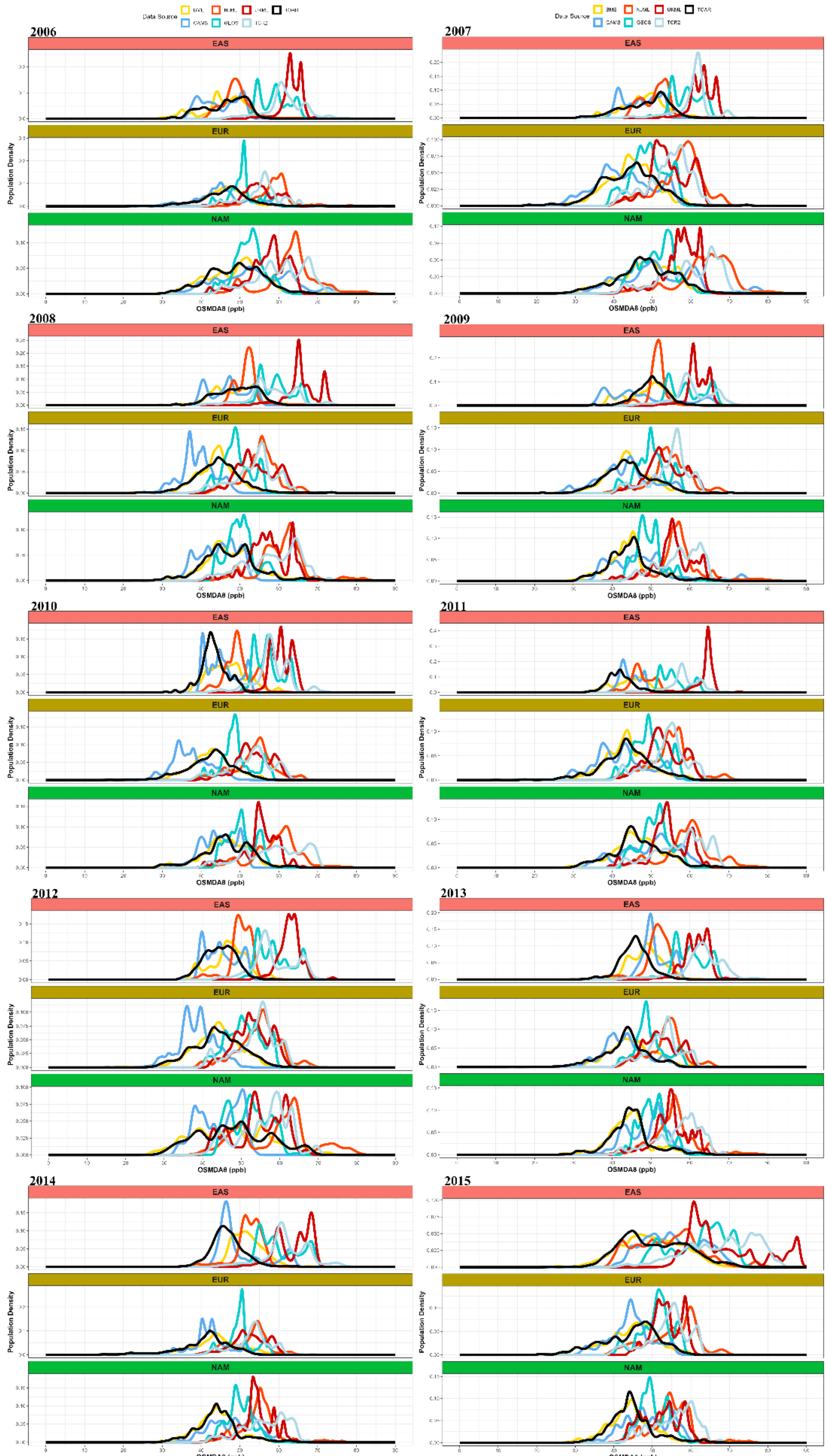

Data Source
2006
2007
2008
2009
2010
2011
2012
2013
2014
2015
EAS
EUR
NAM
Population Density
OSMDA8 (ppb)

Figure S7. The Yearly trends for six datasets for different regions, where ozone is expressed as population-weighted OSMDA8.

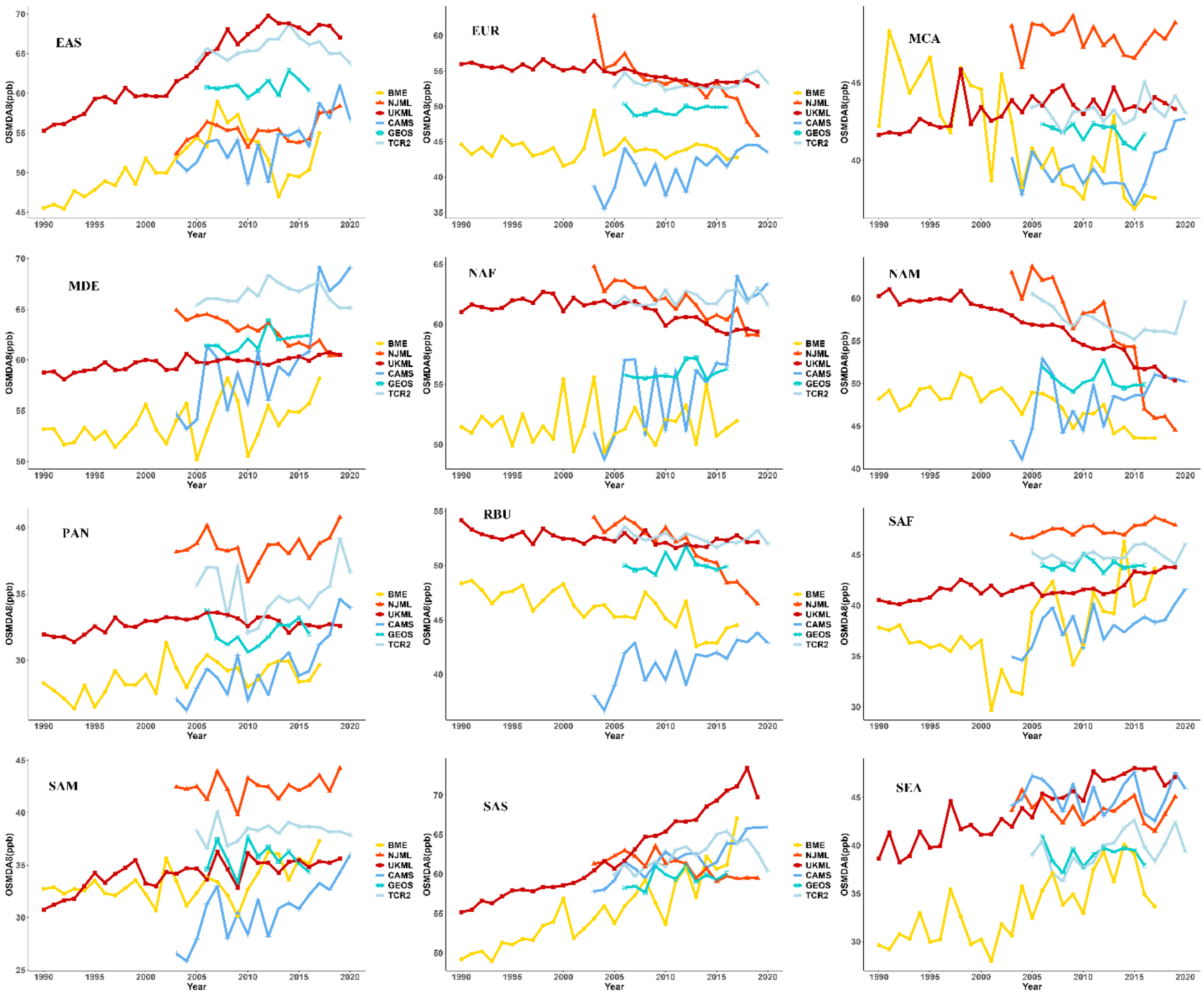

Figure S8. The Yearly trends for six datasets for different regions where ozone is expressed as area-weighted OSMDA8.

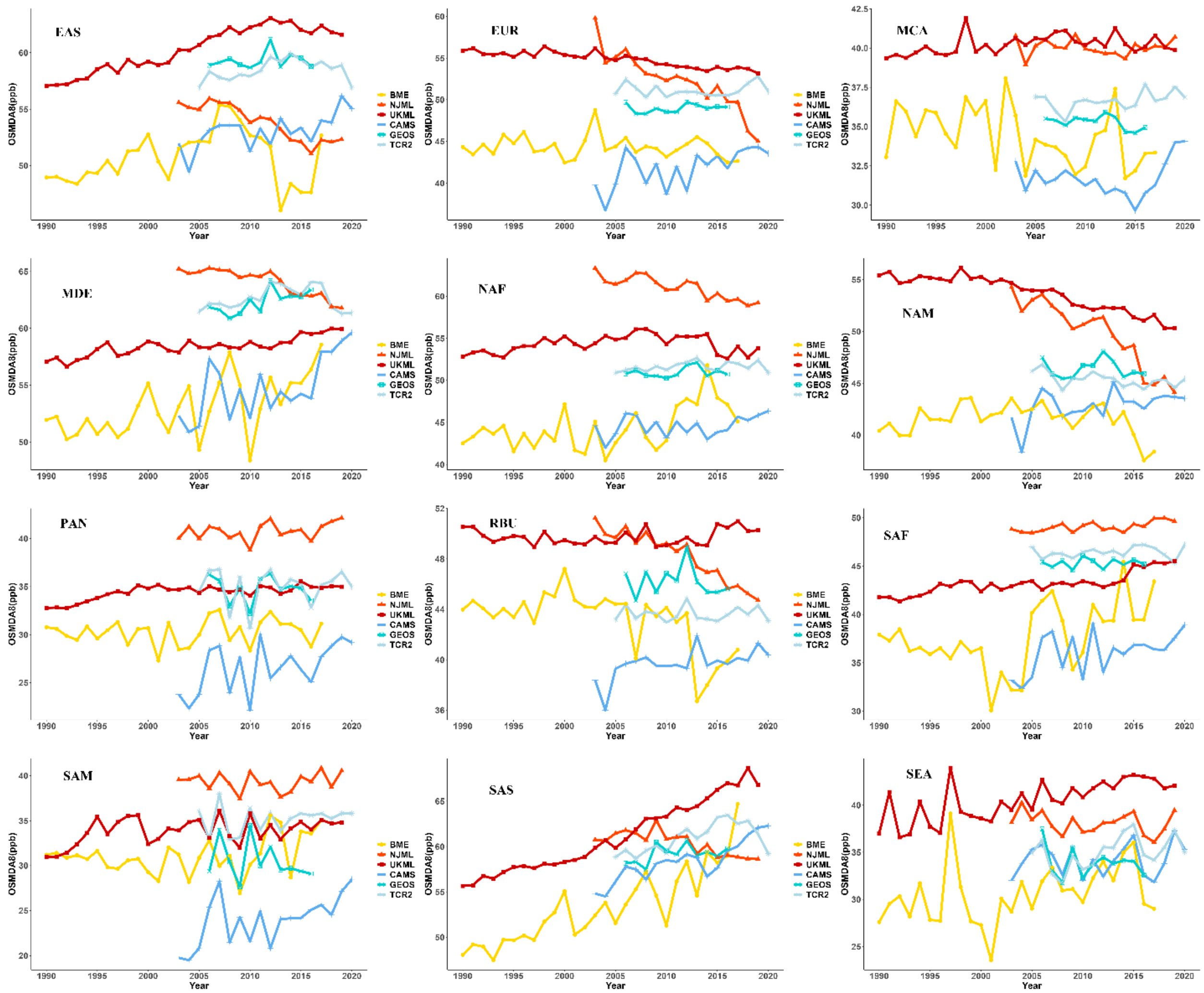

Figure S9. Each year ensemble means of six datasets from 2006 to 2016

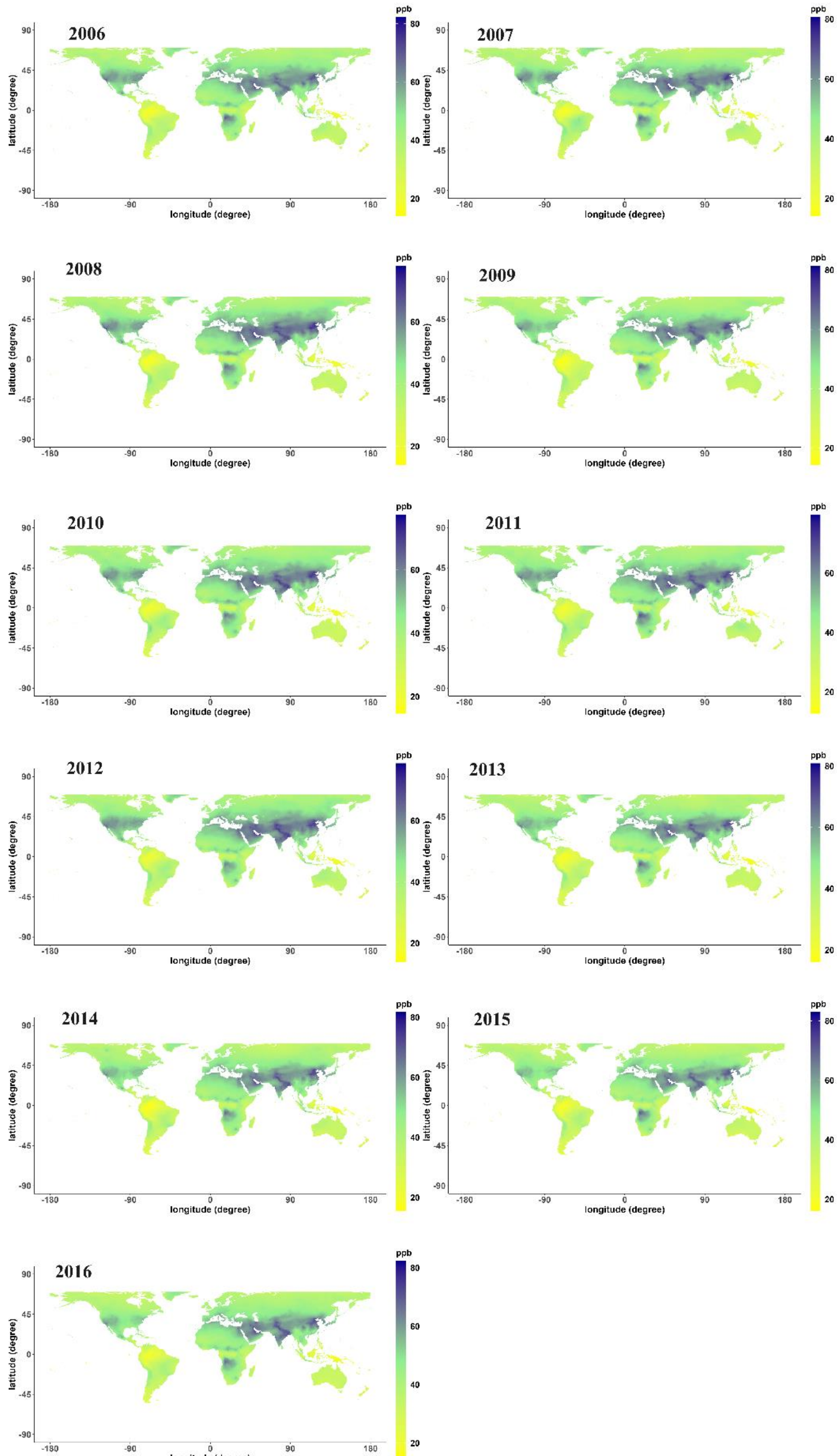

Figure S10. Each year standard deviations of six datasets from 2006 to 2016

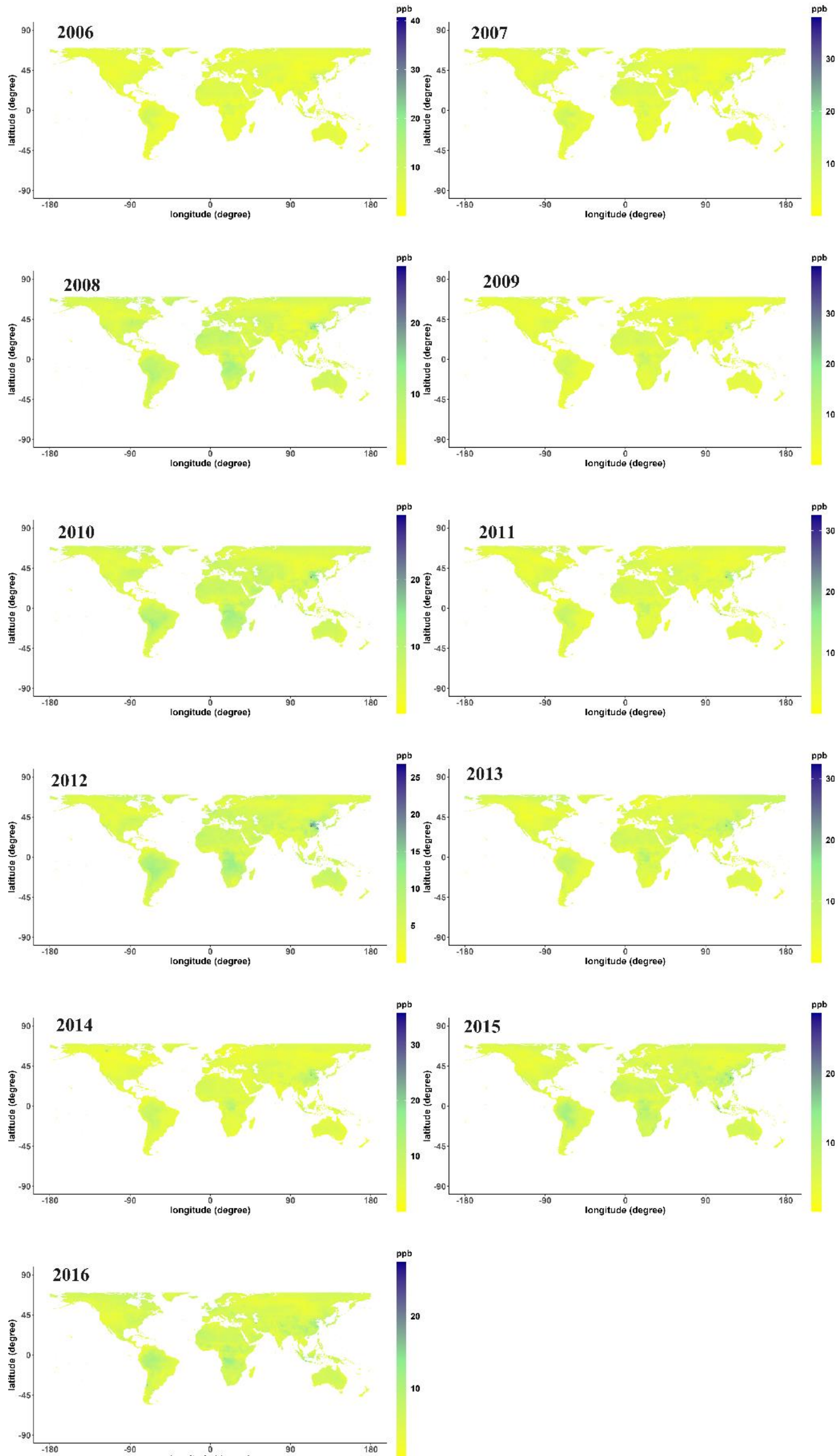

Figure S11. Each year the difference in each grid cell between the six datasets and the ensemble mean (Figure S5) from 2006 to 2016. Positive values indicate that the estimate of the dataset is higher than the ensemble mean. Negative values indicate that the estimate of the dataset is lower than the ensemble mean of the six datasets.

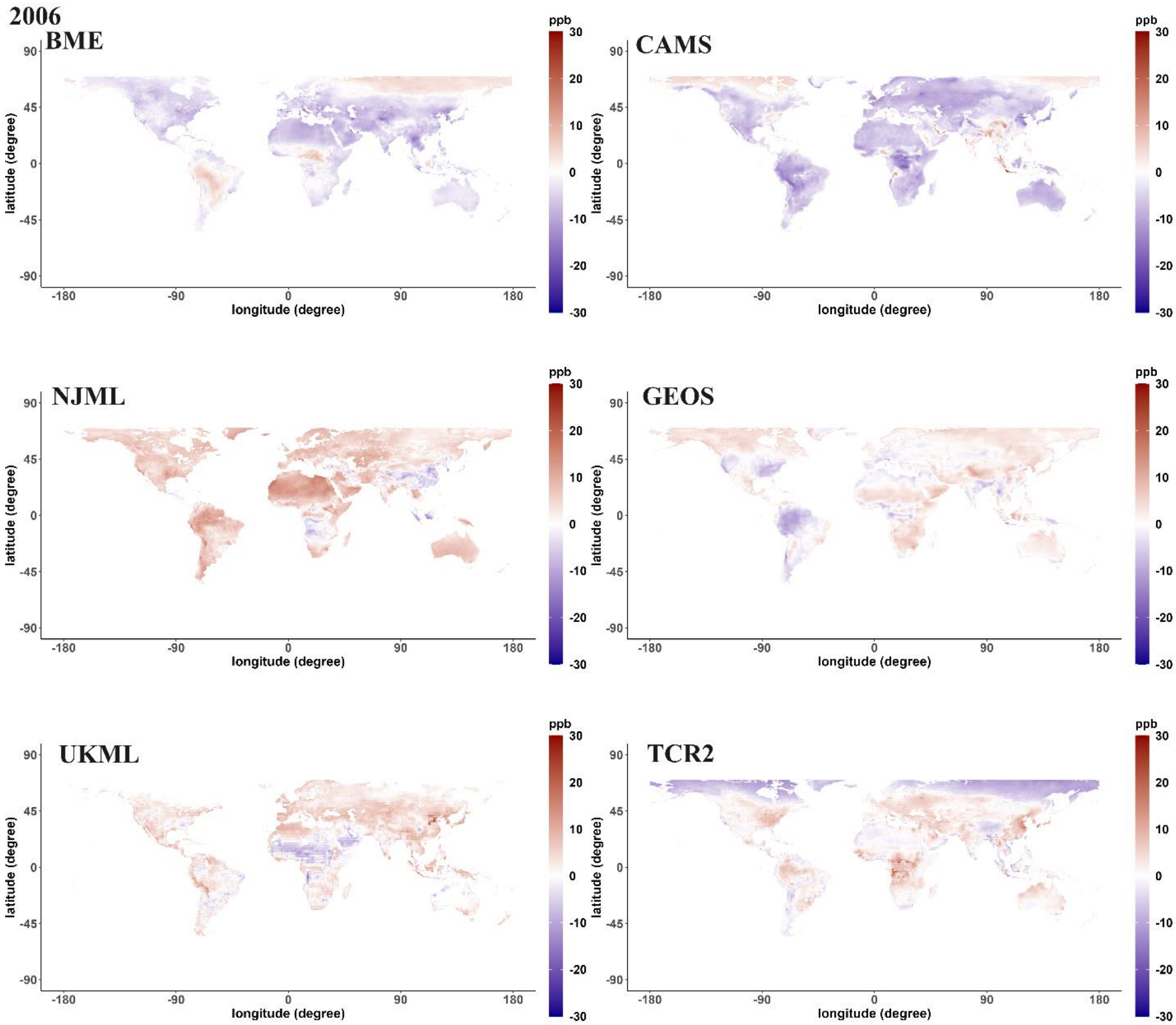

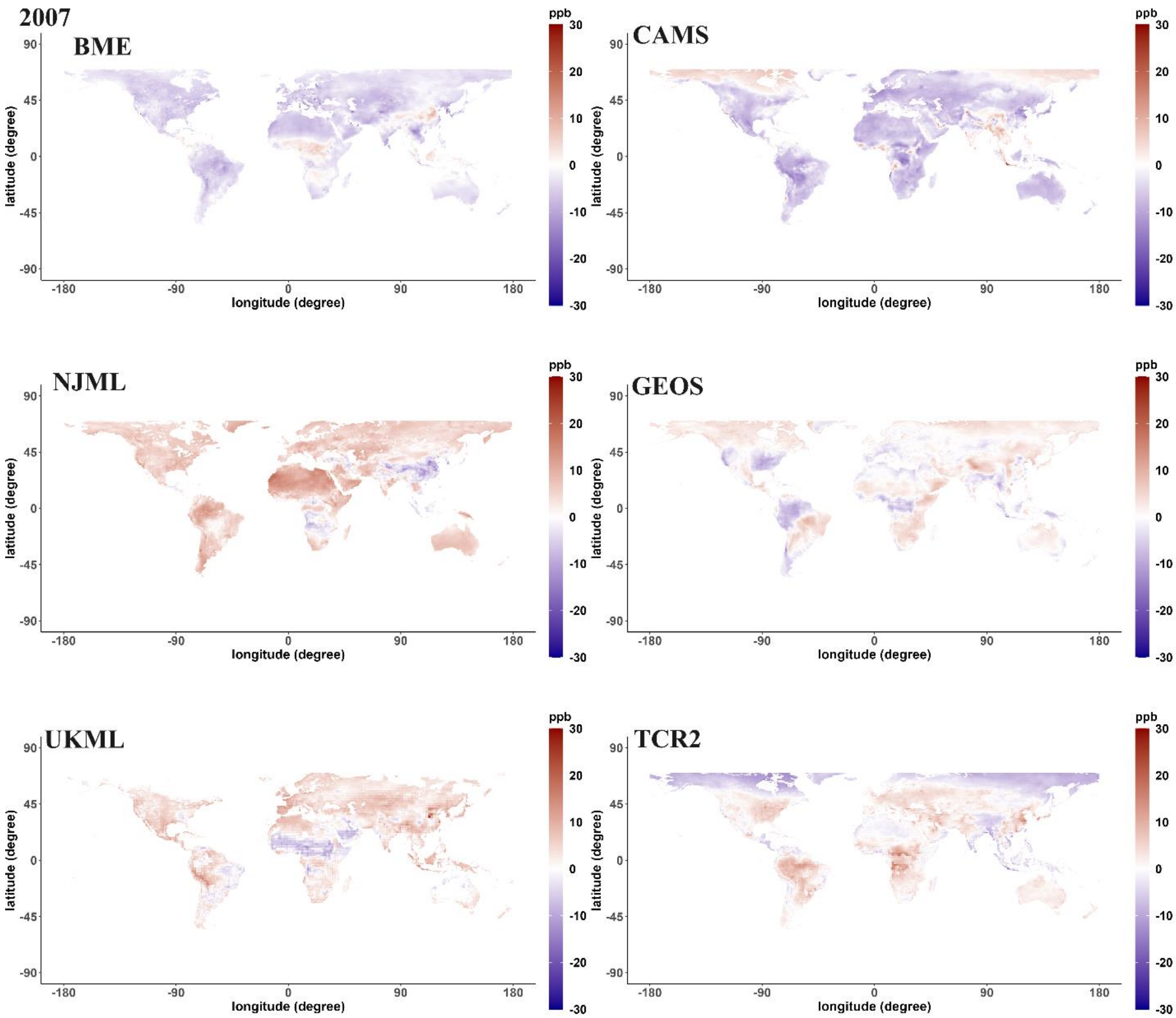
2007
BME
CAMS
NJML
GEOS
UKML
TCR2
latitude (degree)
longitude (degree)
ppb
30
20
10
0
-10
-20
-30
90
45
0
-45
-90
-180
-90
0
90
180

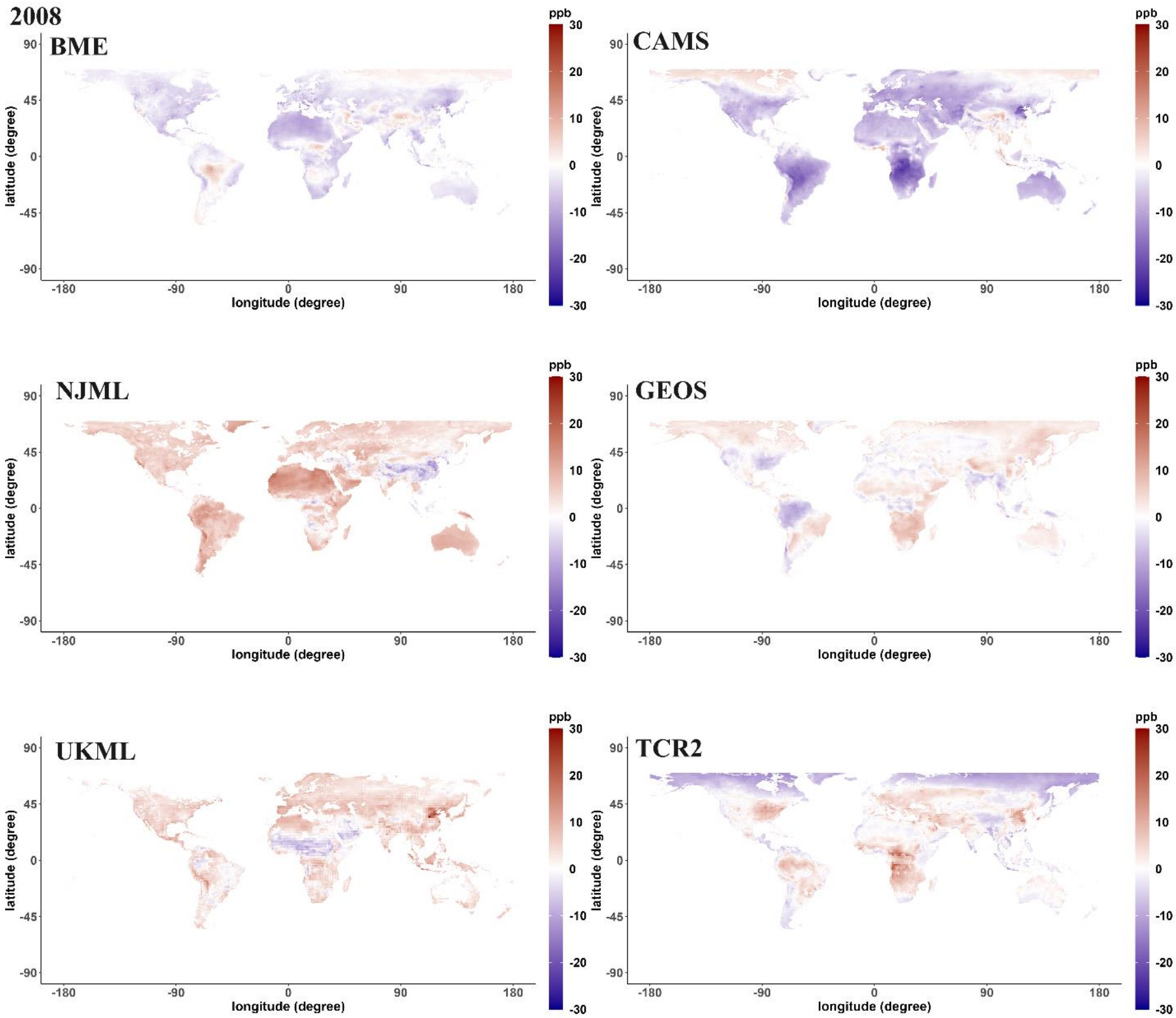
2008
BME
CAMS
NJML
GEOS
UKML
TCR2
ppb
30
20
10
0
-10
-20
-30
latitude (degree)
90
45
0
-45
-90
longitude (degree)
-180
-90
0
90
180

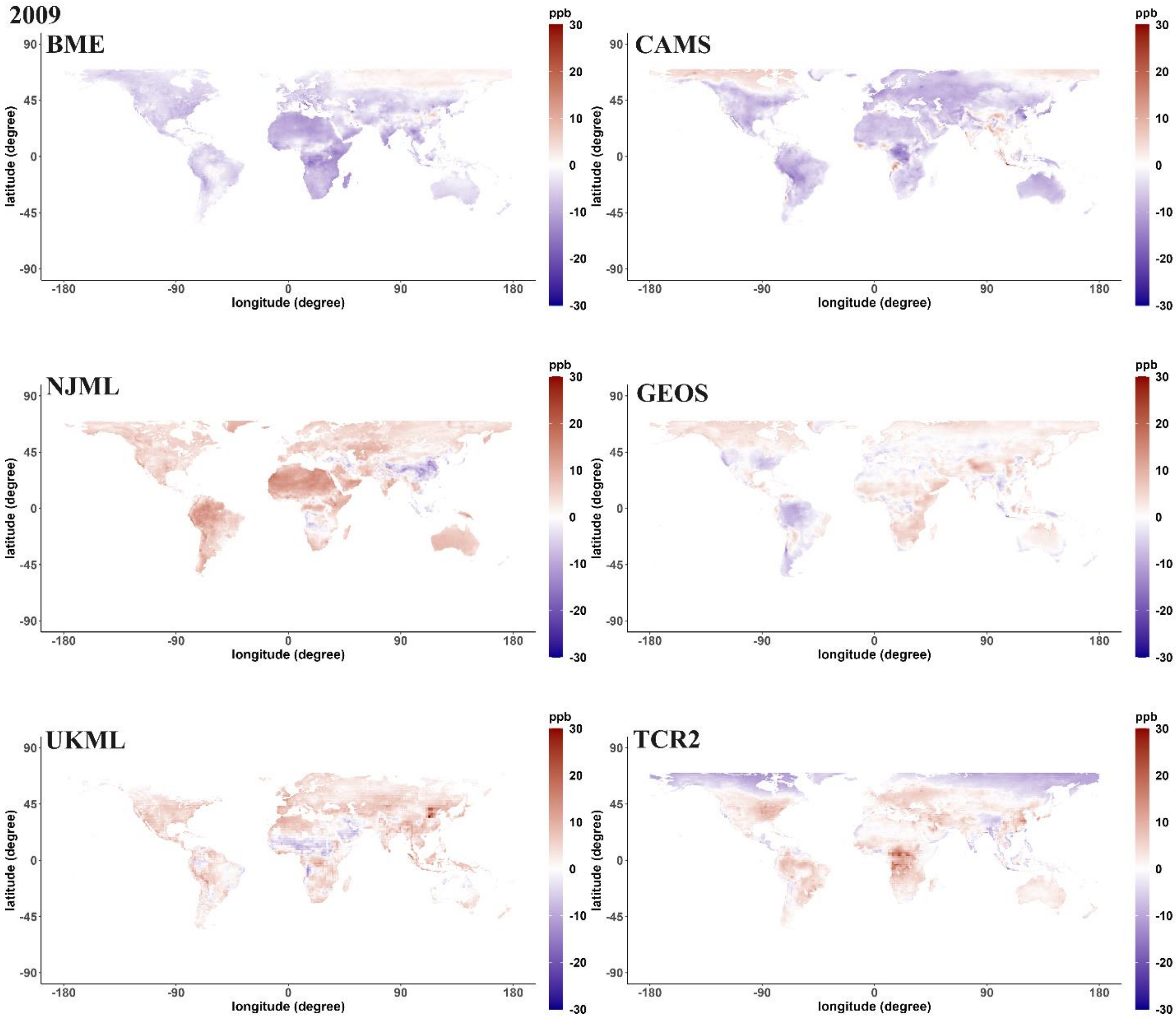
2009
BME
CAMS
NJML
GEOS
UKML
TCR2
ppb
latitude (degree)
longitude (degree)

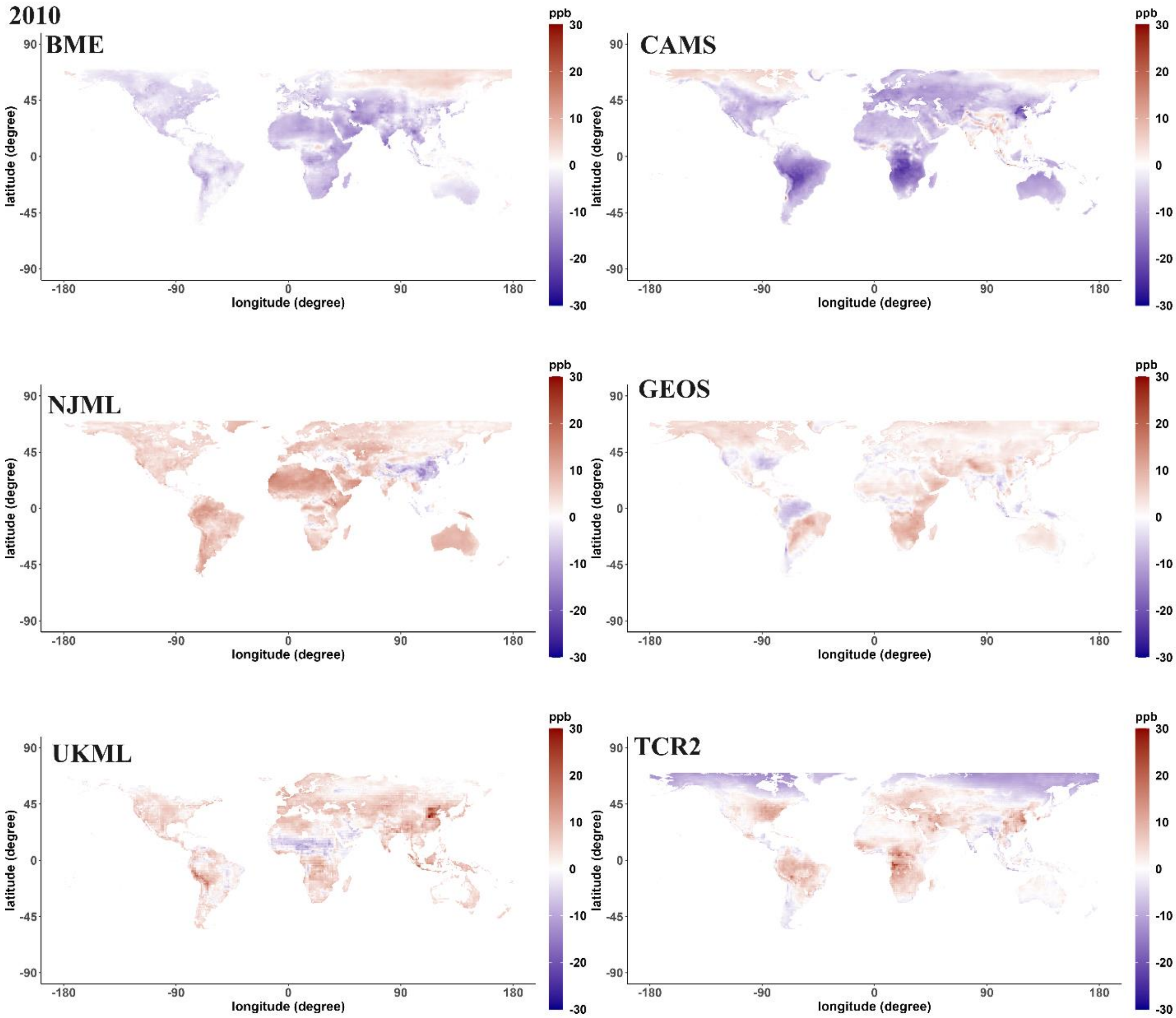
2010
BME
CAMS
NJML
GEOS
UKML
TCR2
ppb
30
20
10
0
-10
-20
-30
latitude (degree)
90
45
0
-45
-90
longitude (degree)
-180
-90
0
90
180

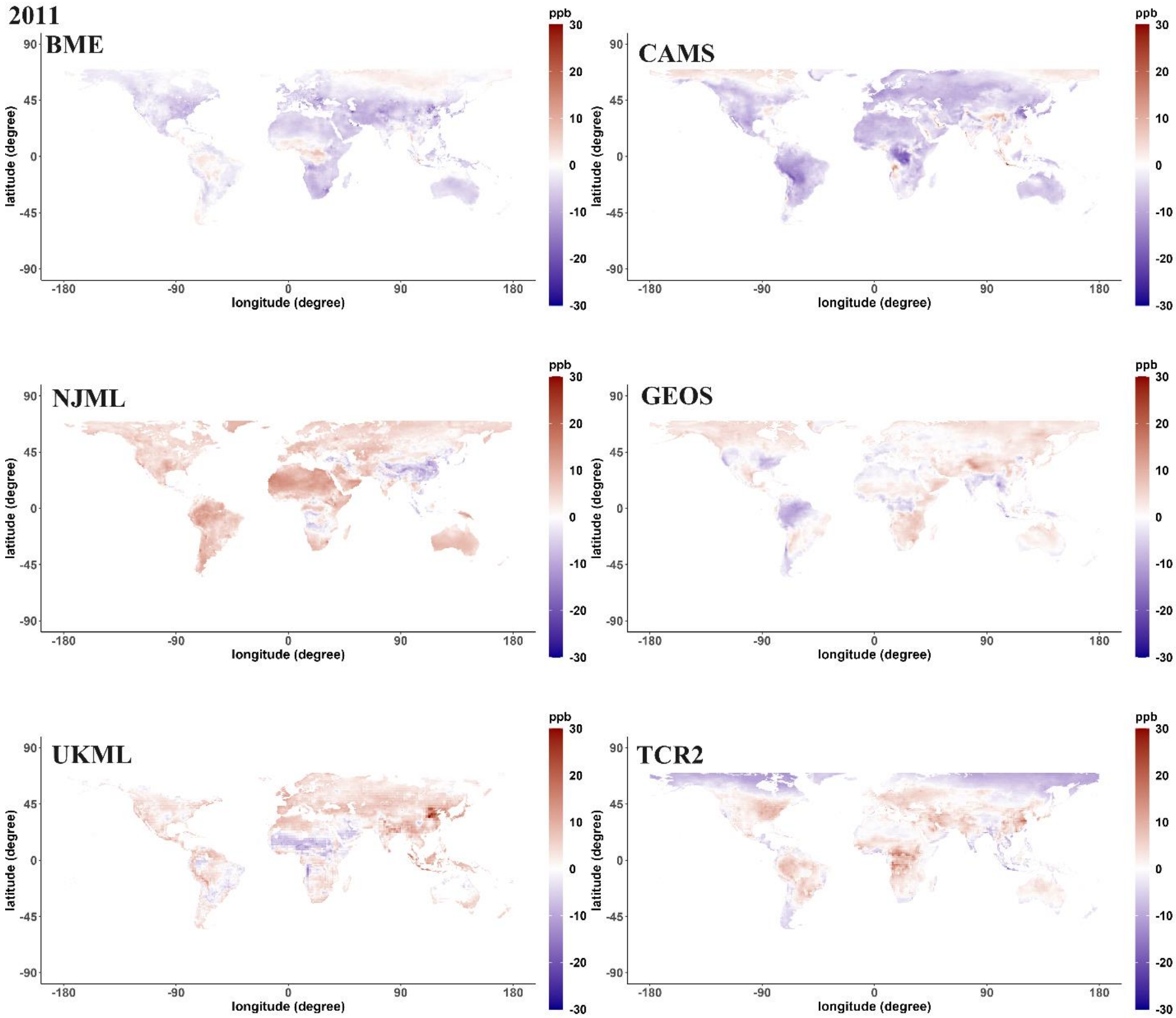
2011
BME
CAMS
NJML
GEOS
UKML
TCR2
ppb
latitude (degree)
longitude (degree)

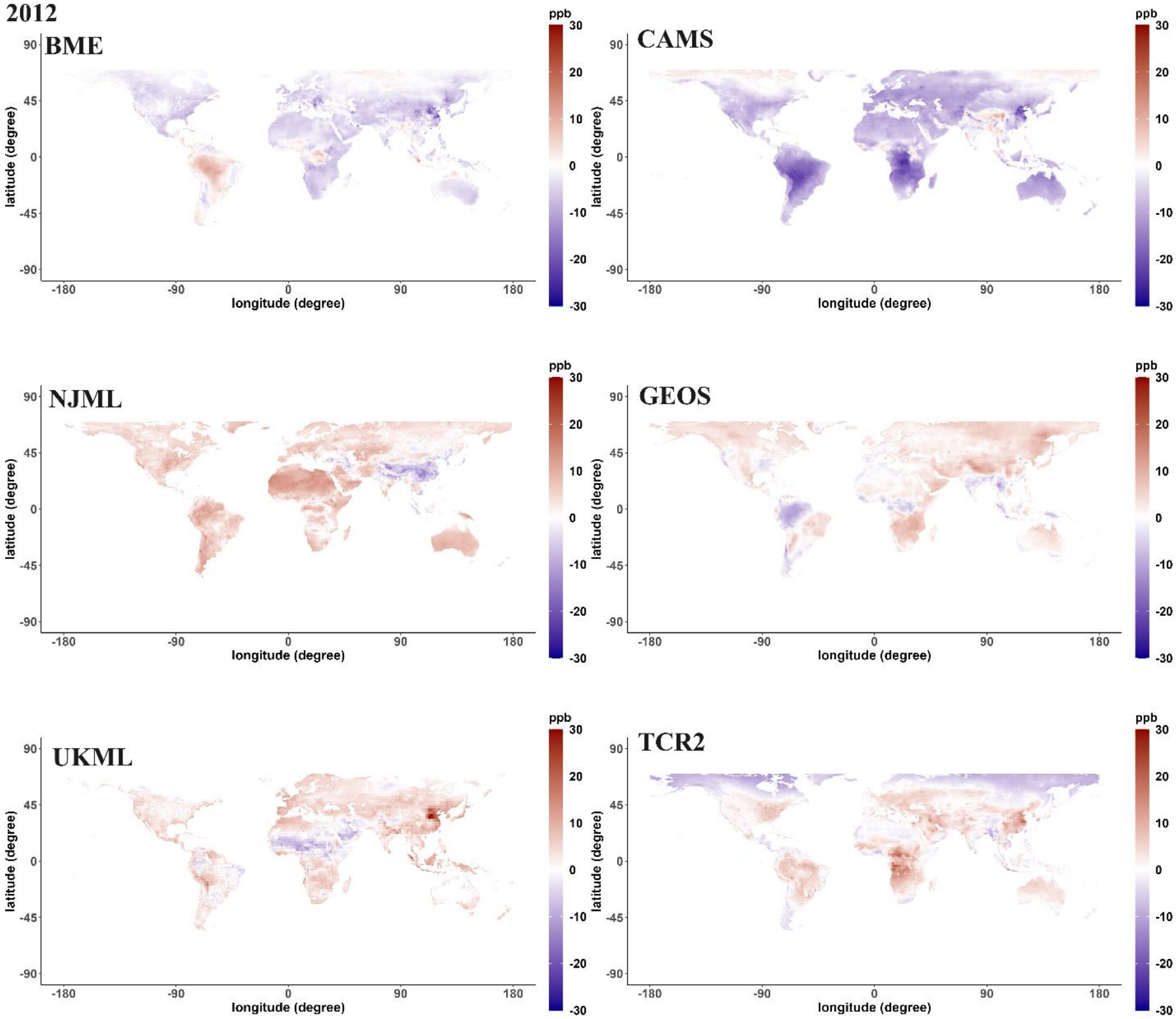
2012
BME
CAMS
NJML
GEOS
UKML
TCR2
ppb
30
20
10
0
-10
-20
-30
latitude (degree)
longitude (degree)
90
45
0
-45
-90
-180
-90
0
90
180

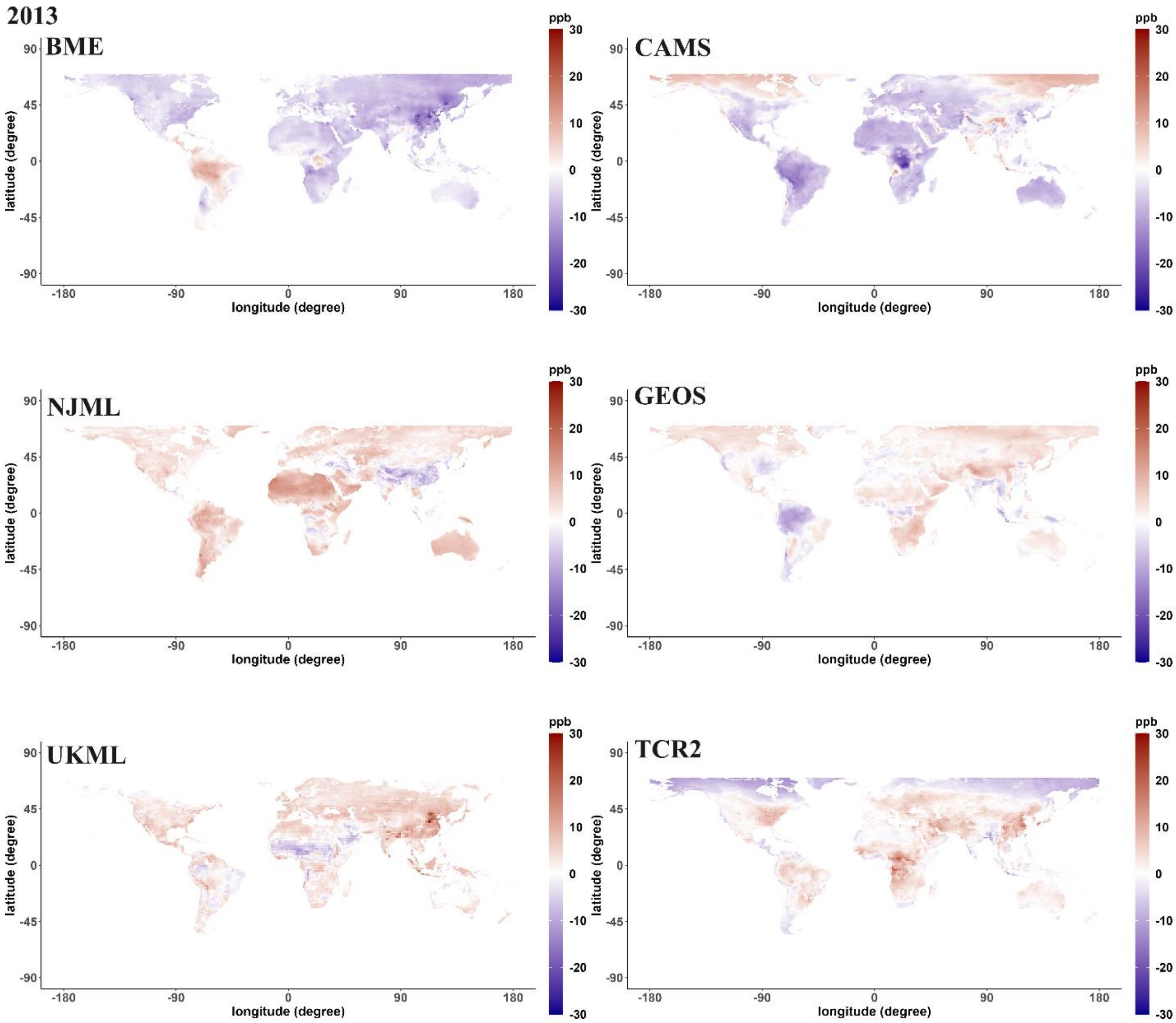
2013
BME
CAMS
NJML
GEOS
UKML
TCR2
ppb
30
20
10
0
-10
-20
-30
latitude (degree)
90
45
0
-45
-90
longitude (degree)
-180
-90
0
90
180

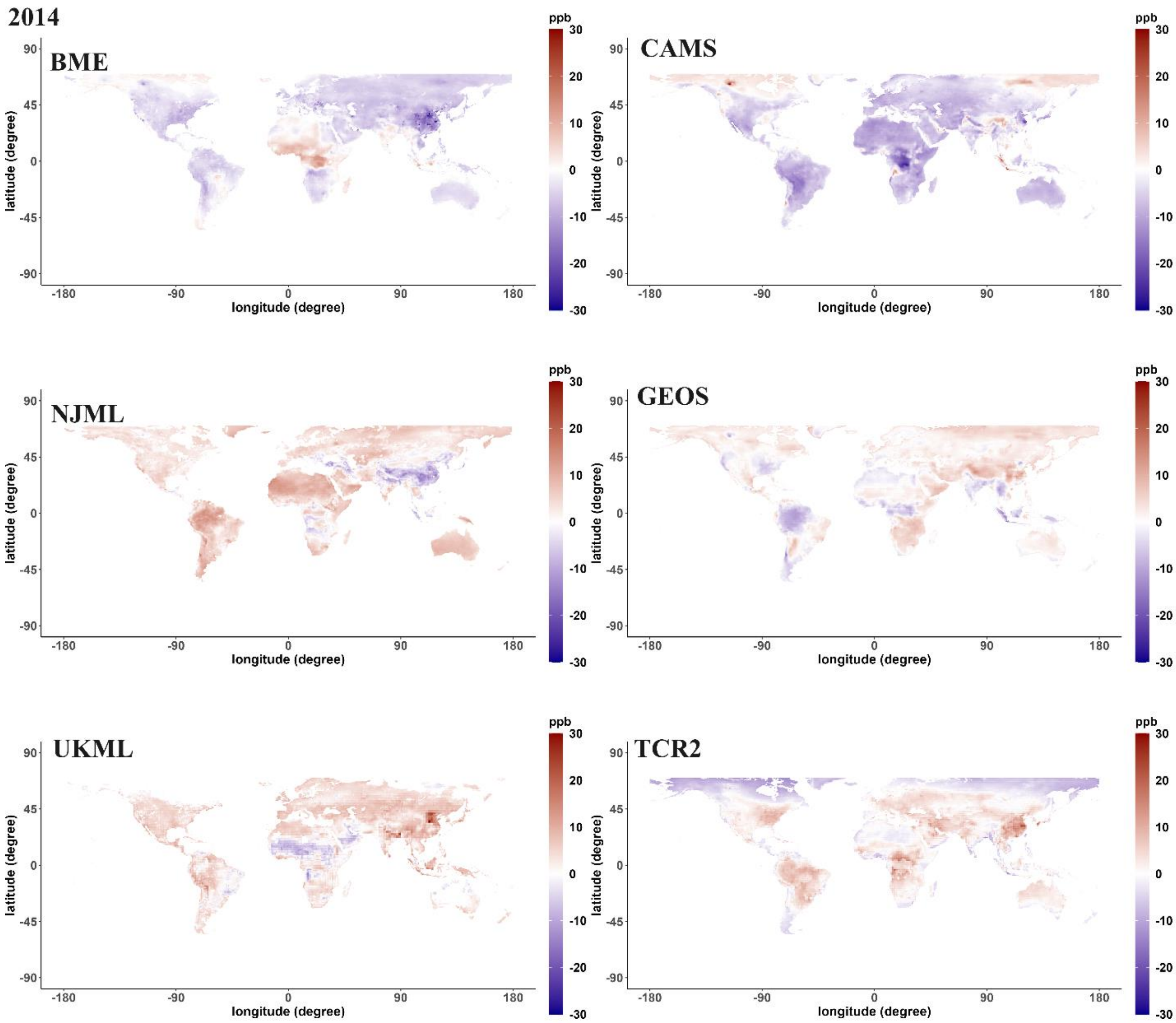
2014
BME
CAMS
NJML
GEOS
UKML
TCR2
ppb
30
20
10
0
-10
-20
-30
latitude (degree)
90
45
0
-45
-90
longitude (degree)
-180
-90
0
90
180

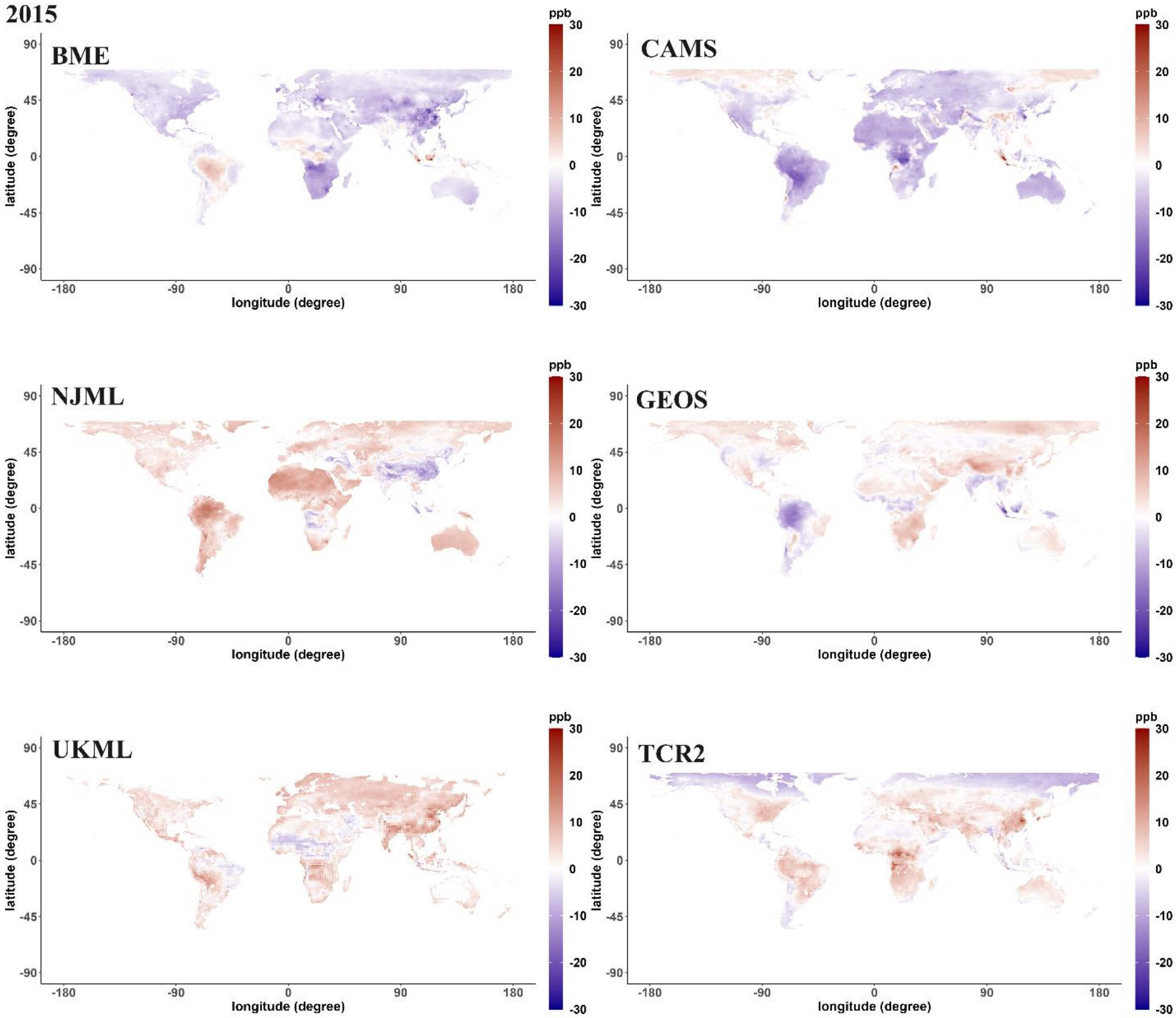
2015
BME
CAMS
NJML
GEOS
UKML
TCR2
ppb
latitude (degree)
longitude (degree)

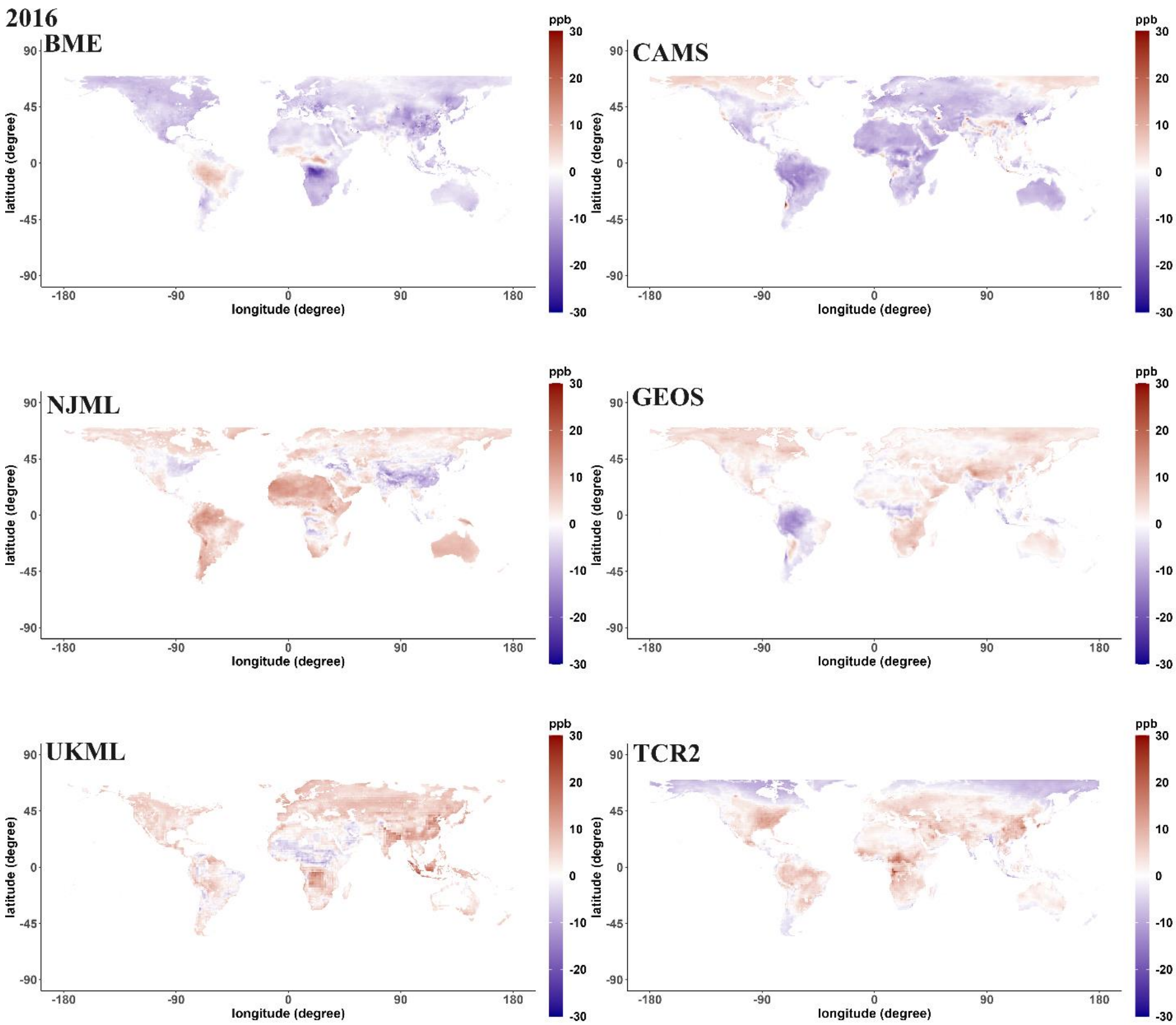
2016
BME
CAMS
NJML
GEOS
UKML
TCR2
ppb
latitude (degree)
longitude (degree)

Figure S12: The Lower and Upper bound of population exposed to yearly ozone metric (OSDMA8) which represent the 95% prediction interval for the estimate, from 2006 to 2016 in different regions. The horizontal axis represents ozone concentrations, and the vertical axis represents population size. The definitions of different regions are included in Table S7.

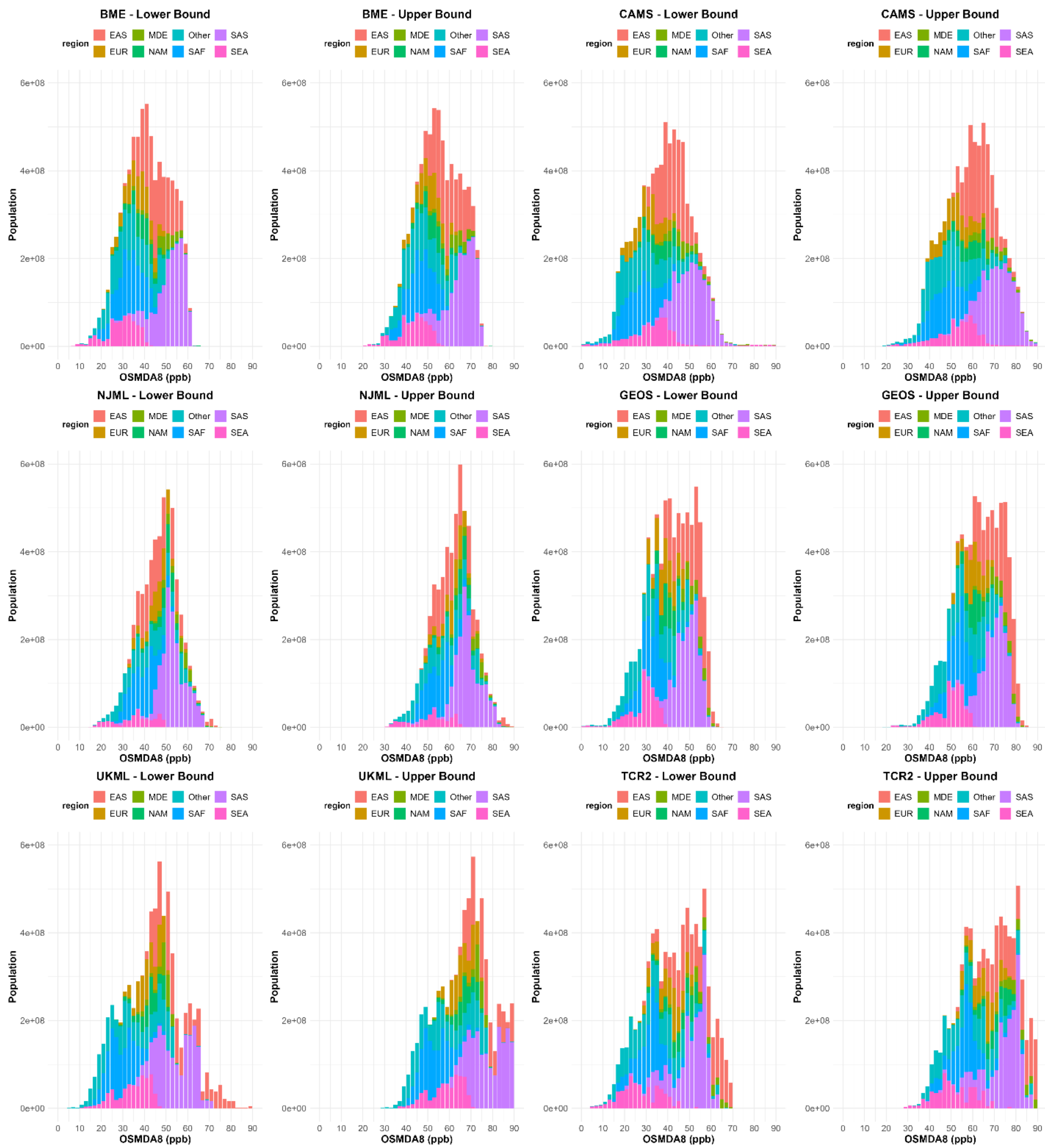

References

Global Modeling and Assimilation Office (GMAO) (2015), MERRA-2 instM_2d_gas_Nx: 2d, Monthly mean,Instantaneous, Single-Level, Assimilation, Aerosol Optical Depth Analysis V5.12.4, Greenbelt, MD, USA, Goddard Earth Sciences Data and Information Services Center (GES DISC), Accessed: [*2015*], 10.5067/XOGNBQEPLUC5

Adachi, Y., Yukimoto, S., Deushi, M., Obata, A., Nakano, H., Tanaka, T., Hosaka, M., Sakami, T., Yoshimura, H., Hirabara, M., Shindo, E., Tsujino, H., Mizuta, R., Yabu, S., Koshiro, T., Ose, T., and Kitoh, A.: Basic performance of a new Earth system model of the Meteorological Research Institute (MRI-ESM1), Papers in Meteorology and Geophysics, 64, 1-19, 10.2467/mripapers.64.1, 2013.

Amante, C. and Eakins, B. W.: ETOPO1 Global Relief Model converted to PanMap layer format, PANGAEA [dataset], 10.1594/PANGAEA.769615, 2009.

Archibald, A. T., O'Connor, F. M., Abraham, N. L., Archer-Nicholls, S., Chipperfield, M. P., Dalvi, M., Folberth, G. A., Dennison, F., Dhomse, S. S., Griffiths, P. T., Hardacre, C., Hewitt, A. J., Hill, R. S., Johnson, C. E., Keeble, J., Köhler, M. O., Morgenstern, O., Mulcahy, J. P., Ordóñez, C., Pope, R. J., Rumbold, S. T., Russo, M. R., Savage, N. H., Sellar, A., Stringer, M., Turnock, S. T., Wild, O., and Zeng, G.: Description and evaluation of the UKCA stratosphere–troposphere chemistry scheme (StratTrop vn 1.0) implemented in UKESM1, Geosci. Model Dev., 13, 1223-1266, 10.5194/gmd-13-1223-2020, 2020.

Bentsen, M., Olivië, D. J. L., Seland, Ø., Toniazzo, T., Gjermundsen, A., Graff, L. S., Debernard, J. B., Gupta, A. K., He, Y., Kirkevåg, A., Schwinger, J., Tjiputra, J., Aas, K. S., Bethke, I., Fan, Y., Griesfeller, J., Grini, A., Guo, C., Ilicak, M., Karset, I. H. H., Landgren, O. A., Liakka, J., Moseid, K. O., Nummelin, A., Spensberger, C., Tang, H., Zhang, Z., Heinze, C., Iversen, T., and Schulz, M.: NCC NorESM2-MM model output prepared for CMIP6 ScenarioMIP ssp245, Earth System Grid Federation [dataset], 10.22033/ESGF/CMIP6.8255, 2019.

Bhartia, P. K., McPeters, R. D., Mateer, C. L., Flynn, L. E., and Wellemeyer, C.: Algorithm for the estimation of vertical ozone profiles from the backscattered ultraviolet technique, Journal of Geophysical Research: Atmospheres, 101, 18793-18806, https://doi.org/10.1029/96JD01165, 1996.

Bishop, C.: Pattern Recognition and Machine Learning, in, 140-155, 10.1117/1.2819119, 2006.

Boersma, K., Eskes, H., Richter, A., De Smedt, I., Lorente, A., Beirle, S., Van Geffen, J., Peters, E., Van Roozendael, M., and Wagner, T.: QA4ECV NO2 tropospheric and stratospheric vertical column data from OMI (Version 1.1)[Data set], Royal Netherlands Meteorological Institute (KNMI), 2017.

Boersma, K. F., Eskes, H. J., and Brinksma, E. J.: Error analysis for tropospheric NO2 retrieval from space, Journal of Geophysical Research: Atmospheres, 109, https://doi.org/10.1029/2003JD003962, 2004.

Boersma, K. F., Eskes, H. J., Dirksen, R. J., van der A, R. J., Veefkind, J. P., Stammes, P., Huijnen, V., Kleipool, Q. L., Sneep, M., Claas, J., Leitão, J., Richter, A., Zhou, Y., and Brunner, D.: An improved tropospheric NO₂ column retrieval algorithm for the Ozone Monitoring Instrument, Atmos. Meas. Tech., 4, 1905-1928, 10.5194/amt-4-1905-2011, 2011.

Bowman, K. W., Rodgers, C. D., Kulawik, S. S., Worden, J., Sarkissian, E., Osterman, G., Steck, T., Ming, L., Eldering, A., Shephard, M., Worden, H., Lampel, M., Clough, S., Brown, P., Rinsland, C., Gunson, M., and Beer, R.: Tropospheric emission spectrometer: retrieval method and error analysis, IEEE Transactions on Geoscience and Remote Sensing, 44, 1297-1307, 10.1109/TGRS.2006.871234, 2006.

Consortium, E. C.-E.: EC-Earth-Consortium EC-Earth3-AerChem model output prepared for CMIP6 CMIP historical, Earth System Grid Federation [dataset], 10.22033/ESGF/CMIP6.4701, 2020.
Atmospheric Chemistry Observations & Modeling, National Center for Atmospheric Research, University Corporation for Atmospheric Research. (2020). CESM2.1 The Community Atmosphere Model with Chemistry (CAM-chem) Outputs as Boundary Conditions. Research Data Archive at the National Center for Atmospheric Research, Computational and Information Systems Laboratory. https://doi.org/10.5065/CKR4-GP38. Accessed 20 November 2024.
Danabasoglu, G.: NCAR CESM2-WACCM model output prepared for CMIP6 CMIP historical, Earth System Grid Federation [dataset], 10.22033/ESGF/CMIP6.10071, 2019.
Deeter, M. N., Edwards, D. P., Francis, G. L., Gille, J. C., Martínez-Alonso, S., Worden, H. M., and Sweeney, C.: A climate-scale satellite record for carbon monoxide: the MOPITT Version 7 product, Atmos. Meas. Tech., 10, 2533-2555, 10.5194/amt-10-2533-2017, 2017.
Deeter, M. N., Martínez-Alonso, S., Edwards, D. P., Emmons, L. K., Gille, J. C., Worden, H. M., Pittman, J. V., Daube, B. C., and Wofsy, S. C.: Validation of MOPITT Version 5 thermal-infrared, near-infrared, and multispectral carbon monoxide profile retrievals for 2000–2011, Journal of Geophysical Research: Atmospheres, 118, 6710-6725, https://doi.org/10.1002/jgrd.50272, 2013.
Deeter, M. N., Martínez-Alonso, S., Edwards, D. P., Emmons, L. K., Gille, J. C., Worden, H. M., Sweeney, C., Pittman, J. V., Daube, B. C., and Wofsy, S. C.: The MOPITT Version 6 product: algorithm enhancements and validation, Atmos. Meas. Tech., 7, 3623-3632, 10.5194/amt-7-3623-2014, 2014.
Doelling, D. R., Sun, M., Nguyen, L. T., Nordeen, M. L., Haney, C. O., Keyes, D. F., and Mlynczak, P. E.: Advances in Geostationary-Derived Longwave Fluxes for the CERES Synoptic (SYN1deg) Product, Journal of Atmospheric and Oceanic Technology, 33, 503-521, https://doi.org/10.1175/JTECH-D-15-0147.1, 2016.
Friedl, M., Sulla-Menashe, D: MCD12C1 MODIS/Terra+Aqua Land Cover Type Yearly L3 Global 0.05Deg CMG V006 [dataset], https://doi.org/10.5067/MODIS/MCD12C1.006, 2015.
Garcia, R. R., Smith, A. K., Kinnison, D. E., Cámara, Á. d. l., and Murphy, D. J.: Modification of the Gravity Wave Parameterization in the Whole Atmosphere Community Climate Model: Motivation and Results, Journal of the Atmospheric Sciences, 74, 275-291, https://doi.org/10.1175/JAS-D-16-0104.1, 2017.
Gettelman, A., Mills, M. J., Kinnison, D. E., Garcia, R. R., Smith, A. K., Marsh, D. R., Tilmes, S., Vitt, F., Bardeen, C. G., McInerny, J., Liu, H.-L., Solomon, S. C., Polvani, L. M., Emmons, L. K., Lamarque, J.-F., Richter, J. H., Glanville, A. S., Bacmeister, J. T., Phillips, A. S., Neale, R. B., Simpson, I. R., DuVivier, A. K., Hodzic, A., and Randel, W. J.: The Whole Atmosphere Community Climate Model Version 6 (WACCM6), Journal of Geophysical Research: Atmospheres, 124, 12380-12403, https://doi.org/10.1029/2019JD030943, 2019.
Good, P., Sellar, A., Tang, Y., Rumbold, S., Ellis, R., Kelley, D., and Kuhlbrodt, T.: MOHC UKESM1.0-LL model output prepared for CMIP6 ScenarioMIP ssp245, Earth System Grid Federation [dataset], 10.22033/ESGF/CMIP6.6339, 2019.
Greg E. Bodeker, S. K., & Jordis S. Tradowsky: BS Filled Total Column Ozone Database V3.4.1 (3.4.1) [dataset], https://doi.org/10.5281/zenodo.7447757, 2022.
Gutjahr, O., Putrasahan, D., Lohmann, K., Jungclaus, J. H., von Storch, J. S., Brüggemann, N., Haak, H., and Stössel, A.: Max Planck Institute Earth System Model (MPI-ESM1.2) for the High-Resolution Model Intercomparison Project (HighResMIP), Geosci. Model Dev., 12, 3241-3281, 10.5194/gmd-12-3241-2019, 2019.

Hao, N., Koukouli, M. E., Inness, A., Valks, P., Loyola, D. G., Zimmer, W., Balis, D. S., Zyrichidou, I., Van Roozendael, M., Lerot, C., and Spurr, R. J. D.: GOME-2 total ozone columns from MetOp-A/MetOp-B and assimilation in the MACC system, Atmos. Meas. Tech., 7, 2937-2951, 10.5194/amt-7-2937-2014, 2014.
Hegglin, M., Kinnison, D., Lamarque, J.-F., and Plummer, D.: CCMI ozone in support of CMIP6 - version 1.0, Earth System Grid Federation [dataset], 10.22033/ESGF/input4MIPs.1115, 2016.
Herman, R. and Kulawik, S.: Tropospheric Emission Spectrometer TES Level 2 (L2) Data User's Guide, D-38042, version 6.0, Jet Propulsion Laboratory, California Institute of Technology, Pasadena, CA, available at: http://tes. jpl. nasa. gov/documents (last access: 30 June 2014), 2013.
Hersbach, H., Bell, B., Berrisford, P., Hirahara, S., Horányi, A., Muñoz Sabater, J., Nicolas, J., Peubey, C., Radu, R., Schepers, D., Simmons, A., Soci, C., Abdalla, S., Abellan, X., Balsamo, G., Bechtold, P., Biavati, G., Bidlot, J., Bonavita, M., and Thépaut, J. N.: The ERA5 global reanalysis, Quarterly Journal of the Royal Meteorological Society, 146, 10.1002/qj.3803, 2020.
Hoesly, R. M., Smith, S. J., Feng, L., Klimont, Z., Janssens-Maenhout, G., Pitkanen, T., Seibert, J. J., Vu, L., Andres, R. J., Bolt, R. M., Bond, T. C., Dawidowski, L., Kholod, N., Kurokawa, J. I., Li, M., Liu, L., Lu, Z., Moura, M. C. P., O'Rourke, P. R., and Zhang, Q.: Historical (1750–2014) anthropogenic emissions of reactive gases and aerosols from the Community Emissions Data System (CEDS), Geosci. Model Dev., 11, 369-408, 10.5194/gmd-11-369-2018, 2018.
Horowitz, L. W., Naik, V., Paulot, F., Ginoux, P. A., Dunne, J. P., Mao, J., Schnell, J., Chen, X., He, J., John, J. G., Lin, M., Lin, P., Malyshev, S., Paynter, D., Shevliakova, E., and Zhao, M.: The GFDL Global Atmospheric Chemistry-Climate Model AM4.1: Model Description and Simulation Characteristics, Journal of Advances in Modeling Earth Systems, 12, e2019MS002032, https://doi.org/10.1029/2019MS002032, 2020.
Horowitz, L. W., Naik, V., Sentman, L., Paulot, F., Blanton, C., McHugh, C., Radhakrishnan, A., Rand, K., Vahlenkamp, H., Zadeh, N. T., Wilson, C., Ginoux, P., He, J., John, J. G., Lin, M., Paynter, D. J., Ploshay, J., Zhang, A., and Zeng, Y.: NOAA-GFDL GFDL-ESM4 model output prepared for CMIP6 AerChemMIP, Earth System Grid Federation [dataset], 10.22033/ESGF/CMIP6.1404, 2018.
Inness, A., Ades, M., Agustí-Panareda, A., Barré, J., Benedictow, A., Blechschmidt, A. M., Dominguez, J. J., Engelen, R., Eskes, H., Flemming, J., Huijnen, V., Jones, L., Kipling, Z., Massart, S., Parrington, M., Peuch, V. H., Razinger, M., Remy, S., Schulz, M., and Suttie, M.: The CAMS reanalysis of atmospheric composition, Atmos. Chem. Phys., 19, 3515-3556, 10.5194/acp-19-3515-2019, 2019.
Janssens-Maenhout, G., Crippa, M., Guizzardi, D., Dentener, F., Muntean, M., Pouliot, G., Keating, T., Zhang, Q., Kurokawa, J., Wankmüller, R., Denier van der Gon, H., Kuenen, J. J. P., Klimont, Z., Frost, G., Darras, S., Koffi, B., and Li, M.: HTAP_v2.2: a mosaic of regional and global emission grid maps for 2008 and 2010 to study hemispheric transport of air pollution, Atmos. Chem. Phys., 15, 11411-11432, 10.5194/acp-15-11411-2015, 2015.
John, J. G., Blanton, C., McHugh, C., Radhakrishnan, A., Rand, K., Vahlenkamp, H., Wilson, C., Zadeh, N. T., Dunne, J. P., Dussin, R., Horowitz, L. W., Krasting, J. P., Lin, P., Malyshev, S., Naik, V., Ploshay, J., Shevliakova, E., Silvers, L., Stock, C., Winton, M., and Zeng, Y.: NOAA-GFDL GFDL-ESM4 model output prepared for CMIP6 ScenarioMIP ssp245, Earth System Grid Federation [dataset], 10.22033/ESGF/CMIP6.8686, 2018.
Josse, B., Simon, P., and Peuch, V. H.: Radon global simulations with the multiscale chemistry and transport model MOCAGE, Tellus, Series B: Chemical and Physical Meteorology, 56B, 339-356, 2004.

KOFFI, L. B., DENTENER, F., JANSSENS-MAENHOUT, G., GUIZZARDI, D., CRIPPA, M., DIEHL, T., GALMARINI, S., and SOLAZZO, E.: Hemispheric Transport of Air Pollution (HTAP): Specification of the HTAP2 experiments: Ensuring harmonized modelling, 2016.
Krasting, J. P., John, J. G., Blanton, C., McHugh, C., Nikonov, S., Radhakrishnan, A., Rand, K., Zadeh, N. T., Balaji, V., Durachta, J., Dupuis, C., Menzel, R., Robinson, T., Underwood, S., Vahlenkamp, H., Dunne, K. A., Gauthier, P. P. G., Ginoux, P., Griffies, S. M., Hallberg, R., Harrison, M., Hurlin, W., Malyshev, S., Naik, V., Paulot, F., Paynter, D. J., Ploshay, J., Reichl, B. G., Schwarzkopf, D. M., Seman, C. J., Silvers, L., Wyman, B., Zeng, Y., Adcroft, A., Dunne, J. P., Dussin, R., Guo, H., He, J., Held, I. M., Horowitz, L. W., Lin, P., Milly, P. C. D., Shevliakova, E., Stock, C., Winton, M., Wittenberg, A. T., Xie, Y., and Zhao, M.: NOAA-GFDL GFDL-ESM4 model output prepared for CMIP6 CMIP, Earth System Grid Federation [dataset], 10.22033/ESGF/CMIP6.1407, 2018.
Krotkov, N. A., Lamsal, L. N., Celarier, E. A., Swartz, W. H., Marchenko, S. V., Bucsela, E. J., Chan, K. L., Wenig, M., and Zara, M.: The version 3 OMI NO2 standard product, Atmos. Meas. Tech., 10, 3133-3149, 10.5194/amt-10-3133-2017, 2017.
Krotkov, N. A., McLinden, C. A., Li, C., Lamsal, L. N., Celarier, E. A., Marchenko, S. V., Swartz, W. H., Bucsela, E. J., Joiner, J., and Duncan, B. N.: Aura OMI observations of regional SO 2 and NO 2 pollution changes from 2005 to 2015, Atmospheric Chemistry and Physics, 16, 4605-4629, 2016.
Lerot, C., Van Roozendael, M., van Geffen, J., van Gent, J., Fayt, C., Spurr, R., Lichtenberg, G., and von Bargen, A.: Six years of total ozone column measurements from SCIAMACHY nadir observations, Atmos. Meas. Tech., 2, 87-98, 10.5194/amt-2-87-2009, 2009.
Li, C., Joiner, J., Krotkov, N. A., and Bhartia, P. K.: A fast and sensitive new satellite SO2 retrieval algorithm based on principal component analysis: Application to the ozone monitoring instrument, Geophysical Research Letters, 40, 6314-6318, https://doi.org/10.1002/2013GL058134, 2013.
Lin, M., Horowitz, L., Payton, R., Fiore, A., and Tonnesen, G.: US surface ozone trends and extremes from 1980 to 2014: Quantifying the roles of rising Asian emissions, domestic controls, wildfires, and climate, Atmospheric Chemistry and Physics, 17, 2943-2970, 10.5194/acp-17-2943-2017, 2017.
Lin, W., Yuan, H., Dong, W., Zhang, S., Liu, S., Wei, N., Lu, X., Wei, Z., Hu, Y., and Dai, Y.: Reprocessed MODIS Version 6.1 Leaf Area Index Dataset and Its Evaluation for Land Surface and Climate Modeling, Remote Sensing, 15, 1780, 10.3390/rs15071780, 2023.
Liu, X., Bhartia, P. K., Chance, K., Froidevaux, L., Spurr, R. J. D., and Kurosu, T. P.: Validation of Ozone Monitoring Instrument (OMI) ozone profiles and stratospheric ozone columns with Microwave Limb Sounder (MLS) measurements, Atmos. Chem. Phys., 10, 2539-2549, 10.5194/acp-10-2539-2010, 2010.
Livesey, N., Read, W., Wagner, P., Froidevaux, L., Lambert, A., Manney, G., Valle, L., Pumphrey, H., Santee, M., and Schwartz, M.: Version 4.2 x level 2 data quality and description document, JPL D-33509 Rev, 2017.
Lloyd, C. T., Chamberlain, H., Kerr, D., Yetman, G., Pistolesi, L., Stevens, F. R., Gaughan, A. E., Nieves, J. J., Hornby, G., MacManus, K., Sinha, P., Bondarenko, M., Sorichetta, A., and Tatem, A. J.: Global spatio-temporally harmonised datasets for producing high-resolution gridded population distribution datasets, Big Earth Data, 3, 108-139, 10.1080/20964471.2019.1625151, 2019.

Lu, X., Hong, J., Zhang, L., Cooper, O. R., Schultz, M. G., Xu, X., Wang, T., Gao, M., Zhao, Y., and Zhang, Y.: Severe Surface Ozone Pollution in China: A Global Perspective, Environmental Science & Technology Letters, 5, 487-494, 10.1021/acs.estlett.8b00366, 2018.
Marsh, D. R., Mills, M. J., Kinnison, D. E., Lamarque, J.-F., Calvo, N., and Polvani, L. M.: Climate Change from 1850 to 2005 Simulated in CESM1(WACCM), Journal of Climate, 26, 7372-7391, https://doi.org/10.1175/JCLI-D-12-00558.1, 2013.
McPeters, R. D., Bhartia, P. K., Haffner, D., Labow, G. J., and Flynn, L.: The version 8.6 SBUV ozone data record: An overview, Journal of Geophysical Research: Atmospheres, 118, 8032-8039, https://doi.org/10.1002/jgrd.50597, 2013.
Mulcahy, J. P., Jones, C., Sellar, A., Johnson, B., Boutle, I. A., Jones, A., Andrews, T., Rumbold, S. T., Mollard, J., Bellouin, N., Johnson, C. E., Williams, K. D., Grosvenor, D. P., and McCoy, D. T.: Improved Aerosol Processes and Effective Radiative Forcing in HadGEM3 and UKESM1, Journal of Advances in Modeling Earth Systems, 10, 2786-2805, https://doi.org/10.1029/2018MS001464, 2018.
Neubauer, D., Ferrachat, S., Siegenthaler-Le Drian, C., Stoll, J., Folini, D. S., Tegen, I., Wieners, K.-H., Mauritsen, T., Stemmler, I., Barthel, S., Bey, I., Daskalakis, N., Heinold, B., Kokkola, H., Partridge, D., Rast, S., Schmidt, H., Schutgens, N., Stanelle, T., Stier, P., Watson-Parris, D., and Lohmann, U.: HAMMOZ-Consortium MPI-ESM1.2-HAM model output prepared for CMIP6 CMIP, Earth System Grid Federation [dataset], 10.22033/ESGF/CMIP6.1622, 2019.
Qu, Z., Daven, K. H., Owen, R. C., and Jessica, L. N.: Global (2°x2.5°) top-down NOx emissions from OMI DOMINO product (2005-2016) (V1), Harvard Dataverse [dataset], doi:10.7910/DVN/QBAQZA, 2020a.
Qu, Z., Daven, K. H., Owen, R. C., and Jessica, L. N.: Global (2°x2.5°) top-down NOx emissions from OMI NASA product (2005-2016) (V1), Harvard Dataverse [dataset], doi:10.7910/DVN/HVT1FO, 2020b.
Qu, Z., Henze, D. K., Capps, S. L., Wang, Y., Xu, X., Wang, J., and Keller, M.: Monthly top-down NOx emissions for China (2005–2012): A hybrid inversion method and trend analysis, Journal of Geophysical Research: Atmospheres, 122, 4600-4625, https://doi.org/10.1002/2016JD025852, 2017.
Schultz, M. G., Schröder, S., Lyapina, O., Cooper, O. R., Galbally, I., Petropavlovskikh, I., von Schneidemesser, E., Tanimoto, H., Elshorbany, Y., Naja, M., Seguel, R. J., Dauert, U., Eckhardt, P., Feigenspan, S., Fiebig, M., Hjellbrekke, A.-G., Hong, Y.-D., Kjeld, P. C., Koide, H., Lear, G., Tarasick, D., Ueno, M., Wallasch, M., Baumgardner, D., Chuang, M.-T., Gillett, R., Lee, M., Molloy, S., Moolla, R., Wang, T., Sharps, K., Adame, J. A., Ancellet, G., Apadula, F., Artaxo, P., Barlasina, M. E., Bogucka, M., Bonasoni, P., Chang, L., Colomb, A., Cuevas-Agulló, E., Cupeiro, M., Degorska, A., Ding, A., Fröhlich, M., Frolova, M., Gadhavi, H., Gheusi, F., Gilge, S., Gonzalez, M. Y., Gros, V., Hamad, S. H., Helmig, D., Henriques, D., Hermansen, O., Holla, R., Hueber, J., Im, U., Jaffe, D. A., Komala, N., Kubistin, D., Lam, K.-S., Laurila, T., Lee, H., Levy, I., Mazzoleni, C., Mazzoleni, L. R., McClure-Begley, A., Mohamad, M., Murovec, M., Navarro-Comas, M., Nicodim, F., Parrish, D., Read, K. A., Reid, N., Ries, L., Saxena, P., Schwab, J. J., Scorgie, Y., Senik, I., Simmonds, P., Sinha, V., Skorokhod, A. I., Spain, G., Spangl, W., Spoor, R., Springston, S. R., Steer, K., Steinbacher, M., Suharguniyawan, E., Torre, P., Trickl, T., Weili, L., Weller, R., Xiaobin, X., Xue, L., and Zhiqiang, M.: Tropospheric Ozone Assessment Report: Database and metrics data of global surface ozone observations, Elementa: Science of the Anthropocene, 5, 10.1525/elementa.244, 2017.

Schupfner, M., Wieners, K.-H., Wachsmann, F., Steger, C., Bittner, M., Jungclaus, J., Früh, B., Pankatz, K., Giorgetta, M., Reick, C., Legutke, S., Esch, M., Gayler, V., Haak, H., de Vrese, P., Raddatz, T., Mauritsen, T., von Storch, J.-S., Behrens, J., Brovkin, V., Claussen, M., Crueger, T., Fast, I., Fiedler, S., Hagemann, S., Hohenegger, C., Jahns, T., Kloster, S., Kinne, S., Lasslop, G., Kornblueh, L., Marotzke, J., Matei, D., Meraner, K., Mikolajewicz, U., Modali, K., Müller, W., Nabel, J., Notz, D., Peters-von Gehlen, K., Pincus, R., Pohlmann, H., Pongratz, J., Rast, S., Schmidt, H., Schnur, R., Schulzweida, U., Six, K., Stevens, B., Voigt, A., and Roeckner, E.: DKRZ MPI-ESM1.2-HR model output prepared for CMIP6 ScenarioMIP ssp245, Earth System Grid Federation [dataset], 10.22033/ESGF/CMIP6.4398, 2019.
Schwartz, M., Froidevaux, L., Livesey, N. and Read, W: MLS/Aura Level 2 Ozone (O3) Mixing Ratio V004 [dataset], 10.5067/Aura/MLS/DATA2017, 2015.
Seland, Ø., Bentsen, M., Oliviè, D. J. L., Toniazzo, T., Gjermundsen, A., Graff, L. S., Debernard, J. B., Gupta, A. K., He, Y., Kirkevåg, A., Schwinger, J., Tjiputra, J., Aas, K. S., Bethke, I., Fan, Y., Griesfeller, J., Grini, A., Guo, C., Ilicak, M., Karset, I. H. H., Landgren, O. A., Liakka, J., Moseid, K. O., Nummelin, A., Spensberger, C., Tang, H., Zhang, Z., Heinze, C., Iversen, T., and Schulz, M.: NCC NorESM2-LM model output prepared for CMIP6 CMIP historical, Earth System Grid Federation [dataset], 10.22033/ESGF/CMIP6.8036, 2019.
Sellar, A. A., Jones, C. G., Mulcahy, J. P., Tang, Y., Yool, A., Wiltshire, A., O'Connor, F. M., Stringer, M., Hill, R., Palmieri, J., Woodward, S., de Mora, L., Kuhlbrodt, T., Rumbold, S. T., Kelley, D. I., Ellis, R., Johnson, C. E., Walton, J., Abraham, N. L., Andrews, M. B., Andrews, T., Archibald, A. T., Berthou, S., Burke, E., Blockley, E., Carslaw, K., Dalvi, M., Edwards, J., Folberth, G. A., Gedney, N., Griffiths, P. T., Harper, A. B., Hendry, M. A., Hewitt, A. J., Johnson, B., Jones, A., Jones, C. D., Keeble, J., Liddicoat, S., Morgenstern, O., Parker, R. J., Predoi, V., Robertson, E., Siahaan, A., Smith, R. S., Swaminathan, R., Woodhouse, M. T., Zeng, G., and Zerroukat, M.: UKESM1: Description and Evaluation of the U.K. Earth System Model, Journal of Advances in Modeling Earth Systems, 11, 4513-4558, https://doi.org/10.1029/2019MS001739, 2019.
Sellar, A. A., Walton, J., Jones, C. G., Wood, R., Abraham, N. L., Andrejczuk, M., Andrews, M. B., Andrews, T., Archibald, A. T., de Mora, L., Dyson, H., Elkington, M., Ellis, R., Florek, P., Good, P., Gohar, L., Haddad, S., Hardiman, S. C., Hogan, E., Iwi, A., Jones, C. D., Johnson, B., Kelley, D. I., Kettleborough, J., Knight, J. R., Köhler, M. O., Kuhlbrodt, T., Liddicoat, S., Linova-Pavlova, I., Mizielinski, M. S., Morgenstern, O., Mulcahy, J., Neininger, E., O'Connor, F. M., Petrie, R., Ridley, J., Rioual, J.-C., Roberts, M., Robertson, E., Rumbold, S., Seddon, J., Shepherd, H., Shim, S., Stephens, A., Teixiera, J. C., Tang, Y., Williams, J., Wiltshire, A., and Griffiths, P. T.: Implementation of U.K. Earth System Models for CMIP6, Journal of Advances in Modeling Earth Systems, 12, e2019MS001946, https://doi.org/10.1029/2019MS001946, 2020.
Shindell, D. T., Pechony, O., Voulgarakis, A., Faluvegi, G., Nazarenko, L., Lamarque, J. F., Bowman, K., Milly, G., Kovari, B., Ruedy, R., and Schmidt, G. A.: Interactive ozone and methane chemistry in GISS-E2 historical and future climate simulations, Atmos. Chem. Phys., 13, 2653-2689, 10.5194/acp-13-2653-2013, 2013.
Strode, S. A., Ziemke, J. R., Oman, L. D., Lamsal, L. N., Olsen, M. A., and Liu, J.: Global changes in the diurnal cycle of surface ozone, Atmospheric Environment, 199, 323-333, https://doi.org/10.1016/j.atmosenv.2018.11.028, 2019.
Studies, N. G. I. f. S.: NASA-GISS GISS-E2.1H model output prepared for CMIP6 CMIP, Earth System Grid Federation [dataset], 10.22033/ESGF/CMIP6.1421, 2018a.

Studies, N. G. I. f. S.: NASA-GISS GISS-E2.1G model output prepared for CMIP6 CMIP, Earth System Grid Federation [dataset], 10.22033/ESGF/CMIP6.1400, 2018b.
Studies, N. G. I. f. S.: NASA-GISS GISS-E2.1G model output prepared for CMIP6 ScenarioMIP ssp245, Earth System Grid Federation [dataset], 10.22033/ESGF/CMIP6.7415, 2020.
Sudo, K., Takahashi, M., and Akimoto, H.: CHASER: A global chemical model of the troposphere 2. Model results and evaluation, Journal of Geophysical Research: Atmospheres, 107, ACH 9-1-ACH 9-39, https://doi.org/10.1029/2001JD001114, 2002.
Tang, Y., Rumbold, S., Ellis, R., Kelley, D., Mulcahy, J., Sellar, A., Walton, J., and Jones, C.: MOHC UKESM1.0-LL model output prepared for CMIP6 CMIP historical, Earth System Grid Federation [dataset], 10.22033/ESGF/CMIP6.6113, 2019.
Teyssèdre, H., Michou, M., Clark, H. L., Josse, B., Karcher, F., Olivié, D., Peuch, V. H., Saint-Martin, D., Cariolle, D., Attié, J. L., Nédélec, P., Ricaud, P., Thouret, V., van der A, R. J., Volz-Thomas, A., and Chéroux, F.: A new tropospheric and stratospheric Chemistry and Transport Model MOCAGE-Climat for multi-year studies: evaluation of the present-day climatology and sensitivity to surface processes, Atmos. Chem. Phys., 7, 5815-5860, 10.5194/acp-7-5815-2007, 2007.
Tilmes, S., Lamarque, J. F., Emmons, L. K., Kinnison, D. E., Ma, P. L., Liu, X., Ghan, S., Bardeen, C., Arnold, S., Deeter, M., Vitt, F., Ryerson, T., Elkins, J. W., Moore, F., Spackman, J. R., and Val Martin, M.: Description and evaluation of tropospheric chemistry and aerosols in the Community Earth System Model (CESM1.2), Geosci. Model Dev., 8, 1395-1426, 10.5194/gmd-8-1395-2015, 2015.
von Clarmann, T., Höpfner, M., Kellmann, S., Linden, A., Chauhan, S., Funke, B., Grabowski, U., Glatthor, N., Kiefer, M., Schieferdecker, T., Stiller, G. P., and Versick, S.: Retrieval of temperature, H₂O, O₃, HNO₃, CH₄, N₂O, ClONO₂ and ClO from MIPAS reduced resolution nominal mode limb emission measurements, Atmos. Meas. Tech., 2, 159-175, 10.5194/amt-2-159-2009, 2009.
von Storch, J.-S., Putrasahan, D., Lohmann, K., Gutjahr, O., Jungclaus, J., Bittner, M., Haak, H., Wieners, K.-H., Giorgetta, M., Reick, C., Esch, M., Gayler, V., de Vrese, P., Raddatz, T., Mauritsen, T., Behrens, J., Brovkin, V., Claussen, M., Crueger, T., Fast, I., Fiedler, S., Hagemann, S., Hohenegger, C., Jahns, T., Kloster, S., Kinne, S., Lasslop, G., Kornblueh, L., Marotzke, J., Matei, D., Meraner, K., Mikolajewicz, U., Modali, K., Müller, W., Nabel, J., Notz, D., Peters-von Gehlen, K., Pincus, R., Pohlmann, H., Pongratz, J., Rast, S., Schmidt, H., Schnur, R., Schulzweida, U., Six, K., Stevens, B., Voigt, A., and Roeckner, E.: MPI-M MPIESM1.2-HR model output prepared for CMIP6 HighResMIP, Earth System Grid Federation [dataset], 10.22033/ESGF/CMIP6.762, 2017.
Watanabe, S., Hajima, T., Sudo, K., Nagashima, T., Takemura, T., Okajima, H., Nozawa, T., Kawase, H., Abe, M., Yokohata, T., Ise, T., Sato, H., Kato, E., Takata, K., Emori, S., and Kawamiya, M.: MIROC-ESM 2010: model description and basic results of CMIP5-20c3m experiments, Geosci. Model Dev., 4, 845-872, 10.5194/gmd-4-845-2011, 2011.
Wu, T., Zhang, F., Zhang, J., Jie, W., Zhang, Y., Wu, F., Li, L., Yan, J., Liu, X., Lu, X., Tan, H., Zhang, L., Wang, J., and Hu, A.: Beijing Climate Center Earth System Model version 1 (BCC-ESM1): model description and evaluation of aerosol simulations, Geosci. Model Dev., 13, 977-1005, 10.5194/gmd-13-977-2020, 2020.
Wu, T., Yu, R., Lu, Y., Jie, W., Fang, Y., Zhang, J., Zhang, L., Xin, X., Li, L., Wang, Z., Liu, Y., Zhang, F., Wu, F., Chu, M., Li, J., Li, W., Zhang, Y., Shi, X., Zhou, W., Yao, J., Liu, X., Zhao, H.,

Yan, J., Wei, M., Xue, W., Huang, A., Zhang, Y., Zhang, Y., Shu, Q., and Hu, A.: BCC-CSM2-HR: a high-resolution version of the Beijing Climate Center Climate System Model, Geosci. Model Dev., 14, 2977-3006, 10.5194/gmd-14-2977-2021, 2021.
Yool, A., Palmiéri, J., Jones, C. G., Sellar, A. A., de Mora, L., Kuhlbrodt, T., Popova, E. E., Mulcahy, J. P., Wiltshire, A., Rumbold, S. T., Stringer, M., Hill, R. S. R., Tang, Y., Walton, J., Blaker, A., Nurser, A. J. G., Coward, A. C., Hirschi, J., Woodward, S., Kelley, D. I., Ellis, R., and Rumbold-Jones, S.: Spin-up of UK Earth System Model 1 (UKESM1) for CMIP6, Journal of Advances in Modeling Earth Systems, 12, e2019MS001933, https://doi.org/10.1029/2019MS001933, 2020.
Yukimoto, S., Koshiro, T., Kawai, H., Oshima, N., Yoshida, K., Urakawa, S., Tsujino, H., Deushi, M., Tanaka, T., Hosaka, M., Yoshimura, H., Shindo, E., Mizuta, R., Ishii, M., Obata, A., and Adachi, Y.: MRI MRI-ESM2.0 model output prepared for CMIP6 ScenarioMIP ssp245, Earth System Grid Federation [dataset], 10.22033/ESGF/CMIP6.6910, 2019a.
Yukimoto, S., Adachi, Y., Hosaka, M., Sakami, T., Yoshimura, H., Hirabara, M., Tanaka, T. Y., Shindo, E., Tsujino, H., Deushi, M., Mizuta, R., Yabu, S., Obata, A., Nakano, H., Koshiro, T., Ose, T., and Kitoh, A.: A New Global Climate Model of the Meteorological Research Institute: MRI-CGCM3 —Model Description and Basic Performance&mdash, Journal of the Meteorological Society of Japan. Ser. II, 90A, 23-64, 10.2151/jmsj.2012-A02, 2012.
Yukimoto, S., Kawai, H., Koshiro, T., Oshima, N., Yoshida, K., Urakawa, S., Tsujino, H., Deushi, M., Tanaka, T., Hosaka, M., Yabu, S., Yoshimura, H., Shindo, E., Mizuta, R., Obata, A., Adachi, Y., and Ishii, M.: The Meteorological Research Institute Earth System Model Version 2.0, MRI-ESM2.0: Description and Basic Evaluation of the Physical Component, Journal of the Meteorological Society of Japan. Ser. II, 97, 931-965, 10.2151/jmsj.2019-051, 2019b.
Yukimoto, S., Kawai, H., Koshiro, T., Oshima, N., Yoshida, K., Urakawa, S., Tsujino, H., Deushi, M., Tanaka, T., Hosaka, M., Yabu, S., Yoshimura, H., Shindo, E., Mizuta, R., Obata, A., Adachi, Y., and Ishii, M.: The Meteorological Research Institute Earth System Model Version 2.0, MRI-ESM2.0: Description and Basic Evaluation of the Physical Component, Journal of the Meteorological Society of Japan, 97, 10.2151/jmsj.2019-051, 2019c.
Zhang, J., Wu, T., Shi, X., Zhang, F., Li, J., Chu, M., Liu, Q., Yan, J., Ma, Q., and Wei, M.: BCC BCC-ESM1 model output prepared for CMIP6 CMIP, Earth System Grid Federation [dataset], 10.22033/ESGF/CMIP6.1734, 2018.
Zhang, L., Lin, M., Langford, A. O., Horowitz, L. W., Senff, C. J., Klovenski, E., Wang, Y., Alvarez Ii, R. J., Petropavlovskikh, I., Cullis, P., Sterling, C. W., Peischl, J., Ryerson, T. B., Brown, S. S., Decker, Z. C. J., Kirgis, G., and Conley, S.: Characterizing sources of high surface ozone events in the southwestern US with intensive field measurements and two global models, Atmos. Chem. Phys., 20, 10379-10400, 10.5194/acp-20-10379-2020, 2020.
Ziemke, J. R., Oman, L. D., Strode, S. A., Douglass, A. R., Olsen, M. A., McPeters, R. D., Bhartia, P. K., Froidevaux, L., Labow, G. J., Witte, J. C., Thompson, A. M., Haffner, D. P., Kramarova, N. A., Frith, S. M., Huang, L. K., Jaross, G. R., Seftor, C. J., Deland, M. T., and Taylor, S. L.: Trends in global tropospheric ozone inferred from a composite record of TOMS/OMI/MLS/OMPS satellite measurements and the MERRA-2 GMI simulation, Atmos. Chem. Phys., 19, 3257-3269, 10.5194/acp-19-3257-2019, 2019.